# MY RESULTS IN MATHEMATICAL GEOPHYSICS

## THESIS SUBMITTED TO THE HUNGARIAN ACADEMY OF SCIENCES FOR THE DOCTOR OF SCIENCES DEGREE

Microsoft

**Dr. Gábor Korvin**

**Budapest, 2020**

# "MY RESULTS IN MATHEMATICAL GEOPHYSICS" – A THESIS SUBMITTED TO THE HUNGARIAN ACADEMY OF SCIENCES FOR THE DOCTOR OF SCIENCES DEGREE

Dr. Gábor Korvin, Budapest

LIST OF CONTENTS

# 0. PREFACE

In 1992, I wrote in the *Preface* of my book on fractals[1]:

> "The book will also be useful to applied mathematicians, physicists and computer scientists looking for new fields for research. A group of these people have devoted a a life-time to deconvolve, unwrap, filter, simulate, krige, predict, up- and downward continue, to cross-plot and transform and prewhiten, in general to apply the latest what mathematics, physics and electronics have to offer to improve data quality and build better geological models. Their endeavors are often met with suspicion or hostility: the bitter words of John Dowds[2] are still valid: "… in the Report, *Information Theory* was mentioned, but I decided it best to avoid unfamiliar words such as entropy, ergodic, Markovian, etc. as these words can cause antagonisms."

The present *Dissertation* is dedicated to these fine and brave people; to the mathematicians, physicists and engineers who became Earth scientists.

Thanks and acknowledgments are due to my late Professors, Pál Turán who trained me as pure mathematician, and Alfréd Rényi who turned me to Applied Mathematics (he asked me: "Do you want to deal all your life with equations, or with people?").

My work has been partly supported, for many years, by the *King Abdulaziz City for Science and Technology*, Saudi Arabia, through their several projects in the *National Science Technology Innovation Plan*. I am also grateful for the financial support from the Project no. 168638 *SENERCONACYT-Hidrocarburos Yacimiento Petrolero como un Reactor Fractal* which enabled me to visit and work with the Research Group of Professor Oleschhko in Juriquilla, Querétaro, Mexico. I am grateful for *Saudi Aramco* (Dhahran, Saudi Arabia) for their support and the core samples, and the *King Fahd University of Petroleum and Minerals* (*KFUPM*, Dhahran, Saudi Arabia), my home Institution for almost 25 years.

Thanks are due to my former partners in Research, Drs. Klavdia Oleschko, Nabil Akbar, Saleh Saner, Ahmed Mohiuddin, Abdulazeez Abdulraheem, and to all my dear students whom I gave a hard time by including mathematical derivations in my *Geophysics* lectures, especially to those who became my graduate students and even co-authors[3].

Budapest, 31st of March, 2020

---

[1] Korvin, G. 1992a. *Fractal Models in the Earth Sciences*. Amsterdam: Elsevier.
[2] Dowds, J.P. 1969. Oil rocks: Information theory: Markov chains: Entropy. *Quart. Col. Sch. Mines* 64: 275-293.
[3] In *Appendix 4* I list my papers co-authored by my students.

## 1. INTRODUCTION

“I KEEP six honest serving-men
(They taught me all I knew);
Their names are What and Why and When
And How and Where and Who.”
(Kipling: I Keep Six Honest Serving Men)

### 1.A. MY RESEARCH METHODOLOGY. A CASE HISTORY


On door # 269, my office for 24 years at the *Earth Sciences Department* of the *King Fahd University for Petroleum and Minerals* (Dhahran, Saudi Arabia), I placed two short mottos, very much loved by my students, not so much by my different Chairmen, who frequently asked me to “immediately remove them”. The “Laugh at your problems …”, that I bought at a Novelty Gift Store at Surfers Paradise, Queensland, expressed (and still does) my personal attitude; the other, that I learned from an American experimental physicist friend of mine, expressed (and still does) how I did research. Research, for me, involves exploring an unknown territory, *terra incognita*, with a hope and firm belief, that at the end something will come up, that the data – as all my research had been based on measured geophysical or petrophysical data that I considered *sacrosanct* – would reveal their hidden pattern and help me find the laws of nature what they express.

Galileo Galilei is attributed with the saying, "Mathematics is the language in which God has written the universe." Actually the quote paraphrases his words in *Opere Il Saggiatore*: "[The universe] cannot be read until we have learnt the language and become familiar with the characters in which it is written. It is written in mathematical language, and the letters are triangles, circles and other geometrical figures, without which it is humanly impossible to comprehend a single word." (My late professor, Alfred Rényi, wrote a beautiful Galilean dialogue on this[4]). I subscribe to this view, and can only add that the more complicated a geophysical process, the more complex are its measured data series, and this increased complexity would require advanced mathematical tools, rather than "triangles, circles and other geometrical figures" to encode their hidden message.

I illustrate my philosophy of research on a simple problem (unpublished), which I came across around 2010 when, as consultant to a large Mexican Oil Company, I tried to explain the strange "staircase like" signals observed on *pressure build-up curves* measured in offshore boreholes through carbonate deposits, and to decide, are they just instrument noise, or do they carry geologically meaningful information[5]. Figure 1 shows the *measured data* (Ku-42), and some similar pressure build-up curves from my previous experience, containing similar DS ( = *Devil's Staircase*) signals.

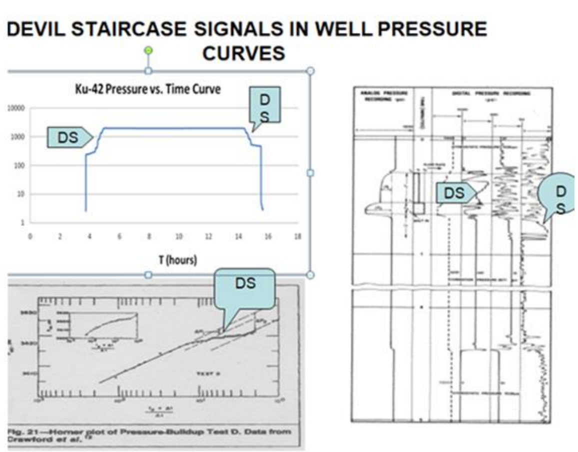


[4] Alfréd Rényi 1967. *Dialogues on Mathematics*. San Francisco: Holden-Day, Inc.

[5] Financial Support, and data, from the Project #168638 SENERCONACYT *Hidrocarburos Yacimiento Petrolero como un Reactor Fractal* are gratefully acknowledged.

Fig.1. a-c. DS (Devil's Staircase) signals, a) - on the pressure buildup curve measured in the Ku-42 borehole (offshore Mexico), b) – Horner plot of a Pressure Build-up Test, and c) – a Schlumberger *RFT* (*Repeated Formation Tester*) pressure log.

I followed, as always, *heuristic steps* to solve the problem:

*Step 1.* First I always ask myself the basic question of *heuristics*[6]: "Does the problem remind you of something from previous readings and studies?". *Yes*, these signals did remind me of the *Devil's Staircase signal which I* came across in *mathematics*, where *DS* is defined as integral of the *Cantor set*; and in *physics* where it described the development of magnetization of spin systems in an increasing external magnetic field[7].

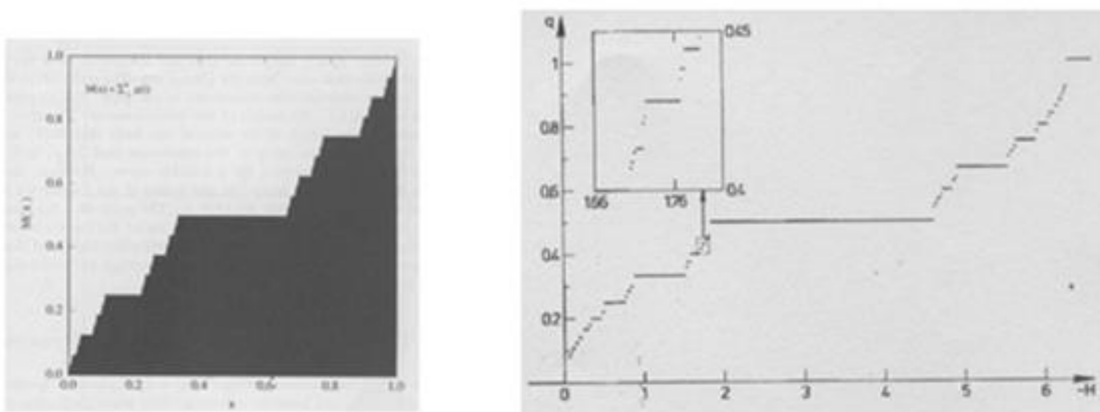

Fig, 2. A. *Devil's Staircase* as (a) integral of a random *Cantor set*, and (b) magnetization of a 1-D Ising spin system in an increasing external magnetic field. (From Bak and Bruisma, 1982).

I checked the self-similarity of these signals at different magnifications (Fig. 3):

[6] G. Polya, *How to Solve It*, 2nd ed., Princeton University Press, 1957.
[7] P. Bak, R. Bruisma: One-dimensional Ising model and the complete Devil's staircase. *Phys. Rev. Let.*, 49 (1982): 249-251.


Fig. 3 The Ku-42 pressure build-up curve at different magnifications.

*Step 2*. In mathematics, the *Devil's Staircase* occurs in the evolution of dynamic quantities over some fractal set, a *Cantor bar, Sierpinski Carpet* or *Menger Sponge*. I made outcrop and microscopic studies to check whether carbonate rocks can indeed be described by such fractal models?

**STRANGE FRACTAL PHENOMENA IN PRESSURE TRANSIENT ANALYSIS**

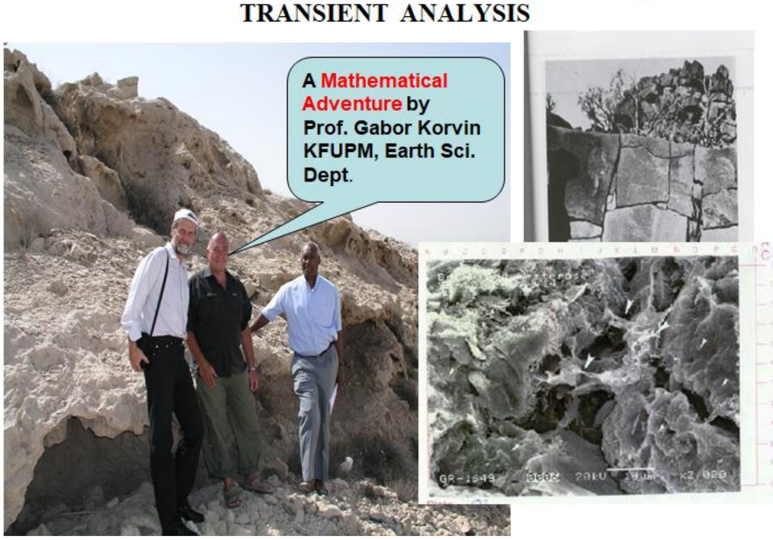


Fig.4. On the left, Dr. Korvin (in black shirt) with Colleagues at a carbonate outcrop (in Dhahran, Saudi Arabia). On the right, closer view of the outcrop, and SEM image of a sample.

I found that *yes*, vugular carbonates look similar at the outcrop, hand-specimen, and SEM (Scanninng Electron Microscopy) scales, that is, they are *fractal*, and they resemble reasonably well the *Menger Sponge* construction. (Figs. 4 & 5).

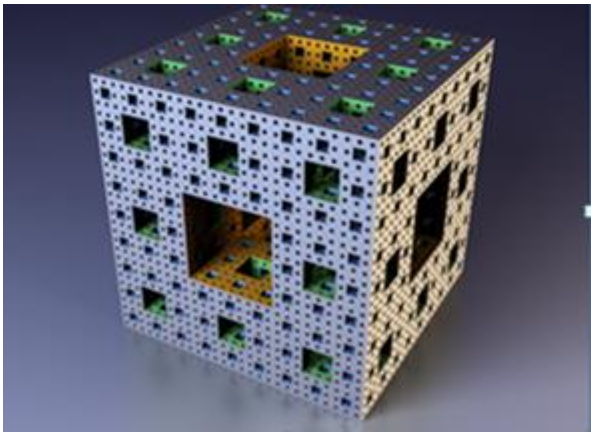
Fig. 5. The Menger Sponge[8]

*Step 3*. But what are the *physical processes* that could lead to DS-like signals in the pressure build-up curves? In our case I found two, physicaly plausible, models, described by different PDFs (partial differential equations). The first suggests to take the

## PRESSURE EQUILIBRATION APPROACH

**Basic assumption: Every step of the DS corresponds to a pressure equilibration between adjacent domains.**

$$\frac{\partial P}{\partial t} = \frac{k}{\Phi \mu c_t} \frac{\partial^2 P}{\partial x^2}$$

*Consider two adjacent domains D1 and D2 of the reservoir, of respective volumes V1 and V2, which are at time t=0 at pressures P1 and P2. Suppose the two volumes (that can be two fractures, two vugs, a vug and a fracture, two blocks of porous matrices, etc.) are in contact with each other. After pressure equilibration, what will be the common equilibrium pressure, and the characteristic time scale t after which equilibrium will be reached?*

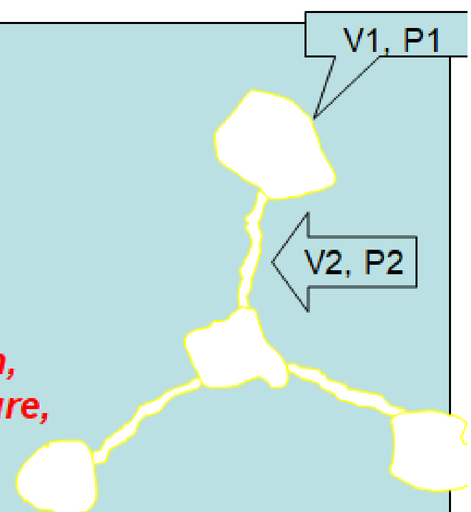


SOLVING THIS PROBLEM BY DIFFUSION EQUATION ESTABLISHES A TRANSFORM BETWEEN DS STEP SIZES t & DOMAIN SIZES x.

---

[8] Korvin, G. *Fractal Models in the Earth Sciences*. Amsterdam: Elsevier 1992: 93.

Fig. 6.a. Scheme of the *Pressure Equilibration* approach. The model of *connected compartments* on the right is similar to the *pore model* discussed in our 2014 paper.[9] In the PDE (diffusion equation): $P$ is pressure, $t$ time, $x$ is a spatial coordinate, $k$ permeability, $\Phi$ porosity, $\mu$ viscosity, $c_t$ total compressibility[10].

The second plausible physical model is the Washburn Equation[11] approach:

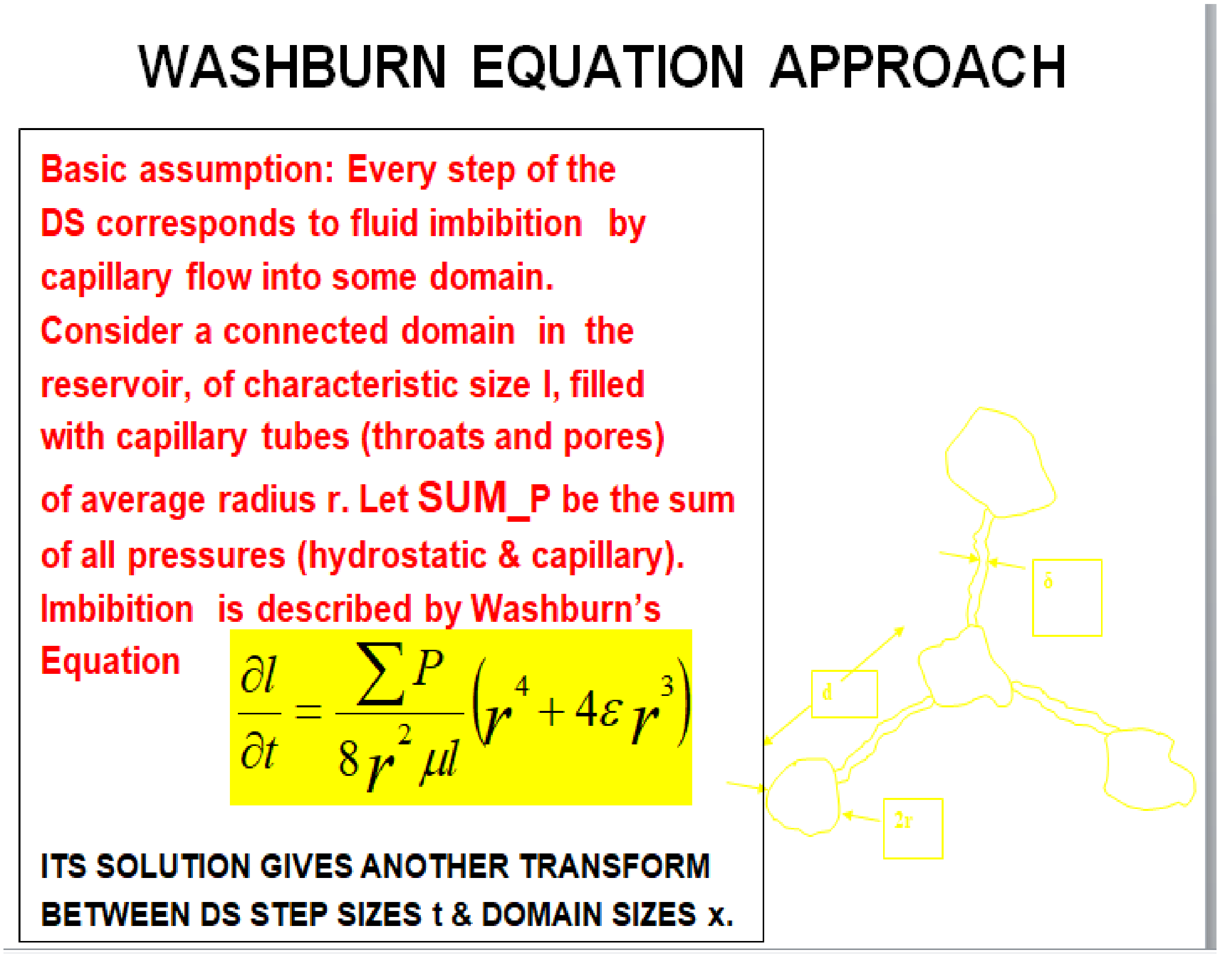


.

Fig. 6.b. Scheme of the *Washburn Equation* approach. In the PDE (Washburn equation) the total time $t$ of imbibition into a block of characteristic size $x$ satisfies $x^2 \approx \frac{\gamma D t}{4\mu}$ where $x$ [m] is block-size, $D$ [m] is throat diameter, $t$ [sec] is time, $\gamma$ [N/m] is surface tension, $\mu$ [Pa sec] is

---

[9] Korvin, G., Oleschko, K. & Abdulraheem, A. 'A simple geometric model of sedimentary rock to connect transfer and acoustic properties'. *Arabian Journal of Geosciences* 7(3)2014: 1127-1138.
[10] Doddy Abdassah & Iraj Ershaghi: Triple-porosity systems for representing naturally fractured reservoirs. *SPE Formation Evaluation*, April 1986, 113-127.
[11] Edward W. Washburn (1921). "The Dynamics of Capillary Flow". *Physical Review*. 17 (3): 273-283; F.A.L. Dullien: *Porous Media: Fluid Transport and Pore Structure*. Acad. Press, NY, 1979.

dynamic viscosity. I assumed[12] a value $\gamma = 0.035\ N\ m$ for the oil/water/grain system, and a viscosity $\mu = 2cp = 2\times10^{-3}\ Pa\ sec$ which was documented for this well.

*Step 4*. If there are more than one possible physical models to explain a phenomenon, *all of them must be used* and (*Step 5*) their results compared!

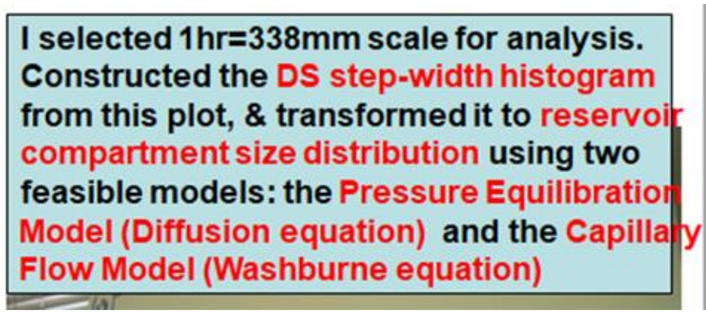


Fig. 7. Scheme of using the two models

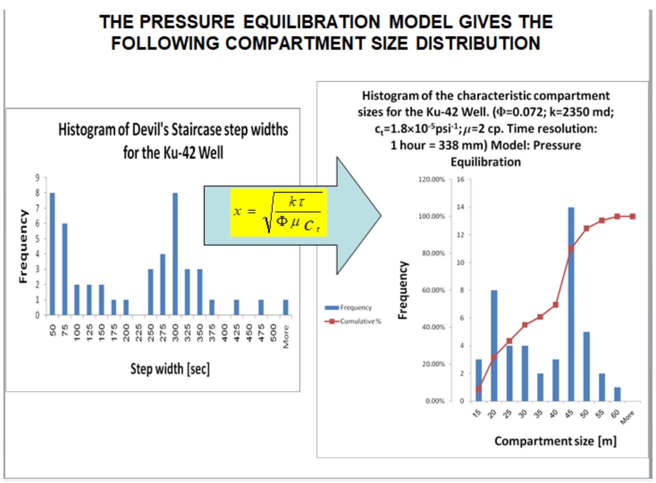


Fig.8.a. Compartment size histogram computed from the Devil's Staircase step durations, using the Pressure Equilibration model

[12] From C.L.Vavra, Kaldi, J.G. and Sneider, R.M. (1992). Capillary pressure. *In*: *Development Geology Manual*. AAPG Methods in Exploration Series No. 10, Tulsa, OK.; Wayne M. Ahr: *Geology of Carbonate Reservoirs. The Identification, Description, and Characterization of Hydrocarbon Reservoirs in Carbonate Rocks*. John Wiley & Sons, Inc., Hoboken, NJ, 2008.

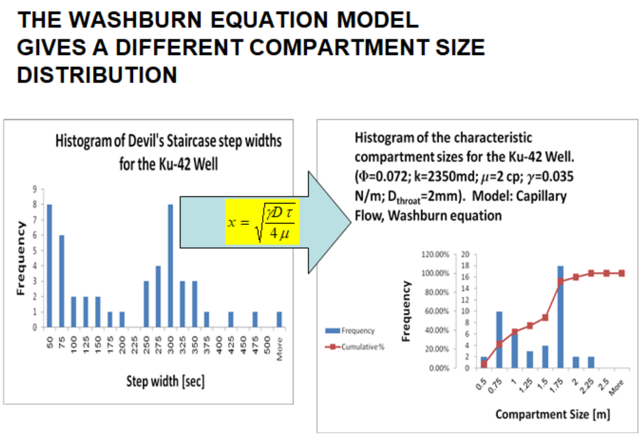


Fig.8.b. Compartment size histogram computed from the Devil's Staircase step durations, using the Washburn Equation model.

As we see in Figs. (8a-b), the results are very different! In the *Pressure Equilibration* model the median compartment size is $\approx 45m$, in the *Washburn Equation* model x ≈ 1.5m.

The respective compartment-size estimates are: $x = \sqrt{\frac{kt}{\Phi \mu c_t}}$ (Pressure Equilibration model), and $x = \sqrt{\frac{\gamma D t}{4\mu}}$ (Washburne Equation model). The Washburn model, which assumes non-vugular carbonate, leads to much smaller (by one magnitude smaller!) compartment sizes than the pressure equilibration model. In order to decide which of the two models should be used we need *independent information*. One way to get an independent estimate for the value of *D* (diameter of the communication channel between adjacent compartments) is to use Lucia's porosity-permeability plot (Fig. 9) for limestones and dolostones[13], where the parameters along the straight lines are the "throat" diameters. One can also use wire-log data including bore-hole wall imaging, or the Schlumberger *Z*-plot (total porosity – transit time plot, see Fig. 10) where carbonates with separate vugs will plot with a smaller slope than the non-vuggy compact carbonates[14].

[13] F. Jerry Lucia: *Carbonate Reservoir Characterization*. Springer, Berlin-Heidelberg, 1998.
[14] Lucia *op.cit.* p. 71.

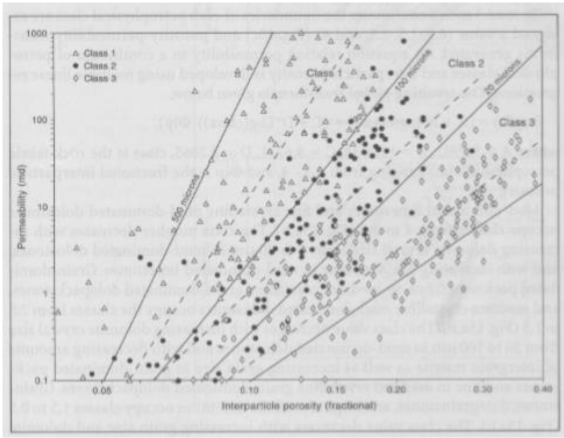


Fig.9

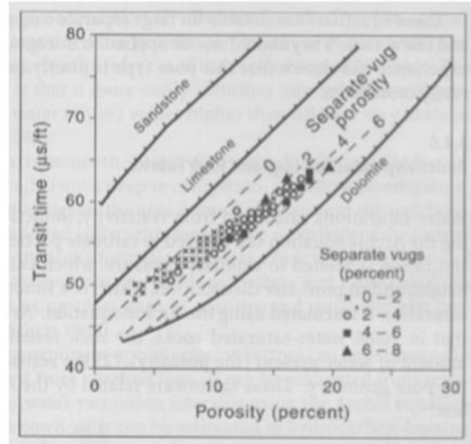


Fig. 10.

Fig, 9. Lucia's porosity-permeability plot. The parameters along the straight lines are the diameters of the channels connecting adjacent compartments.

Fig. 10. Schlumberger Z-plot. Vuggy carbonates plot with a smaller slope than the non-vuggy compact carbonates

The basic rule in all my works had been: "*Devil is in the details*". Watch out for the small details! In this case history, I noticed a small detail, the small oscillations on the pressure buildup curves which were *signals, not noise*!

1.B. HOW DID I USE THESE HEURISTIC STEPS IN MY WORKS?

1.B.1. "SELECT THE PROPER MATHEMATICAL APPARATUS!"

In my works, I used many modern tools of applied and theoretical mathematics, such as:

> Calculus of Variation; Campbell's Theorems (Poisson processes); Differential geometry; Fractal geometry; Homogenization Methods; Hunt's theorem (Weierstrass function); Information Theory; Integral geometry; Invariant Imbedding; Means and their inequalities; Multifractal measures; Random fields; Random graphs; Stochastic differential equations; Toeplitz Forms.

1.B.2. "SELECT A PHYSICAL PROCESS FOR MODELING THE PROBLEM!"

I have found powerful analogies in the following fields of Physics to model the problem at hand:

> Effective Medium approximations; Electrodynamics; Fluid Transport; Geodynamics; Hydrodynamics; Mechanics of Granular Bodies; Percolation Theory; Phase transitions; Radiophysics; Rock Physics; Statistical Physics;Theory of Elasicity; Turbulence; Wave Propagation.

## 1.B.3. "MAKE FIELD EXPERIMENTS, LABORATORY-, OUTCROP AND/OR MICROSCOPIC STUDIES!"

I had twenty-eight (28) theoretical studies, but most of my works were based on field experiments, laboratory-, outcrop and/or microscopic measurements. Whenever possible, my theoretical results were also checked against published measured data[15]. Sources for my papers had been:

> Laboratory Rock Physics measurements (in 9 studies); *GPR* Field work (in 7 studies), Microscopy (in 7 studies); Reflection Seismic data (in 6 studies); Outcrop study (in 3 studies); Well log data (in 3 studies); Seismic field experiment (in 2 studies); Remote sensing data (in 2 studies); Aerial photographs (in 2 studies); Published Rock. Phys. data (in 1 study); Meteorological data (in 1 study); Measured soil physics data (in 1 study); Published agricultural data (in 1 study); Geographical data (in 1study); Gravity and aeromagnetic anomaly maps (in 1 study).

[15] As e.g. the theory developed in Korvin, G. 1983b. 'General theorem on mean wave attenuation'. *Geophysical Transactions* 29(3):191-202 (awarded by the *Best Technical Paper of the Year* by the *Hungarian Geophysicists' Association*) was used to explain *measured seismological data* (of Aki 1980).

## 1.B.4. "USE ALL PLAUSIBLE MODELS!"

If there were more than one plausible physical models explaining or describing the measured data, I always used all of them simultaneously, and checked their different answers.

In my 1992 book[16], when treating the *RNG* (*Renormalization Group*) approach to the *bond percolation problem on the square lattice,* I mentioned that Madden's upscaling model leads to the correct critical percolation probability $p_c=0.5$ , while the Young and Stinchcombe model yields $p_c=0.618$. On pp. 210-215, treating the *RNG* approach to rock damage, I point out that the upscaling rule of Allègre et al. leads to a critical probability $p_c=0.5896$, while a slightly different upscaling by Turcotte gives $p_c=0.49$.

In an experimental study[17] of my group we pointed out that the permeability model of the Russian Mosolov and Dinaryev gives the permeability – porosity law $k \propto \phi^{2/(3-D)}$ where *k* is permeability, *D* is fractal dimension of the pore surface, while the model of the German researchers Pape *et al.* would yield $k \propto \phi^{(D-1)/(3-D)}$ . In the study we used *both* models to estimate the fractal dimension of the pore surface from the experimental data[18]. (See *op.cit*. Tables I. & II, and Figs. 6 & 7).

In the (unpublished) *Introductory Case History* of this Dissertation there are (at least) two different physical phenomena which could be used to explain the *Devil's Staircase* signals on the pressure up-build record: the *Pressure Equilibration Model* and the *Washburn Equation Model* (Figs. 6.a&b), and they lead to different results (Figs. 8.a & b)

## 1.B.5. MY GOLDEN RULE: "WATCH OUT FOR THE DETAILS!"

My tortuous road to *fractals* started in early 1970s, in ELGI, the legendary Eötvös Lóránd Geophysical Institute. As a budding applied mathematician and seismic programmer, I was honored to be asked by my older Colleagues, Tamás Bodoky, Lóránd Sédy, János Lányi, István Rákóczy and István Liptai to interpret - physically and mathematically - and write up in a nice English-language paper, their 2-years-long series of field experiments (1968-1969, in a near-surface sandy complex of the *Nyírség Region*) aiming to find the basic characteristics of the seismic signal generated by underground explosions[19]. I was very much puzzled by one of the results, namely the dependence of the seismic amplitude *A* (corrected for spherical divergence), on charge weight *C* (Fig. 12, from Bodoky et al. 1971).

---

[16] Korvin 1992a: 23-27.
[17] Korvin et al. 2001.
[18] Korvin et al. 2001: Tables I. & II, and Figs. 6 & 7.
[19] Bodoky, T., Korvin, G., Liptai, I. & Sipos, J. 'An analysis of the initial seismic pulse near underground explosions'. *Geophysical Transactions* 21(3-4)1971: 7-26.

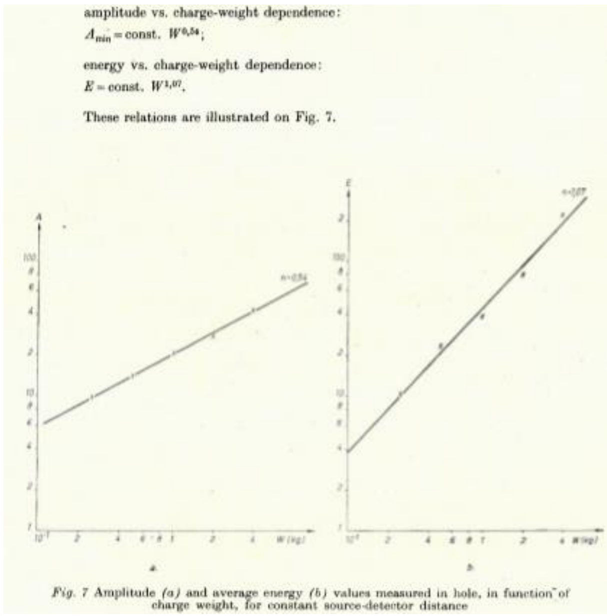


Fig. 12.

The measured data, plotted on double-logarithmic graph paper, perfectly fitted the rule $A \propto C^{0.54}$ what I found strange (*a small detail*!). O'Brien (1960) found experimentally $A \propto C^{2/3}$ and I expected the same from dimensional arguments, because a (spherical) charge $C$ has the linear size $\propto C^{1/3}$, it will create a spherical cavity whose size is also proportional to $C^{1/3}$ , the equivalent radiator's surface around it is proportional to $C^{2/3}$, and – by the integral form of Huyghen's principle – the spherical-divergence-corrected seismic amplitude will also be proportional to $C^{2/3}$. How could we obtain $A \propto C^{0.54}$ ? There are two possible reasons: *a)* the source was not spherical, but consisted of $N$ pieces of dynamite sticks of diameter *2r* and length *l*; *b)* or only a part of the surface of the equivalent radiator of radius $R_{eq}$ whose area S scaled as $S \propto R_{eq}^{1.62}$ radiated coherent seismic energy. (Note, "1.62" enters as surface dimension instead of the theoretical "2" in $A \propto C^{2/3}$ ). Case a) can be excluded, because in the experiment the charge weight was varied by using $N$ dynamite sticks, that is $C$ increased as $C = N \times r^2 \pi l \propto N$, that is by theory $R_{eq} \propto C^{1/3}$ and $A \propto C^{2/3}$. The remaining possibility is that only a *1.62-dimensional* part of the equivalent radiator is emitting coherent seismic energy. In 1972 Mandelbrot's *Fractals: Form, Chance and Dimension* (1st Edition), then his *The Fractal Geometry of Nature* (1982) came out – reading them, I understood that the explosive-generated cavity had a rough surface, and only a 1.62-dimensional part of it contributed to the coherent seismic energy. By noting this small detail ($A \propto C^{0.54}$ instead of $A \propto C^{2/3}$) helped me to find (one) niche for my further studies, *fractals*. In 1992 my book on *fractals* appeared, followed by 20 papers on their diverse applications, some of them co-authored by Saudi Arabian and Mexican students and Colleagues. I must add, that I could only notice this *small detail*, because that time (1971) we still plotted and interpreted graphs, such as those on Fig. 12, *manually*, and in this process the data points have become personal friends, *they talked to me*!

## 2. MY MAIN FIELDS OF RESEARCH

Apart from my studies in history, linguistics, pure mathematics, etc., which are outside this *Doctoral Dissertation* (but are included in my *List of Publications*), and not mentioning my Seminar- and Conference talks, my research has focused on seven fields: *Wave propagation in random media; Entropy; Mean-field rock physics; Fractals; Petrophysics of porous rocks; Seismic Processing*, and *Geodynamics.* Only the first five will be summarized in what follows.

### #1: Wave propagation in random media

Example: Korvin, G. 'Is the optical image of a non-Lambertian fractal surface fractal?' *IEEE Geoscience and Remote Sensing Letters* 2(4)2005:380-383. (*Paper submitted together with my Dissertation*). Other related papers: Korvin et al. 2017; Adetunji et al. 2008; Oleschko et al. 2008; Korvin & Oleschko 2004; Al-Ali et al, 2003; Oleschko et al. 2003; Oleschko et al. 2002; Mohiuddin et al. 2001; Korvin 1985; Korvin1983b; Korvin1982b; Korvin & Armstrong1981; Korvin 1980; Korvin1978b; Korvin 1977 &1978; Korvin 1977; Korvin 1973; Bodoky et al. 1971.

### #2. Entropy

Example: Korvin, G. 'Shale compaction and statistical physics'. *Geophysical Journal – Royal Astronomical Society* 78 (1)1984: 35-50. (*Paper submitted together with my Dissertation*). Other related papers: Korvin. 2020d; Islam el-Deek et al. 2017; Korvin et al. 2013; Korvin. 2009; Oleschko et al. 2004; Korvin 2000.

### #3. Mean-field rock physics

Example: Korvin, G. 'Axiomatic characterization of the general mixture rule'. *Geoexploration* 19(4)1982: 267-276. (*Paper submitted together with my Dissertation*). Other related papers: Korvin 2012; Korvin1978.

### #4. Fractals

Examples: Korvin, G. 'Fractured but not fractal: Fragmentation of the Gulf of Suez basement'. *Pure and Applied Geophysics PAGEOPH* 131(1-2)1989: 289-305. (*Paper submitted together with my Dissertation*); Korvin, G. *Fractal Models in the Earth Sciences*. Amsterdam: Elsevier 1992. (*Book submitted together with my Dissertation*). Other related papers: Arizabalo et al. 2015; Velásquez Valle et al. 2013; Torres-Argüelles et al. 2011; Velázquez-García et al. 2010; Oleschko et al. 2010; Arizabalo et al. 2006; Nieto-Samaniego et al. 2005; Arizabalo et al. 2004; Hassan et al. 2002; Choudhury et al. 2002; Korvin et al. 2001; Korvin 1996; Korvin 1993.

### #5. Petrophysics of porous rocks

Example: G. Korvin. ‘Permeability from Microscopy: Review of a Dream’. *Arabian J. of Science & Engineering* 41(6)2016: 2045-2065. (*Paper submitted together with my Dissertation*). Other related papers: Minhas et al. 2016; Abdlmutalib et al. 2015; Korvin et al. 2014; Abdulraheem et al. 2007; Korvin. & Lux1972..

## 3. SHORT DESCRIPTIONS AND MAIN RESULTS

### 3.1. WAVE PROPAGATION IN RANDOM MEDIA

#### 3.1.A. STOCHASTIC PERTURBATION APPROACH

My research in this area relied on two modern tools of mathematics: *random- field theory*[20], and *perturbation theory of stochastic partial differential equations (PDFs)*[21], and used two important theorems: *Campbell's Theorem*[22] (applicable – as e.g. in Korvin 1978b - when the wave scatterers are *Poisson-distributed* in space) and *Hunt's Theorem*[23] (used - as e.g. in Oleschko et al. 2002 - when the wave scatterers are fractally distributed in space).

*Random fields* are generalizations of the random (or “stochastic”) functions along a line. A *random function*, $\{f(x)\}_\alpha$ is a family of functions depending on a random parameter $\alpha$, where the independent variable *x* varies along some line. A given *f(x)* picked at random from among all possible $\{f(x)\}_\alpha$-s is a *realization*. At some fixed pont of the line $x_1$, $f(x_1)$ is a *random value*, it attains different values *y* with the probabilities $Prob\ [f(x_1) < y] = F(x_1, y)$ . The following expected values[24] (taken with respect to α, i.e. over all realizations of $\{f(x)\}_\alpha$ ) are often enough to characterize a random function : $\langle f(x_1)\rangle$, $\langle f^2(x_1)\rangle$, $\langle f(x_1)\cdot f(x_2)\rangle$, termed *mean value*, *mean square value* and *autocorrelation function*. A random function is *translation invariant* if its statistical properties do not change with respect to a shift along the line, in particular, if $\langle f(x)\rangle = \langle f(0)\rangle$; $\langle f^2(x)\rangle = \langle f^2(0)\rangle$; $\langle f(x_1)\cdot f(x_2)\rangle = \langle f(0)\cdot f(x_2 - x_1)\rangle :=$ $R_{ff}(|x_1 - x_2|)$ where the function $R_{ff}$ is the *autocorrelation function* (*ACF*) of *f(x).* It is an *even function*, $R(\xi) = R(-\xi)$ . assumes its maximum at $\xi = 0$ , $R_{ff}(0) = \langle f^2(x)\rangle$. The *normalized autocorrelation function* is $\rho_{ff}(\xi) = R_{ff}(\xi)/\langle f^2(x)\rangle$.

If **x**(x,y) or **x***(x,y,z)* is point of the 2- resp. 3-dimensional Euclidean space, then $\{f(x,y)\}_\alpha$ resp. $\{f(x,y,z)\}_\alpha$ are called *random fields* over the plane or space, a given field f(**x**) picked out at random is a *realization* of the field.

---

[20] Chernov, L. A., 1960: *Wave Propagation in a Random Medium*. McGraw Hill, New York.
[21] Karal, F. C. Jr .-Keller , J. B., 1964: Elastic, electromagnetic and other waves in a random medium. *J. Math. Phys*. 5 No 4, pp 537-549; Keller, J. B., 1964: Stochastic equations and wave propagation in random media. *Proc. Symp. Appl. Math.* 16: 145-701.
[22] Rytov, S. M. 1966*: Introduction to Statistical Radiophysics*. Nauka, Moscow (In Russian).
[23] B.R. Hunt 1998. The Hausdorff dimension of graphs of Weierstrass functions . *Proc.Am.Math.Soc*.,126:791.
[24] The expected value of a quantity $\nu$ is denoted by $\bar{\nu}$ or $\langle \nu\rangle$ **.**

A random field is *homogeneous* if its statistical properties are invariant with respect to a shift, that is if $\langle f(\boldsymbol{x})\rangle$ and $\langle f^2(\boldsymbol{x})\rangle$ are constant, and the autocorrelation function only depends on the difference of **x** and **y** $\langle f(\boldsymbol{x})f(\boldsymbol{y})\rangle \coloneqq R_{ff}(\boldsymbol{x},\mathbf{y}) \equiv R_{ff}(\boldsymbol{x}-\mathbf{y})$. If the statistical properties of the field are also invariant with respect to rotations and reflections, we speak about an *homogeneous and isotropic random field*. In such a field the autocorrelation is a function of the magnitude of $\mathbf{x}-\boldsymbol{y}$: $\langle f(\boldsymbol{x})f(\boldsymbol{y})\rangle = R_{ff}(|\boldsymbol{x}-\mathbf{y}|)$. The autocorrelation function $R(r) = a^2 exp(-r/r_0)$, where $= \sqrt{[(x_1-y_1)^2+(x_2-y_2)^2+(z_1-z_2)^2]}$, belongs to an isotropic field, here $r_0$ is the *correlation distance,* it is that value of *r* for which the autocorrelation function decreases to $1/e$ times its value at $r = 0$.

The main ideas of *Keller's method of stochastic perturbations*[25] are as follows: Suppose the wave $u_0$ satisfies the linear equation $Lu_0 = 0$ (Eq.1). The operator is perturbed as

$L \to L - \varepsilon L_1(\gamma) - \varepsilon^2 L_2(\gamma) + O(\varepsilon^3)$ (Eq. 2)

where $\varepsilon, |\varepsilon \ll 1|$ is a measure of the strength of inhomogeneities of the medium, $L_1(\gamma)$ and $L_2(\gamma)$ are operators depending on the random variable $\gamma \in \Gamma$, of *pdf* (probability density function) $\rho(\gamma)$. Expectations with respect to $\rho(\gamma)$ are denoted as $\langle f\rangle = \int_\Gamma f(\gamma)\rho(\gamma)d\gamma$. The solution to the random equation

$[L - \varepsilon L_1(\gamma) - \varepsilon^2 L_2(\gamma) + O(\varepsilon^3)] = 0$ (Eq. 3)

is a random function of $\gamma$ . Let us try to find the *expected wave* $\langle u\rangle$. Suppose $L^{-1}$ exists and is bounded, then from Eqs. (1 & 3)

$u = u_0 + \varepsilon L^{-1}(L_1 + \varepsilon L_2) + O(\varepsilon^3)$ (Eq. 4).

Solving (Eq. 4) by *successive iterations*, we get:

$u = u_0 + \varepsilon L^{-1}L_1 u_0 + \varepsilon^2(L^{-1}L_1\,L^{-1} + L^{-1}L_2\,)u_0 + O(\varepsilon^3)$ (Eq.5)

Taking expectances, $\langle u\rangle = u_0 + \varepsilon L^{-1}\langle L_1\rangle u_0 + \varepsilon^2(L^{-1}\langle L_1 L^{-1} L_1\rangle + \langle L_2\rangle)u_0 + O(\varepsilon^3)$ (Eq.6). Solving for $u_0$ and substituting back to (Eq. 6):

$\langle u\rangle = u_0 + \varepsilon L^{-1}\langle L_1\rangle\langle u\rangle + \varepsilon^2 L^{-1}(\langle L_1\,L^{-1}L_1\rangle - \langle L_1\rangle L^{-1}\langle L_1\rangle + \langle L_2\rangle)u + O(\varepsilon^3)$ (Eq. 7). Applying L to both sides, dropping the $O(\varepsilon^3)$ term and assuming that $\langle L_1\rangle = 0$ , we get Keller's equation:

$(L - \varepsilon^2\langle L_1 L^{-1} L_1\rangle - \varepsilon^2\langle L_2\rangle)\langle u\rangle = 0$ (Eq. 8).

---

[25] Karal, F. C. J r . & Kelle r , J. B., 1964: Elastic, electromagnetic and other waves in a random medium. *J. Math. Phys*. 5 No 4: 537-549; Keller, J. B., 1964: Stochastic equations and wave propagation in random media. *Proc. Symp. Appl. Math.* 16: 145-170.

To apply (Eq. 8), we need to express the operator $\langle L_1 L^{-1} L_1 \rangle$. Denote by $I$ the unit operator, and by $\delta$ Dirac's delta function, and introduce the Green's function $G(\mathbf{x}, \boldsymbol{x}')$ defined as

$L \cdot G(\boldsymbol{x}, \boldsymbol{x}') = I \cdot \delta(\mathbf{x} - \boldsymbol{x}')$ . Then $L^{-1} f = \int G(\mathbf{x}, \mathbf{x}') f(\mathbf{x}') d\mathbf{x}'$, and in (Eq. 8) $\langle L_1 \, L^{-1} L_1 \rangle \langle u \rangle = L_1(\mathbf{x}) \int G(\boldsymbol{x}, \mathbf{x}') L_1\,(x') \langle u(x') \rangle \, d\boldsymbol{x}'$ . With this, Keller's (Eq. 8) becomes

$L(\mathbf{x})\langle u(\mathbf{x})\rangle$-$\varepsilon^2 \langle L_1(\mathbf{x})\rangle \int G(\mathbf{x}.x') L_1\,(\boldsymbol{x}') \langle u(x') dx' \rangle - \varepsilon^2 \langle L_2(\mathbf{x})\rangle \langle u(\mathbf{x})\rangle$=0 (Eq. 9 ).

In my studies I applied this equation for many random wave propagation problems, here I only summarize how I dealt with *plane wave propagation and scattering on 3-dimensional, and 1-dimensional velocity inhomogeneities.*[26] We begin with the (*x*-*f* domain) wave equation $\Delta u + \frac{\omega^2}{c^2} u = 0$ (Eq. 10), where the velocity distribution is given as a power series in terms of the small parameter $\varepsilon$: $c = c_0 + a\varepsilon + b\varepsilon^2 + O(\varepsilon^3)$ (Eq. 11). I used in my works three different velocity models[27]:

*Model 1*: $c(\mathbf{x}) = c_0(\mathbf{x}) + \varepsilon(\mathbf{x})$ (Eq. 12a)

*Model 2*: $c(\mathbf{x}) = c_0(\mathbf{x})[1 + \varepsilon(\mathbf{x})]$ (Eq. 12b)

*Model 3*: $c(\mathbf{x}) = \frac{c_0(\mathbf{x})}{1+\varepsilon(\mathbf{x})} = c_0(\mathbf{x}) - c_0(\mathbf{x})\varepsilon(\mathbf{x}) + c_0(\mathbf{x})\varepsilon^2(\mathbf{x}) + O(|\varepsilon|^3)$ (Eq. 12c)

Matching Eqs. (12.a-c) with the general form (Eq. 11), the coefficients *a, b* are:

| Model # | Velocity Model | a | b | Eq. # |
|---|---|---|---|---|
| Model 1. | $c(\mathbf{x}) = c_0(\mathbf{x}) + \varepsilon(\mathbf{x})$ | 1 | 0 | 13a |
| Model 2. | $c(\mathbf{x}) = c_0(\mathbf{x})[1 + \varepsilon(\mathbf{x})]$ | $c_0(\mathbf{x})$ | 0 | 13b |
| Model 3. | $c(\mathbf{x}) = \frac{c_0(\mathbf{x})}{1 + \varepsilon(\mathbf{x})}$ $=c_0(\mathbf{x}) - c_0(\mathbf{x})\varepsilon(\mathbf{x}) + c_0(\mathbf{x})\varepsilon^2(\mathbf{x}) + O(\lvert\varepsilon\rvert^3)$ | $c_0(\mathbf{x})$ | $c_0(\mathbf{x})$ | 13c |

Introducing the average wave-number $k_0 = \omega / c_0$ , expanding $\omega^2/c^2$ into a power series in $\varepsilon$ and dropping $O(\varepsilon^3)$ terms, the wave equation becomes:

[26] Korvin, G. 1977. 'Certain problems of seismic and ultrasonic wave propagation in a medium with inhomogeneities of random distribution. II. Wave attenuation and scattering on random inhomogeneities'. *Geophysical Transactions* 24(Supplement 2): 1-38.
[27] These were introduced in Eqs. (25.a, b, c) in Korvin, G. 'Certain problems of seismic and ultrasonic wave propagation in a medium with inhomogeneities of random distribution.' *Geophysical Transactions* 21(1973): 5-34.

$\Delta u(\mathbf{x}) + k_0^2[1 + \gamma_1\varepsilon(\mathbf{x}) + \gamma_2\varepsilon^2(\mathbf{x})]u(\mathbf{x}) = \Delta u(\mathbf{x}) + k_0^2[1 + \gamma_1\varepsilon \cdot \mu(\mathbf{x}) + \gamma_2\varepsilon^2 \cdot \mu^2(\mathbf{x})] = 0$ (Eq. 14), where we introduced the normalized random variable $\mu(\mathbf{x}) = \varepsilon(\mathbf{x})/\sqrt{\langle\varepsilon^2(\mathbf{x})\rangle} = \varepsilon(\mathbf{x})/\varepsilon$ (Eq. 15), and the coefficients $\gamma_1$ and $\gamma_2$ are, in case of the three velocity models:

| Model # | Velocity Model | $\gamma_1$ | $\gamma_2$ | Eq. # |
|---|---|---|---|---|
| Model 1. | $c(\mathbf{x}) = c_0(\mathbf{x}) + \varepsilon(\mathbf{x})$ | $-2/c_0$ | $3/c_0^2$ | 16a |
| Model 2. | $c(\mathbf{x}) = c_0(\mathbf{x})[1 + \varepsilon(\mathbf{x})]$ | -2 | 3 | 16b |
| Model 3. | $c(\mathbf{x}) = \dfrac{c_0(\mathbf{x})}{1 + \varepsilon(\mathbf{x})}$ $= c_0(\mathbf{x}) - c_0(\mathbf{x})\varepsilon(\mathbf{x}) + c_0(\mathbf{x})\varepsilon^2(\mathbf{x}) + O(\lvert\varepsilon\rvert^3)$ | 2 | 1 | 16c |

Comparing Eq. (14) with Eq. (2) we identify the operators as

$$\left.\begin{aligned} L &= \Delta + k_0^2 \\ L_1 &= -\gamma_1 k_0^2 \mu(\mathbf{x}) \\ L_2 &= -\gamma_2 k_0^2 \mu^2(\mathbf{x}) \end{aligned}\right\} \qquad \text{(Eq. 17)}$$

Obviously, $\langle L_1\rangle = 0$, $\langle\mu^2(\mathbf{x})\rangle = 1$. Denote the autocorrelation function (*ACF*) of $\mu(\mathbf{x})$ by $N(\mathbf{x}, \mathbf{x}') = \langle\mu(\mathbf{x})\mu(\mathbf{x}')\rangle$ (Eq. 18). The Green function is $G(\mathbf{x}, \mathbf{x}') = -\frac{exp[ik_0|\mathbf{x}-\mathbf{x}'|]}{4\pi|\mathbf{x}-\mathbf{x}'|}$ (Eq.19). In case of *homogeneous isotropic random velocity fields* $N(\mathbf{x}, \mathbf{x}') = \langle\mu(\mathbf{x})\mu(\mathbf{x}')\rangle = N(r)$ (Eq. 20), where $r = |\boldsymbol{r}|$, and Eq. (9) becomes:

$$(\Delta + k_0^2 + \varepsilon^2\gamma_2 k_0^2)\langle u(\mathbf{x})\rangle + \frac{\varepsilon^2\gamma_1^2 k_0^4}{4\pi}\int \frac{exp[ik_0 r]}{r} N(r)\langle u(\mathbf{x}+\mathbf{r})\rangle d\mathbf{r} = 0 \quad \text{(Eq. 21)}$$

Solutions to Eq. (21) are sought for in the *plane-wave* form: $\langle u(\mathbf{x})\rangle = A \cdot \exp[i\mathbf{kx}] = \varphi(\mathbf{x})$ (Eq. 22). To find the volume-integral in Eq. (21), we first integrate over the spherical surface S of radius *r*, centered at **x**. By the mean-value theorem[28] for any solution of the wave equation one has

$\frac{1}{4\pi r^2}\int_S \varphi(\mathbf{x}+\mathbf{r})\, dS = \frac{\sin(kr)}{kr} \cdot \varphi(\mathbf{x})$ (Eq. 23), and from Eq. (21):

$$\left(\Delta + k_0^2 + \varepsilon^2\gamma_2 k_0^2 + \varepsilon^2\frac{k_0^4}{k}\gamma_1^2\int_0^\infty exp[ik_0 r] \cdot \sin(kr) \cdot N(r)dr\right)\varphi(\mathbf{x}) = 0 \qquad \text{(Eq. 24).}$$

Since the plane wave $\varphi$, defined by Eq. (22), evidently satisfies the wave equation

$(\Delta + k^2)\varphi(\mathbf{x}) = 0$ (Eq. 25), we obtain, equating Eqs. (24 and 25), the *dispersion relation*

---

[28] Keller, J. B., 1964: Stochastic equations and wave propagation in random media. *Proc. Symp. Appl. Math*. 16: 145-701.

$$k^2 = k_0^2 + \varepsilon^2\gamma_2 k_0^2 + \varepsilon^2 \frac{k_0^4}{k}\gamma_1^2 \int_0^\infty exp[ik_0 r]\cdot \sin(kr)\cdot N(r)dr, \qquad \text{(Eq. 26)}$$

which is an equation for k. Its solution is the *effective wave-number*, expressing the *global effect* of the inhomogeneous medium. Solving Eq. (26) in powers of $\varepsilon$ (by *successive iterations*), we obtain $\frac{k^2}{k_0^2} \approx 1 + \varepsilon^2\gamma_2 + \frac{\varepsilon^2}{2} k_0\gamma_1^2 \int_0^\infty \sin(2k_0 r)\, N(r)dr - \frac{i}{2}\varepsilon^2 k_0\gamma_1^2 \int_0^\infty [\cos(2k_0 r) - 1]N(r)dr$ (Eq. 27). The imaginary part of $k$ is the attenuation coefficient,

$$\alpha = \frac{\varepsilon^2\,\gamma_1^2 k_0^2}{4}\int_0^\infty (1 - \cos(2k_0 r))\, N(r)dr \qquad \text{(Eq.28).}$$

Denoting the integral in Eq. (28) by $I_\sim^3(k_0)$ (where "3" refers to *3-dimensional* velocity inhomogeneities), and making use of Eqs. (16a-c), the respective values of $\alpha$ for the velocity models (12a, b, c) are:

$$\left.\begin{aligned} \alpha &= \left(\frac{\varepsilon^2}{c_0^2}\right) I_\sim^3(k_0) \\ \alpha &= \varepsilon^2 k_0^2\, I_\sim^3(k_0) \\ \alpha &= \varepsilon^2 k_0^2\, I_\sim^3(k_0) \end{aligned}\right\} \qquad \text{Eqs. (29a-c)}$$

| Model # | Velocity Model (Eqs. 12a-c) | $\gamma_1$ | $\gamma_2$ | Eq. # | $\alpha$ | Eq. # |
|---|---|---|---|---|---|---|
| Model 1. | $c(\mathbf{x}) = c_0(\mathbf{x}) + \varepsilon(\mathbf{x})$ | $-2/c_0$ | $3/c_0^2$ | 16a | $\left(\frac{\varepsilon^2}{c_0^2}\right) I_\sim^3(k_0$ | 29a |
| Model 2. | $c(\mathbf{x}) = c_0(\mathbf{x})[1 + \varepsilon(\mathbf{x})]$ | -2 | 3 | 16b | $\varepsilon^2 k_0^2\, I_\sim^3(k_0)$ | 29b |
| Model 3. | $c(\mathbf{x}) = \frac{c_0(\mathbf{x})}{1+\varepsilon(\mathbf{x})}$ $=c_0(\mathbf{x}) - c_0(\mathbf{x})\varepsilon(\mathbf{x}) + c_0(\mathbf{x})\varepsilon^2(\mathbf{x})$ $+O(\lvert\varepsilon\rvert^3)$ | 2 | 1 | 16c | $\varepsilon^2 k_0^2\, I_\sim^3(k_0)$ | 29c |

The special case (29c) has also been derived by Chernov (1960) and Karal and Keller (1964). For some frequently occurring autocorrelation functions the integral $I_\sim^3(k_0)$ can be easily computed using tabulated formulae of integration:

| Autocorrelation function | Eqn.# | $I^{3}(k_0)$ | Eq. # |
|---|---|---|---|
| $N_1\,(r) = \exp(-r/r_0)$ | 30 | $I_1^{3}(k_0) = \frac{4\, r_0^3 k_0^2}{1 + 4\, r_0^2 k_0^2}$ | 31 |
| $N_2\,(r) = \exp(-r^2/r_0^2\,)$ | 32 | $I_2^{3}(k_0) = \frac{\sqrt{\pi}}{2} r_0(1 - exp[-r_0^2 k_0^2])$ | 33 |
| $N_3\,(r) = \begin{cases} \frac{1}{d}(d - \lvert r \rvert) & if \quad \lvert r \rvert < d \\ 0 & if \quad \lvert r \rvert \geq d \end{cases}$ | 34 | $I_3^{3}(k_0) = \frac{d}{2}\left[1 - \left(\frac{\sin k_0 d}{k_0 d}\right)^2\right]$ | 35 |

The case of *one-dimensional velocity inhomogeneities* can be similarly dealt with[29]. Instead of isotropy, we assume that $\mu$ is stationary, with normalized *ACF N(r).* In the *1-D* case the *dispersion relation* is (instead of Eq. 26)

$k^2 = k_0^2 + \varepsilon^2\gamma_2 k_0^2 + i\varepsilon^2\gamma_1^2 k_0^3 \int_0^\infty exp[ik_0 r] \cdot \cos(kr) \cdot N(r)dr$ (Eq. 36), its solution to first approximation is $\frac{k^2}{k_0^2} \approx 1 + \varepsilon^2\gamma_2 + \frac{i\varepsilon^2\gamma_1^2 k_0}{2} \int_0^\infty (1 + \exp(2ik_0 r))\, N(r)dr$ (Eq. 37), that yields $\alpha = Im\ k \approx \frac{\varepsilon^2\gamma_1^2 k_0^2}{4} \int_0^\infty (1 + \cos 2k_0 r)\, N(r)dr$ (Eq. 38).

For the ACFs $N_1$, $N_2$, and $N_3$ (Eqs. 30, 32, 34) the integral in Eq. (38) can be evaluated as:

$I_1^{1}(k_0) = \frac{2\, r_0 + 4r_0^3 k_0^2}{1 + 4r_0^2 k_0^2}$ (Eq. 39-1)

$I_2^{1}(k_0) = \frac{\sqrt{\pi}}{2}(1 + exp[-\, k_0^2/r_0^2])$ (Eq. 39-2)

$I_3^{1}(k_0) = \frac{d}{2}\left(1 + \left[\frac{\sin k_0 d}{\sin k_0 d}\right]^2\right)$ (Eq. 39-3)

In the low-frequency limit ( $k_0 \ll 1$) we have

$I_1^{3}(k_0), I_2^{3}(k_0), I_3^{3}(k_0) = O(k_0^2);\ I_1^{1}(k_0), I_2^{1}(k_0), I_3^{1}(k_0) = O(1)$ (Eq. 40)

that is, in words: if the wave-length is much *longer than the characteristic size of the inhomogeneities* (low-frequency limit) the attenuation is proportional to $k_0^4$ in case of 3-

[29] See Korvin, G. 1977. 'Certain problems of seismic and ultrasonic wave propagation in a medium with inhomogeneities of random distribution. II. Wave attenuation and scattering on random inhomogeneities'. *Geophysical Transactions* 24(Supplement 2): 1-38, Section 3 (pp. 7-9).

dimensional velocity inhomogeneities (*Rayleigh scattering*). In case of l-dimensional velocity inhomogeneities the attenuation is proportional to $k_0^2$.

Let us now study the *high-frequency behaviour of the absorption coefficient* in case of 3-dimensional velocity-inhomogeneities. We start from the dispersion relation:

$$k^2 = k_0^2 + \varepsilon^2\gamma_2 k_0^2 + \varepsilon^2 \frac{k_0^4}{k}\gamma_1^2 \int_0^\infty exp[ik_0 r]\cdot \sin(kr)\cdot N(r)dr, \quad \text{(Eq. 26)}$$

For the autocorrelation function $N_1\,(r) = \exp(-r/r_0)$ the integral in Eq. (26) can be evaluated, and the first iteration step gives[30] for *k*:

$$k^2 = k_0^2 + \varepsilon^2\gamma_2 k_0^2 - \frac{\varepsilon^2}{2} i k_0^3 \gamma_1^2 \left\{\frac{1}{r^{-1}-2ik_0} - r_0\right\} \qquad \text{(Eq. 41)}$$

Letting $k_0 \to \infty$, we have $\frac{k^2}{k_0^2} = 1 + \varepsilon^2\gamma_2 + \frac{\varepsilon^2\gamma_1^2}{4} + \frac{\varepsilon^2\gamma_1^2}{2} r_0\, k_0 i \to \infty$ (Eq. 42)

what contradicts the experimental fact[31] that for high frequencies the absorption coefficient satisfies Wiener 's causality relation $\lim_{\omega\to\infty} \frac{Im\, k(\omega)}{\omega} = 0$ (Eq. 43). The contradiction indicates that for $k \gg 1$ Eq. (26) must be solved more accurately. By Wiener's relation it is reasonable to assume that for $\omega \to \infty$, *k* behaves as $k \sim k_0\left(\chi_1 + i\frac{\chi_2}{k_0}\right)$ (Eq. 44), where $\chi_1$ and $\chi_2$ are unknown coefficients. Substituting to the dispersion relation (Eq. 26), solving it by iteration, a lengthy computation[32] gives

$$\left.\begin{aligned} \chi_1 &= 1 + \frac{1}{2}|\gamma_1\varepsilon| + O(\varepsilon^3) \\ \chi_2 &= \frac{1}{4r_0} \end{aligned}\right\} \qquad \text{(Eq. 45a, b), i.e., from Eq. (44):}$$

$$\lim_{\omega\to\infty} \alpha(k) = \lim_{\omega\to\infty} Im\, k(\omega) = \frac{1}{4r_0} \qquad \text{(Eq. 46).}$$

Thus, *for very high frequencies, the absorption coefficient tends to a finite limit which is independent of the variance of the velocity inhomogeneities. This limit depends on the geometry (i.e. correlation distance) of the inhomogeneities only*.

### 3.1.B. MULTIPLE SCATTERING: INTEGRAL EQUATION APPROACH

I studied this problem in case of *one-dimensional wave propagation*. Consider an inhomogeneous layer of thickness $L$ situated parallel to the *(x, y)* plane, which contains, between *z= 0* and *z=L*, velocity inhomogeneities of the form $c(\mathrm{z}) = c_0 + \varepsilon(\mathrm{z})$ (1-D case of Eq. 12a),

---

[30] See details in Korvin 1977: 19-24.
[31] Azimi, Sh.A. *et al*. 1968: Impulse and transient characteristics of media with linear and quadratic absorption laws. *Izv. Earth Phys*. No 2: 42-54.
[32] Korvin 1977: 23-24.

and let a plane wave $\varphi = \exp(i\omega t) \cdot u(z)$ coming from the half-space *z < 0* be incident upon this layer. It is assumed that $L$ is much larger than the characteristic size of inhomogeneities. The time-independent part of the plane wave satisfies the wave-equation $u''(z) + \frac{\omega^2}{c^2}u(z) = 0$ (Eq. 47). Introduce the average wave-number $k_0 = \frac{\omega}{c_0}$ and the notation $\nu(z) = \frac{\varepsilon(z)}{c_0}$ (Eq. 48), we can series-develop $\frac{\omega^2}{c^2}$ in Eq. (47) to powers of $\nu$ so that the wave-equation becomes $\left[\frac{d^2}{dz^2} + k_0^2\right] u(z) = -k_0^2\Psi(z)u(z)$ (Eq. 49), where $\Psi(z) = -2\nu(z) + 3\nu^2(z) + O(\nu^3)$ (Eq.50). Transform Eqs. (49-50) to an integral equation of the Fredholm type[33]:

$u(z) = \exp(ik_0 z) - k_0^2 \int_0^L G(z,z')\Psi(z')u(z')dz'$ (Eq.51), where the Green function is $G(z,z') = \frac{1}{2ik_0} exp[ik_0|z - z'|]$. We solve the integral equation by Neumann series (which I proved to be convergent[34] for $k_0 < \frac{2c_0}{5L\varepsilon_{max}}$, where $\varepsilon_{max} = \max_{z\epsilon[0,L]}|\varepsilon(z)|$).

If we define the transmission coefficient *T* and the reflection coefficient *R* by the relations:

$u(z) = \begin{cases} Texp(ik_0 z) & if \quad z \geq L \\ exp(ik_0 z) + Rexp(-ik_0 z) & if \quad z < 0 \end{cases}$ (Eq. 52), the Neumann series gives

$T = 1 + \sum_{n=1}^{\infty} \left(\frac{ik_0}{2}\right)^n \int_0^L \int_0^L ... \int_0^L \exp(-ik_0\, z_1)\exp(ik_0|z_1 - z_2|) \cdots \exp(ik_0 z_n)\, \Psi(z_1) \cdots \Psi(z_n) dz_1 \cdots dz_n$ (Eq. 53)

and

$R = \sum_{n=1}^{\infty} \left(\frac{ik_0}{2}\right)^n \int_0^L \int_0^L ... \int_0^L \exp(ik_0\, z_1)\exp(ik_0|z_1 - z_2|) \cdots \exp(ik_0 z_n)\, \Psi(z_1) \cdots \Psi(z_n) dz_1 \cdots dz_n$ (Eq. 54). Since we are interested in the expected value of $|T|^2$, multiply Eq. (53) by its complex conjugate and omit higher-order terms to find: $\langle TT^* \rangle = 1 - \frac{2\,k_0^2 L}{4} \int_0^\infty \cos(2k_0\; r) \cdot R_{\Psi\Psi}(r)dr$ (Eq. 55), where $R_{\Psi\Psi}(r)$ is the *ACF* of $\Psi$. By Eqs. (48 & 50) $R_{\Psi\Psi} = 4R_{\nu\nu} + O(\nu^3) = \frac{4R_{\varepsilon\varepsilon}}{c_0^2} + O\left(\left|\frac{\varepsilon}{c_0}\right|^3\right)$ (Eq. 56), and we find that for one-dimensional multiple scattering the attenuation coefficient describing the amplitude-decrease for moderate distances *L* is given by

---

[33] Kay, I. & Silverman, R. A., 1958: Multiple scattering by a random number of dielectric slabs. *Nouvo Cimento*, IX. Serie X. Suppl. No 2: 626-645.
[34] Korvin 1977: 12-13.

$\alpha = \frac{k_0^2}{c_0^2}\varepsilon^2 \int_0^\infty \cos(2k_0 r)\, N_{\varepsilon\varepsilon}(r)dr = \frac{\pi\omega^2}{c_0^4} W_{\varepsilon\varepsilon}(2k_0)$ (Eq. 57), where $N_{\varepsilon\varepsilon}(r)$ is the normalized *ACF* , and $W_{\varepsilon\varepsilon}$ is the *power spectrum* of the inhomogeneities. Summing up the results obtained for the velocity model $c(\mathbf{x}) = c_0(\mathbf{x}) + \varepsilon(\mathbf{x})$ (Eq. 12a), we have:

In the 3-dimensional case:

$$\alpha = \frac{\varepsilon^2}{c_0^2}\, k_0^2 \int_0^\infty (1 - cos2k_0 r) N(r)dr \qquad \text{(Eq. 58a)}$$

In the 1-dimensional case:

$$\alpha = \frac{\varepsilon^2}{c_0^2}\, k_0^2 \int_0^\infty (1 + cos2k_0 r) N(r)dr \qquad \text{(Eq. 58b)}$$

In the 1-dimensional case including multiple scattering:

$$\alpha = \frac{\varepsilon^2}{c_0^2}\, k_0^2 \int_0^\infty \cos 2k_0 r\, N(r)dr \qquad \text{(Eq. 58c)}$$

It is easy to show that all the above absorption coefficients are positive. Comparing Eqs. (58b) and (58c), we find that in the *one-dimensional case* the multiple scattering *decreases* the total wave attenuation. Internal multiples "are working against" reflection losses, i.e. decrease them. (*Note*: This result was achieved in the early 1970's, published in 1977. Thirty years later[35] I returned to this problem and proved that *multiple scattering on point-like-scatterers, fractally distributed in the 3-D space, also decreases energy losses in the high-frequency spectra of propagating signals.*)

EXCURSUS 1. ATTENUATION ON REFLECTION COEFFICIENTS

Starting out from the expression Eq, (54) of the reflection operator *R*, its expected value $\langle |R|^2 \rangle$ can be deduced and by simple manipulations[36] we get the "conservation of energy" formula: $\langle |R|^2 \rangle = 1 - \langle |T|^2 \rangle$ (Eq. 59). Then it follows that $\langle |T|^2 \rangle = 1 - \langle |R|^2 \rangle = 1 - \frac{2\pi\,\omega^2 L}{c_0^4} W_{\varepsilon\varepsilon}(2k_0)$ i.e. for a moderate distance *L* one has $\langle |T|^2 \rangle \approx exp\left[-\frac{2\pi\,\omega^2 L}{c_0^4} W_{\varepsilon\varepsilon}(2k_0)\right]$ (Eq. 60). The right-hand side of Eq. (60) can be expressed in terms of *the power spectrum* $W_{rr}$ *of the sequence of reflection coefficients*. Indeed, as I proved in 1973[37] : $R_{rr}(\tau) = -\frac{d^2}{d\tau^e}\frac{R_{rr}(\tau)}{4c_0^2}$ (Eq. 61). Fourier transforming both sides $W_{rr}(\omega) = \frac{\omega^2 R_{rr}(\tau)}{4c_0^2}$, which, expressing ω in terms of $2k_0$ leads to $\langle |T|^2 \rangle = exp[-2\pi L\, W_{rr}(2k_0)]$ (Eq. 62), that is

[35] Korvin, G. & Oleschko, K. 2004. 'Multiple wave scattering from fractal aggregates'. *Chaos, Solitons and Fractals*19(2): 421-425.
[36] Korvin, G. 'Certain problems of seismic and ultrasonic wave propagation in a medium with inhomogeneities of random distribution.' *Geophysical Transactions* 21(1973):5-34.
[37] Korvin 1973, Eq. (51).

the transmission operator for a series of layers is simply connected to the power spectrum of the sequence of reflection coefficients. It should be noted that Eq. (62) of the operator of transmission shows analogy with the formula $|T(\omega)| = exp[-R(\omega)t]$ (Eq. 63) of O'Doherty and Anstey[38], where $T(\omega)$ denotes the amplitude spectrum of the transmitted pulse, $R(\omega)$ is the spectrum of the time-series of the reflection coefficients, and $t$ is two-way time. This result has a special importance in *seismic stratigraphy*, because as I had shown[39], *the statistics of reflection coefficients is connected to the sedimentation history of the sequence of layers*.

### 3.1.C. FURTHER RESULTS AND APPLICATIONS

#### 3.1.C.1. WAVE ATTENUATION IN POROUS ROCKS

I successfully applied[40] this technique and the basic result

$$\alpha = \frac{k_0^2}{c_0^2}\varepsilon^2\int_0^\infty \cos(2k_0 r)\, N_{\varepsilon\varepsilon}(r)dr = \frac{\pi\omega^2}{c_0^4}W_{\varepsilon\varepsilon}(2k_0) \qquad \text{(Eq. 64)}$$

for a probabilistic description of acoustic wave attenuation in porous, two-component rocks. The story goes back to 1961 when Fara and Scheidegger proposed the *ACF* for the description of the statistical geometry of porous media: ". . . Let us assume that an arbitrary line be drawn through a given porous medium whose geometry is to be described. Points on the line are to be defined by giving their arch length *s* from an arbitrarily chosen origin. Then, for certain values of *s* the line will pass through void spaces; for other values of *s* the line will pass through filled spaces. We then introduce a function *f(s)* defined as follows: the value of *f(s)* is defined as +1 if the line at *s* passes through void space; it is defined as equal to -1 if the line passes through filled space"[41]. Fara and Scheidegger then suggested that the autocorrelation function (or the power spectrum) of this random function *f(s)* be used to characterize the statistical properties of the medium. Except in my works, the ideas of Fara and Scheidegger have apparently never been followed up in ultrasonic absorption studies. I could show that *there is a definite relationship between the autocorrelation function of f(s) and the absorption coefficient of ultrasonic waves propagating in the rock*. Instead of the function *f(s)* of Fara and Scheidegger I introduced a function $\varepsilon(x)$ defined along a random line traversing a plane section of the porous rock. Denoting by $c_0$ average velocity: $c_0 = p \cdot c_{fluid} + q \cdot c_{matrix} \equiv p \cdot c_1 + q \cdot c_2$ (Eq. 58), where $p$ is porosity, $q = 1 - p$, $\varepsilon(x)$ is defined as:

---

[38] O'Doherty, R. F., Anstey, N. A.,1971: Reflections on amplitudes. *Geoph. Prosp*. 19 No 3: 430-458.

[39] Korvin, G. 'The kurtosis of reflection coefficients in a fractal sequence of sedimentary layers'. *Fractals-Complex Geometry Patterns and Scaling in Nature and Society* 1(2)1993: 263-268.

[40] Korvin 1977, 1977-78 Part 1., 1980, 1981.

[41] Fara, H.D . Scheidegger, A. E.,1961: Statistical geometry of porous media. *Journal Geoph. Res*. 66 No 10: 3,279-3,284.

$$\varepsilon(x) = \begin{cases} c_1 - c_0 \quad = \varepsilon_1 \qquad if\ the\ line\ at\ x\ passes\ through\ fluid \\ c_2 - c_0 \quad = \varepsilon_2 \quad if\ the\ line\ at\ x\ passes\ through\ a\ solid\ grain \end{cases} \quad \text{(Eq. 65).}$$

Consider first a simplified model of the random function: $\varepsilon(x)$ at any given point $x$ assumes the value $\varepsilon_1$ with probability $p$, and $\varepsilon_2$ with probability $q$, whereas the number of changes of the values in any interval $(x_1, x_2)$ follows a *Poisson distribution of density* $\lambda$. The autocorrelation function is defined as $R_{\varepsilon\varepsilon}(x_1, x_2) = \langle\varepsilon(x_1)\varepsilon(x_2)\rangle$, the average being taken over all realizations of $\varepsilon(x)$. The product $\varepsilon(x_1)\varepsilon(x_2)$ can take the following forms: $\varepsilon(x_1)\varepsilon(x_2) =$
$$\begin{cases} \varepsilon_1^2\ or\ \varepsilon_2^2 \quad if\ there\ are\ an\ even\ number\ of\ changes\ between\ x_1 \& x_2 \\ \quad \varepsilon_1\,\varepsilon_2 \qquad if\ there\ are\ an\ odd\ number\ of\ changes\ between\ x_1 \& x_2 \end{cases}$$

Denoting x= $|x_1 - x_2|$ , $R_{\varepsilon\varepsilon}(x) = \exp(-\lambda x)\left\{(p\varepsilon_1^2 + q\varepsilon_2^2)\sum_{k=0}^{\infty}\frac{(\lambda x)^{2k}}{(2k)!} + \varepsilon_1\,\varepsilon_2\sum_{k=0}^{\infty}\frac{(\lambda x)^{2k+1}}{(2k+1)!}\right\} =$ $\frac{1}{2}[p\varepsilon_1^2 + q\varepsilon_2^2 + \varepsilon_1\,\varepsilon_2] + \frac{1}{2}\exp(-2\lambda x)[p\varepsilon_1^2 + q\varepsilon_2^2 - \varepsilon_1\,\varepsilon_2]$ (Eq. 66)

Observing that $\varepsilon_1 = c_1 - c_0 = q(c_1 - c_2)$, similarly $\varepsilon_2 = c_2 - c_0 = p(c_2 - c_1)$, we get $\langle\varepsilon\rangle = 0$, $\langle\varepsilon^2\rangle = pq(c_1 - c_2)^2$, and Eq. (66) simplifies to

$R_{\varepsilon\varepsilon}(x) = \langle\varepsilon^2\rangle\exp(-\lambda x) = pq(c_1 - c_2)^2\exp(-\lambda x)$ (Eq. 67), the corresponding power spectrum being $W_{\varepsilon\varepsilon}= pq(c_1 - c_2)^2\,\frac{1}{\pi}\cdot\frac{2\lambda}{\omega^2+(2\lambda)^2}$ (Eq. 68). Applying Eq. (57) it is seen that in a two-component porous rock the absorption coefficient is given by $\alpha(k_0) = \frac{\lambda pq}{c_0^2}\cdot\frac{k_0^2}{k_0^2+\lambda^2}$ (Eq. 68), where $k_0 = \omega/c_0$ , $c_0 = p\cdot c_1 + q\cdot c_2$ , $p$ is porosity, $q = 1 - p$ , $\lambda$ is the Poisson-density of pore/grain interfaces along a random line.

From Eq. (68) we see that the coefficient of attenuation in a porous rock:

— *is zero for zero frequency* ;

— increases with $\omega^2$ for low frequencies;

—for high frequencies the attenuation coefficient tends to a finite, frequency-independent, limit.

For a given fixed frequency, the attenuation

— increases as square of the difference between solid and fluid velocities;

— decreases with increasing average velocities;

— attains its maximum as function of porosity when $p$ = 0.5.

From Eq. (68), for $k_0 \ll \lambda$ (low-frequency approximation) we have

$\alpha(\omega) = \frac{1}{\lambda}\frac{pq}{c_0^2}\frac{(c_1-c_2)^2}{c_0^2} = r\cdot\frac{pq}{c_0^2}\cdot\frac{(c_1-c_2)^2}{c_0^2}$ (Eq. 69), where[42] $r \approx 1/\lambda$ . A more precise calculation yields $\alpha(\omega) = \frac{2r_1r_2}{r_1+r_2}\cdot\frac{pq}{c_0^2}\cdot\frac{(c_1-c_2)^2}{c_0^2}$ (Eq. 70). Equations (69 & 70) are formally similar to Ament's[43] equation of scattering on density inhomogeneities: $\alpha(\omega) = \frac{\omega^2}{9\eta}\cdot\frac{pq}{c_0^2}\cdot\frac{(\rho_1-\rho_2)^2}{\rho_0^2}\cdot r^2$ (Eq. 71) where $\eta$ is the viscosity of the fluid, $\rho_1$, $\rho_2$, $\rho_0$ are fluid-, solid- and average densities, $r_1$ and $r_2$ are the average pore- and grain-diameters, respectively. Equation (69) implies that the absorption coefficient is inversely proportional to (the square of the) average velocity—this was confirmed experimentally by a student of mine, L. Gombár[44] .

3.1.C.2. WAVE ATTENUATION AND ROCK ENTROPY

According to Eqs. (68 or 69) the absorption coefficient is a monotonically increasing function of porosity between 0-0.5 and attains its maximum at around $p$ = 0.5. This is confirmed by the experimental findings of Shumway and Hamilton[45] (Fig. 13).

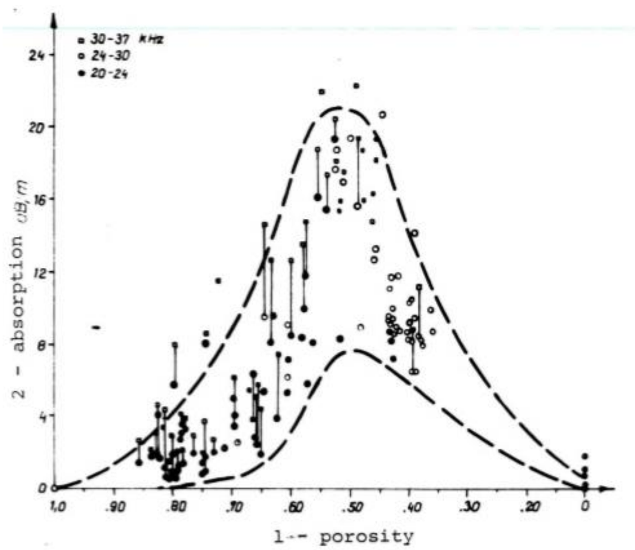


Fig. 13. Absorption coefficient vs. porosity dependence for marine sediments (after Shumway 1960).

In several works of mine[46], I tried to explain this important finding. I considered a more general $n$-component rock model, in which component velocities are $\{c_1, \cdots, c_n\}$, component

---

[42] Korvin 1977: 27.
[43] Ament, W. S., 1953: Sound propagation in gross mixtures. *Journal Ac. Soc. Am*. 25 No. 4: 638-641.
[44] Gombár L.: Correlation of attenuation of elastic waves with other petrophysical and lithological properties, *Geophysical Transactions*, 1983. Vol. 29. No.3: 217-228.
[45] Shumway, G., 1960: Sound speed and absorption studies of marine sediments by a resonance method—Part II. *Geophysics*, 25 No 3: 659-682; Hamilton, E. L.,1972: Compressional wave attenuation in marine sediments. *Geophysics* 37 No 4: 620-646.

probabilities are $\{p_1, \cdots, p_n\}$ with $\sum p_i = 1$, average velocity is $c_0 = \sum p_i\, c_i$, velocity fluctuation is $\varepsilon_i = c_i - c_0$ so that obviously $\langle\varepsilon\rangle = 0$ and – as little algebra[47] yields – $\langle\varepsilon^2\rangle = \sum p_i\, \varepsilon_i^2 = \sum\sum_{i<j}\left(c_i - c_j\right)^2 p_i p_j$ and along any random line traversing the medium the number of interfaces between components obeys a Poisson distribution with parameter $\lambda$. In this model the *ACF* is $\langle\varepsilon(x_1)\varepsilon(x_2)\rangle = R_{\varepsilon\varepsilon}(|x_1 - x_2|) = \langle\varepsilon^2\rangle \exp(-2\lambda|x_1 - x_2|)$ (Eq. 72) where

$$\langle\varepsilon^2\rangle = \sum p_i\, \varepsilon_i^2 = \sum\sum_{i<j}\left(c_i - c_j\right)^2 p_i p_j \quad \text{(Eq. 73).}$$

Assume the velocities $\{c_i\}$ are indepent, and uniformly distributed in an interval $[c_{min}, c_{max}]$, let $\Delta = c_{max} - c_{min}$, then $\langle\left(c_i - c_j\right)^2\rangle = \frac{1}{\Delta^2}\int_{c_{min}}^{c_{max}}\int_{c_{min}}^{c_{max}}\left(c_i - c_j\right)^2 dc_i dc_j = C^2$ (Eq. 74). The expected value of expression (Eq. 72) with respect to the velocity distribution $\{c_1, \cdots, c_n | p_1, \cdots, p_n\}$ is

$$\langle R_{xx}(x)\rangle = C^2 \Sigma\Sigma_{i<j}\, p_i\, p_j\, \exp(-\lambda|x|) = \frac{C^2 \exp(-\lambda|x|)}{2}\Sigma\Sigma_{i\neq j}\, p_i\, p_j$$

$= \frac{C^2 \exp(-\lambda|x|)}{2}\sum_{i=1}^{n} p_i\,(1 - p_i)$ (Eq. 75), where $C^2$ is the constant computed in Eq. (74).

By (Eq. 57), $\alpha = \frac{\pi\omega^2}{c_0^4} \cdot W_{\varepsilon\varepsilon}(2k_0)$, that is the absorption coefficient $\alpha$ is proportional to the power spectrum of the inhomogeneities, the latter is proportional to the *ACF*, consequently by Eq. (75) it is also proportional to the factor $H = \sum_{i=1}^{n} p_i\,(1 - p_i)$ (Eq. 76), expressing the *heterogeneity* of the rock. Obviously, $H = 0$ if one of the probabilities is 1; $H$ attains it maximum for $p_1 = p_2 = \cdots = p_n = \frac{1}{n}$, and $H_{max} = \frac{n-1}{n}$. It is worth-while to compare $H$ with the *Shannon entropy* $E = -\sum_{i=1}^{n} p_i\, log p_i$ (Eq. 77), used by Byryakovskiy[48] to characterize the *heterogeneity of rocks*. The entropy also satisfies that $E = 0$ if any $p_i$=1, it assumes its maximum for $p_1 = p_2 = \cdots = p_n = \frac{1}{n}$, and $E_{max} = \log n$. It can be proved by series development[49] that close to the maximum (if $\sum_{i=1}^{n}\left|\frac{1}{n} - p_i\right| \ll 1$) one has $H_{max} - H = \frac{2}{n}(E_{max} - E)$ (Eq. 78) (see Fig. 14).

---

[46] Korvin 1977-78 Pt.1; Korvin 1980, Korvin 1985.
[47] Korvin 1977-78 Pt.1: 115.
[48] Byryakovskiy, L. A. 1968: Entropy as criterion of heterogeneity of rocks. Soviet Geol. No 3 pp. 135 -138. (In Russian, English translation in *Internat. Geol. Rev*. 10, No 7).
[49] Details can be found in Korvin 1977-78 Pt.1: 112.

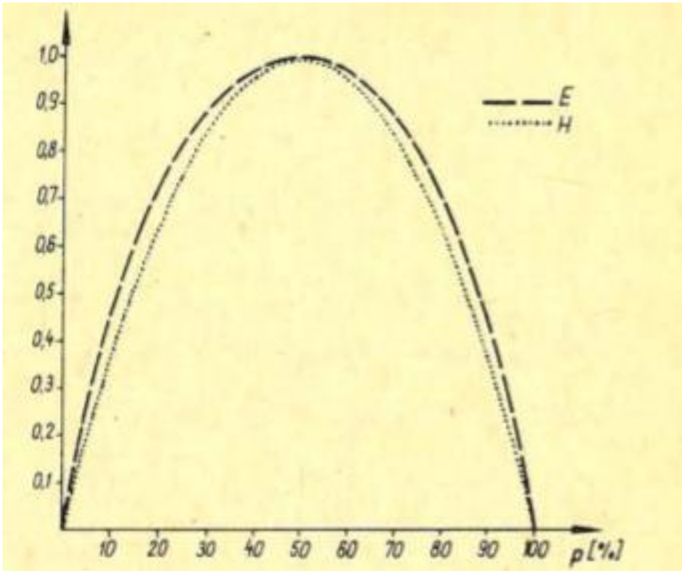


Fig. 14. Relative heterogeneity factor $H/H_{max}$ and relative entropy $E/E_{max}$ for $n = 2$ .

EXCURSUS 2. A SEISMOLOGICAL APPLICATION[50]

The constancy of the "quality factor" $Q$ over a broad frequency range has been widely accepted by seismologists[51]. In seismic exploration as well, a large number of published data[52] prove the nearly linear frequency-dependence of the coefficient of absorption. (The quality factor $Q$ and $\alpha$ are connected by $\frac{1}{Q} = \frac{c_0\alpha}{f\pi}$)[53]. However, in 1980 Aki[54], based on an analysis of the filtered records of some 900 earthquakes occurring in the region of central Japan with focal depths to 150 km conclusively demonstrated that $Q$ for the shear waves in the crust and upper mantle increases with frequency over the range 1-25 Hz, at least in the areas studied.

[50] Korvin, G. 1983b. 'General theorem on mean wave attenuation'. *Geophysical Transactions* 29(3):191-202.
[51] Knopoff, L. 1964: Q. *Rev. Geoph*. 2, 4: 625-660.
[52] Attewell, P. B., Ramana, Y. W. 1966: Wave attenuation and internal friction as functions of frequency in rocks. *Geophysics* 31, 6: 1049-1056
[53] The definitions of the quality factor $Q$, absorption coefficient $\alpha$ and of other measures of attenuation are summarized in Bradley, J. J., Fort, A. N. Jr. 1966: Internal friction in rocks. In: *Handbook of Physical Constants* (Ed. Clark, S. P. Jr). *Geol. Soc. Am. Memoir*, 97: 175-193.
[54] Aki, K. 1980: Attenuation of shear waves in the lithosphere for frequencies from 0.05 to 25 Hz. *Phys. Earth. Planet. Int*. 21, 1: 50-60.

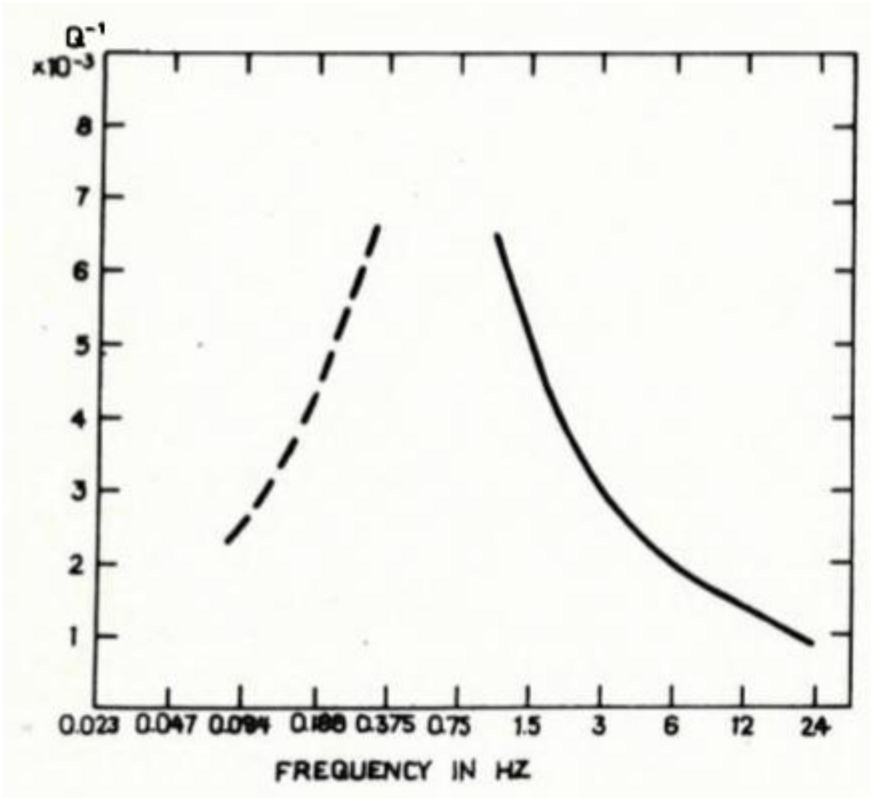

[55]

Fig. 15. Frequency dependence of $Q^{-1}$ (after Aki 1980).

The descending flank of the curve for frequencies higher than 0.75 Hz was fitted by Dainty as $\frac{1}{Q(\omega)} = \frac{1}{Q_i} + g_0 \frac{v}{\omega}$ with $Q_i$ being the intrinsic $Q$ [$Q_i$ = 2000], $v$ the shear wave velocity [assumed to be 3.5 km/sec], $g_0$ = 0.01 km$^{-1}$ for the observations in Japan and $g_0$ = = 0.005 km$^{-1}$ for Central Asia. In 1983 I derived a general asymptotic formula for the high-frequency behavior of the mean field attenuation coefficient (a version of Eq. 46 of this Dissertation) which, for an appropriate and realistic model of the random velocity fluctuation, explained the frequency-dependence of $Q^{-1}$ in Aki's data. This work of mine[56] brought me the *Best Technical Paper of the Year* award from the *MGE* (*Hungarian Geophysicists' Association*).

### 3.1.C.3. AN UNSOLVED PROBLEM[57]: ABSORPTION AND ENTROPY

[55] Dainty, A.M. 1981: A scattering model to explain seismic *Q* observations .in the lithosphere between 1 and 30 Hz. *Geoph. Res. Letters*, 8, 11: 1126-1128.
[56] Korvin, G. 1983b. 'General theorem on mean wave attenuation'. *Geophysical Transactions* 29(3):191-202.
[57] Korvin, G. 'A few unsolved problems of applied geophysics'. *Geophysical Transactions* 31(4)1985:373-389.

In 1978 Beltzer studied elastic wave propagation in randomly porous materials. He concluded that “for low frequency regimes the randomness of porosity leads to an increase in the attenuation and dispersion of the elastic wave”[58]. This is highly plausible and in agreement with the general understanding that the heterogeneity of a medium causes additional dissipation of the propagating elastic wave. (It is well known, for example, that the sound attenuation in crystalline materials is less for a single crystal than for an aggregate.) Prior to Beltzer's work, I had already reported similar conclusions, in connection with elastic waves propagating in a random stack of layers (the hypothesis was published in Korvin1977a, its heuristic proof in Korvin1977-78 Pt.1). My [1980] paper applied stochastic perturbation for the random wave equation in order to generalize Beltzer’s results for rocks of random structure. I could show that in multi-component rocks the low-frequency attenuation coefficient is proportional to (more exactly, *positively correlated with*) the quantity $E = -\sum_{i=1}^{n} p_i \, log p_i$ where $p_i$; $\sum p_i = 1$ is the relative volume ratio of the *i*-th phase. The quantity E measures the *randomness* of the constitution of the rock and, in Russian literature, is termed “rock entropy”[59]. Recall that in the *statistical theory of disordered systems* the entropy *S* of a random aggregate of several components always consists of two parts: $S = S_{configurational} + S_{mixture}$ (Eq. 79, the so-called *Flory-Huggins formula*[60] ) , where $S_{mixture}$ has the same form as the entropy E in our Eq. (77). For 2-component rocks we had: for $k_0 \ll \lambda:\ \alpha(\omega) = \frac{1}{\lambda}\frac{pq}{c_0^2}\frac{(c_1-c_2)^2}{c_0^2} = r \cdot \frac{pq}{c_0^2} \cdot \frac{(c_1-c_2)^2}{c_0^2}$ where $r \approx 1/\lambda$ (Eq, 69). A more precise calculation gave $\alpha(\omega) = \frac{2r_1 r_2}{r_1+r_2} \cdot \frac{pq}{c_0^2} \cdot \frac{(c_1-c_2)^2}{c_0^2}$ (Eq. 70), that is

$$\log \alpha(\omega) = \underbrace{log \frac{1}{c_0^2}}_{constant} + \underbrace{log r}_{configurational\ term} + \underbrace{\log pq}_{mixing\ term} + \underbrace{log \frac{(c_1-c_2)^2}{c_0^2}}_{strength\ of\ heterogeneity\ term}$$

(Eq. 80): *the logarithm*[61] *of the attenuation coefficient contains configurational and mixing terms as in the Flory-Huggins equation* (79).

It is well known that frequency-dependent attenuation, and the resulting velocity dispersion, lead to a distortion of the propagating acoustic pulses; Russian oceonologists[62] speak about the *changes of signal entropy during hydroacoustic propagation.* That is, we can state the following unsolved problem: *Derive attenuation in random media from “conservation of information” principles! In other words, prove that “the loss of information about the signal which had propagated through a random medium equals the gain of information about the statistics of the*

[58] Beltzer A. 1978: The influence of random porosity on elastic wave propagation. *J. Sound Vibr*. 58, No. 2: 251-256.
[59] Byryakovskiy, L. A. 1968: Entropy as criterion of heterogeneity of rocks. *Soviet Geol*. No 3 pp. 135 - 138. (In Russian, English translation in *Internat. Geol. Rev*. 10, No 7).
[60] Ziman J. M. 1979*: Models of Disorder. The Theoretical Physics of Homogeneously Disordered Systems*. Cambridge University Press, Cambridge-London-New York-Melbourne. §. 7.2.
[61] Throughout the paper “log” means *natural logarithm*.
[62] Barkhatov A. N. 1982: *Modelling of the propagation of sound waves in the oceans* (In Russian). Hydro-meteoizdat, Leningrad; Barkhatov A. N., Shmelev I. I. 1969: A study of the under-surface sound channel as communication channel, under model conditions (In Russian). *Akust. Zhurnal* 15, 2.

*medium's inhomogeneities."* To make the hypothesis plausible, I refer to the common observation that high-entropy, very irregular stacks of layers always strongly attenuate the seismic waves propagating through them[63] (Fig. 15).

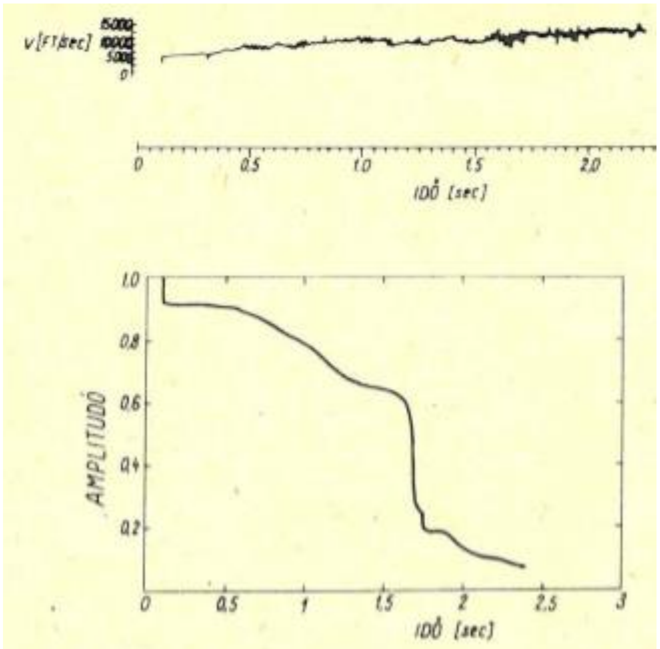


Fig. 15. Anomalously large energy-attenuation due to a high-entropy cyclic series of layers (after Schoenberger and Levin 1974)

## 3.1.D. SCATTERING ON RANDOM SURFACES, FROM A RANDOM HALF-SPACE, AND FROM RANDOM NEAR-SURFACE LAYERS

In each of the following works[64] I was responsible for the physical model, the mathematics, and the write-up of the paper; when there were co-authors, they were responsible for the field work, data collection, and for the software, if needed.

### 3.1.D.1. DIFFUSE REFLECTION FROM A GAUSSIAN RANDOM BOUNDARY[65]

It has been since long a basic problem of Hungarian reflection seismology that in many cases we could not get but intricated diffuse reflections from the uneven surface of the basement. These diffuse reflections consist of random diffraction arrivals coming from the rough surface. They follow the basement reflection as a "*diffuse shadow*" of a few hundred ms length that makes

---

[63] Schoenberger, M. and Levin, F. K. 1974: Apparent attenuation due to intrabed multiples. *Geophysics* 39 No 3: 278-291.
[64] Korvin 1978b, 1982b, 2005; Korvin & Olechko 2004; Korvin et al. 2017; Oleschko et al. 2002, 2003, 2008.
[65] Korvin, G. 1982b. 'Certain problems of seismic and ultrasonic wave propagation in a medium with inhomogeneities of random distribution. III. Statistics of the diffuse reflection shadow following a rough reflecting boundary'. *Geophysical Transactions* 28(1): 8-19.

very difficult to detect eventual deeper reflections. To study this problem, I considered Gaussian, differentiable, random surfaces for the case when the wavelength is much shorter than the characteristic size of the inhomogeneities. Surface-surface multiple scattering and self-shadowing of the random surface[66] have not been taken into account. I derived the expected *temporal behaviour* of the amplitude distribution of the diffuse reflection shadow, using the following measurement geometry:

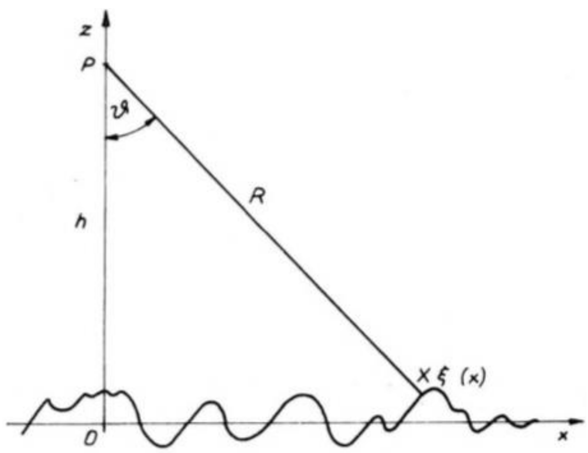


Fig. 16. Measurement geometry.

The random surface is described by the function $\xi(x, y)$ , it is *homogeneous* and *isotropic* with $\langle\xi\rangle = 0, \langle\xi^2\rangle = \sigma^2$ , with Gaussian distribution function $W(\xi) = \frac{1}{\sigma\sqrt{2\pi}} exp[-\xi^2/2\sigma^2]$ (Eq. 81), and correlation function $\langle\xi(x_1, y_1)\xi(x_2, y_2)\rangle = \sigma^2 exp[-r^2/r_0^2]$ (Eq.82) where

$r^2 = (x_1 - x_2)^2 + (y_1 - y_2)^2$, $r_0$ is the *correlation length*. If we consider $\xi(x, y)$ along an arbitrary line, the power spectrum of $\xi$(x) is[67] $E(k) = \frac{r_0}{2\sqrt{\pi}} exp\left[-\frac{k^2}{4} r_0^2\right]$ (Eq. 83)

Suppose that $\xi$ *(x)* is twice continuously differentiable and introduce the variables

$\xi_1 = \frac{\partial\xi}{\partial x}$; $\xi_2 = \frac{\partial^2\xi}{\partial x^2}$. Obviously, $\xi_1$ and $\xi_2$ are also Gaussian and[68] $\langle\xi_1^2\rangle = \gamma_1^2 = \frac{\sigma^2}{r_0^2}$;

$\langle\xi_2^2\rangle = \gamma_2^2 = \frac{6\sigma^2}{r_0^4}$ (Eqs. 84, 85). We select on the (*x, y*) plane an arbitrary straight line passing through the origin, say the axis *x*. Measurements are performed by generating and receiving the waves at point *P = P(0,0, h)*, lying on the *z* axis at a height *h* above the plane (*x, y*) (this case corresponds to *NMO*-corrected seismic time-sections). It is supposed that *P* lies high above the

[66] Beckmann, P.1965: Shadowing of random rough surfaces. *IEEE Trans. AP*-13 No. 3: 384-388.
[67] Tatarski, V. I.1961*: Wave Propagation in a Turbulent Medium*. Dover Publ. Inc. New York.
[68] Rice, S.O.1944, 1945: The mathematical analysis of random noise. *Bell Syst. Techn. J*. 23, No. 3 (1944); 24, No 1 (1945).

random surface, $\sigma^2 \ll h^2$ (Eq. 86) . Let *X* denote the point $\xi(x)$, let $R = \overline{PX}$ (Fig. 16). We obtain a reflection from point *X* if and only if *x* is a *stationary point* of the function $R(x) = \overline{PX}$, that is if $\frac{\partial R}{\partial x} = \frac{\partial}{\partial x}\sqrt{(h-\xi)^2 + x^2} = 0,$ implying $\xi_1\left(1 - \frac{\xi}{h}\right) = \xi_1(1 - \chi\xi) = 0$ (Eq. 87) where we introduced the notation $\chi = 1/h$ . Neglecting the second term on the l.h.s. of Eq. (86) on strength of (Eq. 86), the necessary and sufficient condition of a reflection from $X = \xi(x)$ will be the validity of $\xi_1(x) = \chi\xi$ (Eq. 88). Denote by *N(x) dx* the probability of a reflection arrival from some surface point $\xi(x)$ above the interval (*x, x* + *dx*). Computation[69] gives: $N(x) \approx \frac{\sqrt{6}}{\pi r_0} exp\left(-\frac{1}{12}\frac{r_0^4}{h^2\sigma^2}\right) exp\left[-\frac{1}{2}\chi^2 x^2/\gamma_1^2\right]$ (Eq. 89).

Determine now the expected number of reflections $\mathfrak{N}(x)dx$ coming from the ring between radii *x* and *x* + *dx* around the origin *O* of the (*x, y*) plane. If *v* is the propagation speed of sound waves above the plane (*x, y*) and $R \approx \sqrt{x^2 + h^2}$ , then $\mathfrak{N}(x)dx$ is the expected number of reflection arrivals coming from the surface $\xi$, at time instant *t* = *2R/v*. Some geometry, and integration, give $\mathfrak{N}(x)dx = Ax \cdot exp\left(-\frac{1}{2}\chi^2 x^2/\gamma_1^2\right)dx$ (Eq. 90), with $A = \frac{2\sqrt{6}}{r_0} \cdot exp\left(-\frac{1}{12} \cdot \frac{r_0^4}{h^2\sigma^2}\right)$ (Eq. 91). Since $A = A(h) = O(1)$ and $\gamma_1^2$ is independent of *h*, the *expected total number of reflections from the Gaussian random surface* $\xi(x,y)$ is $N = A \int_0^\infty x \cdot exp\left[-\frac{1}{2}\chi^2 x^2/\gamma_1^2\right]dx = \frac{A\gamma_1^2}{2\chi^2} = O(h^2)$ (Eq. 92). The function $x \cdot exp\left[-\frac{1}{2}\chi^2 x^2/\gamma_1^2\right]$ attains its maximum for $x_{max}$ where $\frac{x_{max}^2}{h^2} = \gamma_1^2$, that is $x_{max} = \pm h\gamma_1$ (Eq. 93). Since, by Eq. (84), $\gamma_1^2$ is the mean square slope of the surface $\xi(x)$ , Eq. (93) has a simple geometric interpretation (Fig. 17).

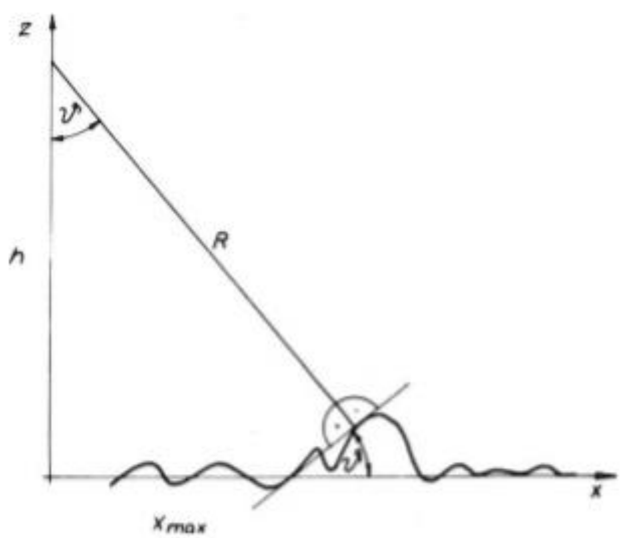


Fig. 17. Condition of reflection from a random Gaussian surface

---

[69] Korvin, G. 1982b: 9-10.

The greatest number of reflections from the random surface $\xi$ (x, y) is obtained for that angle of incidence $\vartheta$ for which $tg\,\vartheta = \langle\left(\frac{\partial\xi}{\partial x}\right)^2\rangle = \gamma_1^2 = \frac{\sigma^2}{r_0^2}$. The corresponding distance $R_{max}$ is, by Eq. (93): $R_{max} \approx h\sqrt{1+\gamma_1^2}$ , or in terms of *two-way travel times*, the maximum number of backscattered reflections is to be expected at $t_{max} \approx t_0\sqrt{1+\gamma_1^2}$ (Eq. 94) where $t = 2R/v$ , $t_0 = 2h/v$, *v* is propagation speed above the (*x*,*y*) plane. (See Table 1). If the propagating wave has the dominant frequency *f* , the corresponding wavelength is $\lambda = v/f$ and the first Fresnel zone on the (*x*, *y*) plane has the radius $x_1 = \sqrt{\lambda h/2}$. The scattering has no important effect unless $r_0 \ll x_1$.

The derivation required the applicability of *geometrical optics* , that is the following five conditions must be satisfied:

| | |
|---|---|
| $\lambda < r_0$ | C.1 |
| $\lambda < h$ | C.2 |
| $\sigma^2 \ll h^2$ | C.3 |
| $r_0 \ll \sqrt{\lambda h/2}$ | C.4 |
| $\frac{1}{h^4} \ll \gamma_2^2 = \langle\xi_2^2\rangle = \frac{6\sigma^2}{r_0^4}$ | C.5 |

Table 1. The diffuse reflection shadow in terms of two-way time:

| | |
|---|---|
| the shadow exists between | $t_0 \le t \le t_0\sqrt{1+3\gamma_1^2}$ |
| it starts with zero expected energy, its energy gradually builds up, attains its maximal value around | $t_{max} = t_0\sqrt{1+\gamma_1^2}$ |
| and from that point on it decreases faster than exponentially until it disappears around | $t_{end} = t_0\sqrt{1+3\gamma_1^2}$ |

As an example, consider the case of v = 4000 m/s; *f* = 40 Hz; *h* = 4000 m; $r_0$ = 250 m; $\sigma^2$ = = 5000 m$^2$ ($\lambda$ = 100 m). It is easy to check that conditions C.l-C.5 are met. The time-history of the diffuse reflection shadow will be:

| | |
|---|---|
| it exists between | $2 \le t \le 2.228\ sec$ |
| it attains its maximal value around | $t_{max} = 2.078\ sec$ |
| it disappears around | $t_{end} = 2.228\ sec$ |

## 3.1.D.2. OPTICAL IMAGE OF A NON-LAMBERTIAN FRACTAL SURFACE[70]

Pentland[71] proved that if a self-affine surface $F(x,y)$ with power spectrum $\propto f^{-\beta}$ (here $f \gg 1$ is *spatial frequency*) is explored with perpendicularly incident light and the diffuse reflection follows Lambert's law $I(x,y) = I_{inc}\gamma(x,y)cos\vartheta(x,y)$ (Eq. 95) where $I_{inc}$ is incident wave intensity, $I(x,y)$ is image-intensity, $\gamma(x,y)$ is reflectance, $\vartheta(x,y)$ angle between surface normal and incident wave direction, then the intensity distribution of the image will have the power spectrum $\propto f^{2-\beta}$ for $f \gg 1$ . He assumed constant reflectance along the surface, and made formal use of the partial derivatives $\frac{\partial F(x,y)}{\partial x}$, $\frac{\partial F(x,y)}{\partial y}$ even though they *almost nowhere exists along the surface $F(x,y)$ if it is fractal*.

First, in 2003, I gave a correct proof to Pentland's Theorem using numerical approximation for the partial derivatives, but still assuming Lambertian reflection. Then, in 2004, I dropped the *Lambertian Ansatz* and only assumed that the reflectance is proportional to the local *focusing/defocusing* factor of the surface. These factors are related to the *Gaussian curvature G(x,y)* of $F(x,y)$ .

Modern *Differential Geometry* helps to express the focusing/defocusing of light by local surface curvatures. Compute first the area of a small cap of intrinsic radius λ on a sphere of radius *R* at the point $(x,y,z) = (Rsin\varphi cos\vartheta, Rsin\varphi sin\vartheta, Rcos\varphi)$. The *intrinsic metric* on the sphere is $(ds)^2 = R^2(d\varphi)^2 + R^2sin^2\vartheta(d\vartheta)^2$; that is $g_{11} = R^2, g_{22} = R^2sin^2\varphi, g_{12} = g_{21} = 0$; the *Gauss curvature* is $G = 1/R^2$. The area of a polar cap of intrinsic radius λ is:

$$(\lambda, \mathrm{R}) = \int_0^{\lambda/R} 2\pi R^2 sin\varphi d\varphi = 2\pi R^2\left(1 - cos\frac{\lambda}{R}\right) \approx \pi\lambda^2 - \frac{1}{R^2}\frac{\pi}{12}\lambda^4 ,$$

this is a special case of *Schoen's Lemma*[72] for general surfaces: "*If the Gauss curvature at the point P=F(x,y) is G(x,y), then the area of a small disk of intrinsic radius $\lambda \ll |G(x,y)|^{-1/2}$ around P is $A(\lambda,G) = \pi\lambda^2 - G\frac{\pi}{12}\lambda^4$* (Eq. 96)." From Eq. (96) the *defocusing factor* (for positive curvature) or *focusing factor* (for negative curvature) is

$I_f \approx 1 + cG(x,y)\lambda^2 + O\left(\lambda^4 \langle\frac{1}{G}\rangle^2\right)$ (Eq. 97), where *c* is a constant, $\lambda$ is wavelength. The *ACF* (autocorrelation function) of the optical image is

$R_{II}$=$\langle I(x_1,y_1)I(x_2,y_2)\rangle = \langle I(P)I(Q)\rangle \approx \langle\{1 - c\lambda^2G(P)\{1 - c\lambda^2G(Q)\}\}\rangle \approx$
$1 + c^2\lambda^4\langle G(P)G(Q)\rangle$ . To relate the *ACF* of *I(x,y)* to the *ACF* of the surface, write

---

[70] Korvin, G. 'Is the optical image of a non-Lambertian fractal surface fractal?' *IEEE Geoscience and Remote Sensing Letters* 2(4)2005:380-383.
[71] Alex P. Pentland 1984. Fractal-Based Description of Natural Scenes. *IEEE Transactions on Pattern Analysis and Machine Intelligence PAMI*-6:661-674.
[72] Schoen, Richard M. (1984), "Conformal deformation of a Riemannian metric to constant scalar curvature", *Journal of Differential Geometry* 20 (2): 479–495.

$G(x,y) = \frac{F_{xx}F_{yy} - F_{xy}^2}{\left(1+F_x^2+F_y^2\right)^2}$ , $F_x = \frac{\partial F}{\partial x}$, $F_{xy} = \frac{\partial^2 F}{\partial x \partial y}$ , $\cdots$, and make the following assumptions:

A1. Smallness: $F_x^2 + F_y^2 \ll 1$

A2. Finiteness: $\langle F_x \rangle = \lim_{X\to\infty} \frac{1}{2X} \int_{-X}^{X} F_x\,(x,y)dx = \lim_{X\to\infty} \frac{1}{2X} [F(x,y)]_{x=-X}^{x=+X} = 0,$

$$\langle F_{xy} \rangle = 0, \cdots$$

A3. *F(x,y)* is isotropic and translation invariant.

I also assumed that the *four-product theorem*[73] approximately holds for the derivatives:

A4. For any four 1st and 2nd -order derivatives: $\langle ABCD \rangle \approx \langle AB \rangle \langle CD \rangle + \langle AC \rangle \langle BD \rangle + \langle AD \rangle \langle BC \rangle$

With these assumptions, neglecting the constant additive term and higher-order terms:

$$\langle G(P)G(Q) \rangle \approx \langle \left[F_{xx}(P)F_{yy}(P) - F_{xy}^2(P)\right]\left[F_{xx}(Q)F_{yy}(Q) - F_{xy}^2(Q)\right] \rangle \cdot$$

$$\cdot \langle \left[1 - 2\left\{F_x^2(P) + F_y^2(P)\right\}\right] \cdot \left[1 - 2\left\{F_x^2(Q) + F_y^2(Q)\right\}\right] \rangle$$

Then I proved (using Wiener's technique[74]), and then applied, the identities:

$$R_{F_{xx}F_{xx}} = \frac{\partial^4}{\partial x^4} R(\xi,\eta);\ R_{F_{yy}F_{yy}} = \frac{\partial^4}{\partial y^4} R(\xi,\eta), \cdots, R_{F_{xx}F_{xy}} = \frac{\partial^4}{\partial x \partial y^3} R(\xi,\eta) \ ,$$

for the computation of $\langle G(P)G(Q) \rangle$ term-by-term in order to derive the sought-for relation between the fractal surface *F(x,y)* and its optical image *I(x,y)* . Assuming that *F(x,y)* scales as

$\langle [F(x,y) - F(x-\xi, y-\eta)]^2 \rangle \propto \delta^{2H}$ (where $= \sqrt{\xi^2 + \eta^2}$ ), I obtained by a very lengthy calculation $R_{II}(\delta) \propto \langle \left[F_{xx}(P)F_{yy}(P) - F_{xy}^2(P)\right]\left[F_{xx}(Q)F_{yy}(Q) - F_{xy}^2(Q)\right] \rangle \cdot$

$$\cdot \left[1 - 2\left\{F_x^2(P) + F_y^2(P)\right\}\right] \cdot \left[1 - 2\left\{F_x^2(Q) + F_y^2(Q)\right\}\right]\Big|_{|P-Q|=\delta} \propto$$
$$\delta^{2H-2}(const_1 - const_2|\delta|^{2H-2}) \approx |\delta|^{2H-2} + O(|\delta|^{4H-4}) \ ,$$

whence Fourier Ttransform gives that for high spatial frequencies the power spectrum of the image falls of as $\propto f^{-2H}$ , that is I proved - without the *Lambertian Ansatz* - that the optical *image inherits the fractal dimension of the mapped surface*.

[73] Julius Bendat 1981. *Nonlinear System Analysis and Identification from Random Data*. New York: Wiley-Interscience.
[74] Wiener, Norbert 1949. *Extrapolation, Interpolation, and Smoothing of Stationary Time Series*. New York: Wiley.

## 3.1.D.3. WAVE SCATTERING ON POISSON-DISTRIBUTED AND FRACTALLY-DISTRIBUTED[75] INHOMOGENEITIES IN A HALF-SPACE

The basic difference between the two cases is, that - in the 3-D space - the total number $\mathfrak{N}$ of scatterers distributed according to a Poisson process of density $\lambda$ in a volume of characterisctic size $R$ scales as $\mathfrak{N} \propto \lambda R^3$, while the total number of fractally distributed scatterers scales as $\mathfrak{N} \propto \lambda R^d$ with $2 < d < 3$. As we shall see, the treatment of the two models requires different mathematical techniques.

### 3.1.D.3.1. SOURCE-GENERATED RANDOM NOISE OVER POISSON-DISTRIBUTED SCATTERERS[76]

We start out from the wave equation $\nabla^2 \mathrm{p} - \frac{1}{c^2}\frac{d^2 p}{dt^2} = 0$ (Eq. 97) where the inhomogeneous velocity is of the form $c = c_0/(1+\varepsilon), \langle\varepsilon\rangle = 0, \langle\varepsilon(x,y,z)^2\rangle = \varepsilon^2 \ll c_0^2$ , termed previously as velocity model (Eq.29.b). Neglecting multiple scattering the solution to Eq. (97) is

$F(t) = \frac{k_0 P_0}{2\pi}\iiint_V \varepsilon(x,y,z)\frac{s\left(t - {}^{2r}/_{c_0}\right)}{r^2}dV$ (Eq. 98), where F is the backscattered signal detected at (0,0,0), $r = \sqrt{x^2+y^2+z^2}$ is the distance to the inhomogeneity, $V$ is the domain containing the inhomogeneities, and $k_0 = 2\pi f_0/c_0$ where $f_0$ is the dominant frequency of the source-signal *s(t)*. In case of isolated "point-like" inhomogeneities ("diffracting points") $\varepsilon(x,y,z) = \sum_i \varepsilon_i\,\delta(x-x_i, y-y_i, z-z_i)$ (Eq. 99), where $(x_i, y_i, z_i)$ are coordinates of the $i^{\text{th}}$ diffracting point and $\delta(x,y,z)$ is the 3-dimensional Dirac delta function. Inserting Eq. (99) into (98) we get $F(t) = \sum_i a_i\ s(t - t_i\,)$ (Eq. 100), where $a_i = \frac{k_0 P_0 \varepsilon_i^2}{2\pi r_i^2};\ t_i = \frac{2r_i}{c_0}$. The function *F(t)* in Eq. (100) can be made *stationary* by the usual *AGC* or *TAR* (*Automatic Gain Control*, *True Amplitude Recovery*) seismic processing steps, the (two-way) arrival times $t_i$ can be assumed Poisson-distributed, because of the *independence*, *homogeneity* and *rarity* of the diffraction points.[77]

We shall need *Campbell's Theorem*[78] about the *ACF* of the function $F(t) = \sum_i a_i\ s(t - t_{i)}$ : *Suppose that the amplitudes $a_i$ are independent Gaussian, with $\langle a_i\,\rangle = 0, \langle a_i^2\rangle = a^2$, the $t_i$ time instants are Poisson-distributed with density $\lambda$, that is the probability that there are exactly N*

[75] Berry called *diffractals* those waves that have encountered fractals. See: M.V. Berry 1979. Diffractals. *Journal of Physics A: Mathematical and General* 12(6): 781-797.
[76] Korvin, G. 1978b. 'Correlation properties of source-generated random noise, scattered on velocity inhomogeneities '. *Acta Geod. Geoph. et Mont. Acad. Sci. Hung*.13(1-2)1978: 201-210.
[77] Jánossy,L., Rényi, A. and Aczél, J. On composed Poisson distributions. Pt.1. Acta Math. 1(1950): 209-224.
[78] R y t o v, S. M., 1966: *Introduction to Statistical Radiophysics*. Nauka, Moscow (In Russian).

*arrivals in a time-interval* $[T, T+\tau]$ *is* $exp[-\lambda\tau]\frac{(\lambda\tau)^N}{N!}$ *, the wavelet s(t) is of zero mean* ($\int_{-\infty}^{\infty} s(t)dt = 0$*, and it is identically zero outside some finite interval* $[T_1, T_2]$*, then*

$R_{FF}(\tau) = \langle F(t)F(t+\tau)\rangle = \lambda a^2 \int_0^{\infty} s(t)s(t+\tau)dt.$ (Eq. 101).

We shall also need a generalization of this formula for the case of cross-correlation, due to Olshevsky[79]:

*Let* $F_1(t) = \sum_i a_i\ s_1(t - t_i, \xi_i)$ *and* $F_2(t) = \sum_j a_j\ s_2(t - t_j, \xi_j)$ *be two processes where* $s_1$ *and* $s_2$ *are different functions, both depending on a random parameter* $\xi$*. If the distribution function of* $\xi$ *is* $W(\xi)$*, and the definition of* $a^2$ *and* $\lambda$ *are as in Campbell's Theorem, then*

$\langle F_1(t)F_2(t+\tau)\rangle = \lambda a^2 \iint_{\xi} W(\xi) \int_0^{\infty} s(t)s(t+\tau)dtd\,\xi$ (Eq. 102)

The measurement geometry is shown in Fig. 18. We shall investigate the spatial-temporal correlation of the source-generated seismic noise $F_1$ observed at receiver $G_1$ at time $t_0$ and at another receiver $G_2$ (which is a distance *r* apart) at time instant $t_0 + \tau$. The geophones are at the points $G_1 = (-r/2, 0{,}0)$ and $G_2 = (r/2, 0{,}0)$, the source is at $O = (0{,}0{,}0)$, the z-axis points downwards. Denote by R the source-diffractor distance $\overline{OD}$, assume that $R \gg r$ (far field).

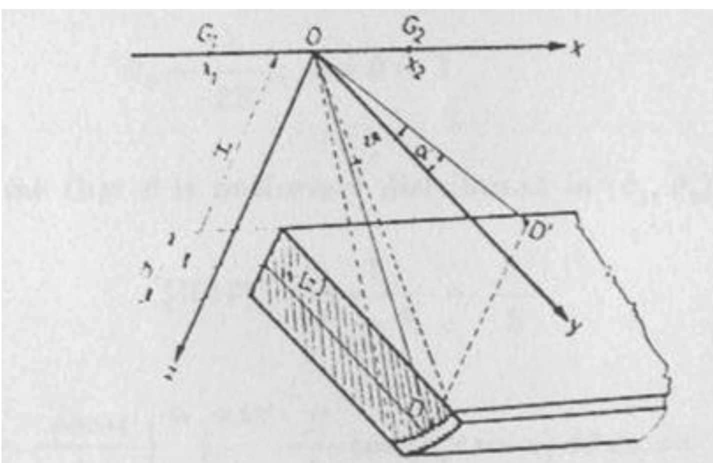


Fig. 18. Measurement geometry: O =source, $G_1$ & $G_2$ are receivers at positions $x_1$ and $x_2$ .

The backscattered noise records received by $G_1$ and $G_2$ are:

$F_1(t) = \sum_i a_i\, s(t - t_i - \frac{\Delta t(\alpha_i, \vartheta_i)}{2})$ (Eq. 103a)

$F_2(t) = \sum_j a_j\, s(t - t_j + \frac{\Delta t(\alpha_j, \vartheta_j)}{2})$ (Eq. 103b),

---

[79] Olshevsky, V.V. 1966. *Statistical Properties of Sea Reverberations*. Nauka, Moscow. (In Russian).

where $\Delta t(\alpha,\vartheta) \sim \frac{r}{c_0} cos\vartheta sin\alpha$ (Eq. 104).

If the distribution of the diffracting points $D_i$ is circularly symmetric, and with respect to depth is *W(z)*, then, putting $z = R \cdot sin\vartheta$, we have $Wz)dz = W(R \cdot sin\vartheta)Rcos\vartheta d\vartheta$ and using *Olshevsky's Theorem* (Eq. 102) we get - after lengthy integrations[80] - the *spatio-temporal correlation* of the two signals:

$$A(r,\tau) = \langle F_1(t)F_2(t+\tau)\rangle \sim const \cdot \lambda \cdot \langle a^2\rangle \frac{R}{2\pi}\int_0^{2\pi}\int_{\vartheta_1}^{\vartheta_2} W(Rsin\vartheta) \cdot \int_{-\infty}^{\infty} s(t - \frac{\Delta t(\alpha,\vartheta)}{2}) \cdot$$

$s\left(t + \tau + \frac{\Delta t(\alpha,\vartheta)}{2}\right) dtcos\vartheta d\vartheta d\alpha \approx const \cdot \lambda \cdot \langle a^2\rangle \frac{R}{2\pi}\int_0^{2\pi}\int_{\vartheta_1}^{\vartheta_2} W(Rsin\vartheta) \cdot \cos[\omega_0 \tau + k_0 rcos\vartheta sin\,\alpha]\, cos\vartheta d\vartheta d\alpha$ (Eq. 105)

where the integration limits are $\vartheta_1 = arc\sin\left(\left(H - \frac{h}{2}\right)/R\right)$; $\vartheta_2 = arc\sin\left(\left(H + \frac{h}{2}\right)/R\right)$. In the derivation I assumed the quasi-harmonicity of *s(t)*, what allowed me to write

$\int_{-\infty}^{\infty} s(t)s(t+\tau)dt \approx const \cdot cos\omega_0\, t$ (Eq. 106) where $\omega_0$ is the apparent circular frequency of the signal.

Three particular cases of Eq. (105) are important:

a) If *r=0*, $A(r,\tau) \approx const \cdot \lambda \cdot \langle a^2\rangle \frac{R}{2\pi}\int_0^{2\pi}\int_{\vartheta_1}^{\vartheta_2} W(Rsin\vartheta) \cdot \cos[\omega_0\, \tau]\, cos\vartheta d\vartheta d\alpha$ that is, by Eq. (106), Eq. (105) reduces to *Campbell's formula*.

b) Let $\tau = 0$ and assume the *scatterers are within a near-surface thin layer*. Then $H = 0, \frac{h}{R} \ll 1$ that is $\vartheta_1 = arc\sin(-h/2R) \approx -\frac{h}{2R}$; $\vartheta_2 \approx \frac{h}{2R}$; $\cos\vartheta \approx 1$. Assuming that $\vartheta$ is uniformly distributed in $(\vartheta_{1,}, \vartheta_2)$, that is $W(\vartheta) = \frac{1}{|\vartheta_1 - \vartheta_2|} \approx \frac{R}{h}$, we obtain for the normalized correlation function
$B(r) = \frac{A(r)}{A(0)} = const \cdot \mathcal{J}_0(k_0\, r)$ (Eq. 106). This correlation function fairly well agrees with the correlation function found in model experiments[81] (Fig. 19).

---

[80] For details see Korvin 1978b: 205.
[81] F. K. Levin & D. J. Robinson 1969. Scattering by a random field of surface scatterers . *Geophysics* 34: 170-179.

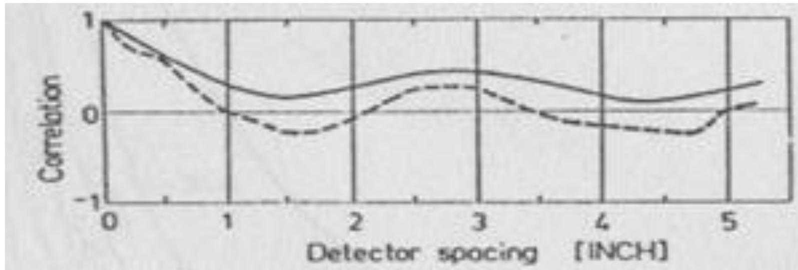


Fig. 19. Experimental correlation function for near-surface scatterers. Solid line: wide band noise, dashed line: filtered noise. From Levin & Robinson (1969).

c) Let $\tau = 0$ and assume the scatterers are *within an infinite half-space*. Then in Eq. (105) $\vartheta$ changes from $-\pi/2$ to 0, $W$ is uniform, and an easy calculation[82] gives the basic result for the normalized correlation function: $B(r) = \frac{A(r)}{A(0)} = \frac{\sin k_0 r}{k_0 r}$ (Eq. 107). The different mathematical forms of Eqs. (106) and (107) can be used to distinguish the two scattering mechanisms (i.e. coming from *near-surface*, or from the *half-space*).

3.1.D.3.2. THE OBSERVED WAVE-FORM OVER FRACTAL SCATTERERS[83]

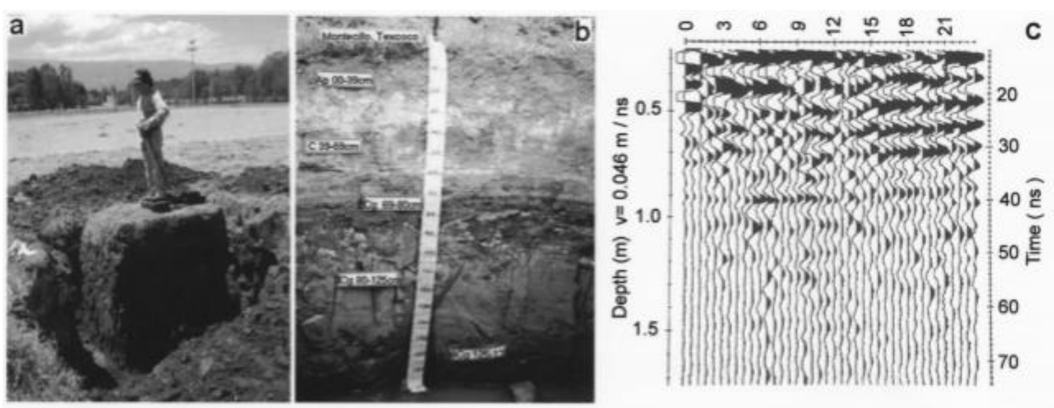


Fig.20. *a*. View of a monolith, removed from the soil at a Mexican site; *b*. its wall, showing macro- and micro-layers; *c*. Common-offset display of the *GPR* (Ground Penetrating Radar, with 225 MHz antenna) measurement, carried out on the top of the monolith. (From Oleschko et al. 2002).

Soil is heterogeneous at a wide range of length scales. Microscopy had proved the fractal nature of soil in the range 0.008 to 3mm; in our field studies in 2002 we extended this range to the

[82] See Korvin 1978b: 207.
[83] Oleschko et al. 2002, 2003, 2008; Korvin et al. 2017.

*macroscale* ($\sim 10^{-2}$ - $\sim 1m$ ). In water-saturated porous soil the high-permittivity points are associated with pore space, which is known to be a *mass fractal*[84], so our basic idea for designing the field experiment shown in Fig. 20 had been that microwaves scattered on these high-permittivity points and recorded by *GPR* would also show a signal with fractal properties. Indeed, I could prove mathematically, that *the backscattered radar signal has the same Hausdorff-dimension*[85] *as the mass-fractal dimension of the high-permittivity points in the explored soil*. Assssume that a narrow-band radar signal is sent to a soil layer between $0 \leq z \leq Z_{max}$, where depth axis points downwards, both source and receivers are at $x = 0, z = 0$. If soil resistivity is between $0.1 - 10\Omega m$, and with moderate permittivity contrasts, multiple scattering can be neglected, and the received signal is $A(t) \propto \sum_{j=1}^{N \gg 1} I_j\,(q_j) n_j(q_j) \exp[iq_j ct]$ Eq. (108), where $I_j(q_j)$ is scattered intensity from a soil element with scattering vector $q_j$, $n_j(q_j)$ is the number of scatterers with the same $q_j$, *c* is average wave velocity in soil. By *Hunt's Theorem*[86] , *if* $A_j(q_j) = I_j(q_j) n_j(q_j)$ *satisfies the conditions (i)* $a|q_j| \leq |q_{j+1}| \leq b|q_j|$ *for some* $1 < a < b$ *and* $for\ all\ j$, *and (ii)*$-1 < \lim_{j \to \infty} \frac{log A_j}{log|q_j|} = -H < 0$, *then A(t) is a self-affine function with Hurst exponent H. The graph of A(t) has a fractal dimension D = 2-H which is the same as the mass fractal dimension of scatterers in the planar soil section.*

We assume that $n_j(q_j)$ scales as $n_j(q_j) \propto |q_j|^{D_m}$ (Eq. 109). As most scatterers are randomly oriented 2-dimensional objects (platelets of clay, cracks, fissures, etc.), for a single scatterer $I_j(q_j) \propto |q_j|^{-2}$ (Eq. 110). In a fractal soil both solid grains and pores belong to a finite number of geometrically decreasing size classes[87], that is in the radar's penetration range only a finite number of scattering vectors $q_j$ can occur, and ordering them by increasing length, condition (i) can be satisfied. By Eqs. (109 &110) $A_j(q_j) = I_j(q_j) n_j(q_j) \propto |q_j|^{D_m - 2}$ and indeed, taking the limit in condition (ii): $-1 < \lim_{j \to \infty} \frac{log A_j}{log|q_j|} = D_m - 2 < 0$ (in the plane of measurement). Consequently, the graph of *A(t)* has the same fractal dimension as the mass fractal dimension of the scatterers in the plane of measurement.

We also verified the relation $D_m = 2 - H$ between the mass fractal dimension of the high-permittivity points in the plane of measurement, and the self-affinity exponent *H* of radar traces by numerically solving[88] the wave equation of the *EM* field:

---

[84] Korvin, G. 1992a. *Fractal Models in the Earth Sciences*. Amsterdam: Elsevier.
[85] Korvin 1992a: 172.
[86] B.R. Hunt 1988.. The Hausdorff dimension of graphs of Weierstrass functions .*Proc.Am.Math.Soc*.,126:791.
[87] Hansen, J. P. and Skjeltorp, A.T.1988. Fractal pore space and rock permeability implications. *Physical Review B (Condensed Matter)* 38(4): 2635-2638.
[88]Details are in Gabor Korvin, Ruben V. Khachaturov, Klaudia Olechko. Gerardo Ronquillo, Maria de Jesus Correa Lopez & Juan-José Garcia. 'Computer simulation of microwave propagation in heterogeneous and fractal media'. Computers & Geosciences 100(2017): 156-165.

$\frac{\partial^2}{\partial z^2}E(x,z) + \kappa^2[sin^2\vartheta_0 + \varepsilon(x,z) - 1]$ (Eq. 111)

where $= \omega/c$ is wave number in vacuum, $\vartheta_0$ yaw-angle of incident wave, $\varepsilon(x,z)$ complex dielectric permittivity. Left- and right boundary conditions are

$E'_z(x,0) + i\gamma_0 E(x,0) = 2i\gamma_0 e_0$ (Eq, 112.a)

$E'_z(x,L) - i\gamma_0 E(x,L) = 0$ (Eq, 112.b)

where $i = \sqrt{-1}$, $\gamma_0 = \kappa \sin\vartheta_0$ , $\gamma = \kappa\sqrt{sin^2\vartheta_0 + \varepsilon(x,L) - 1}$, and $e_0$ is initial wave amplitude. Equation (111) was approximated to the 2nd order by a symmetric difference scheme, and solved by the complex version of Samarskii's sweep method[89].

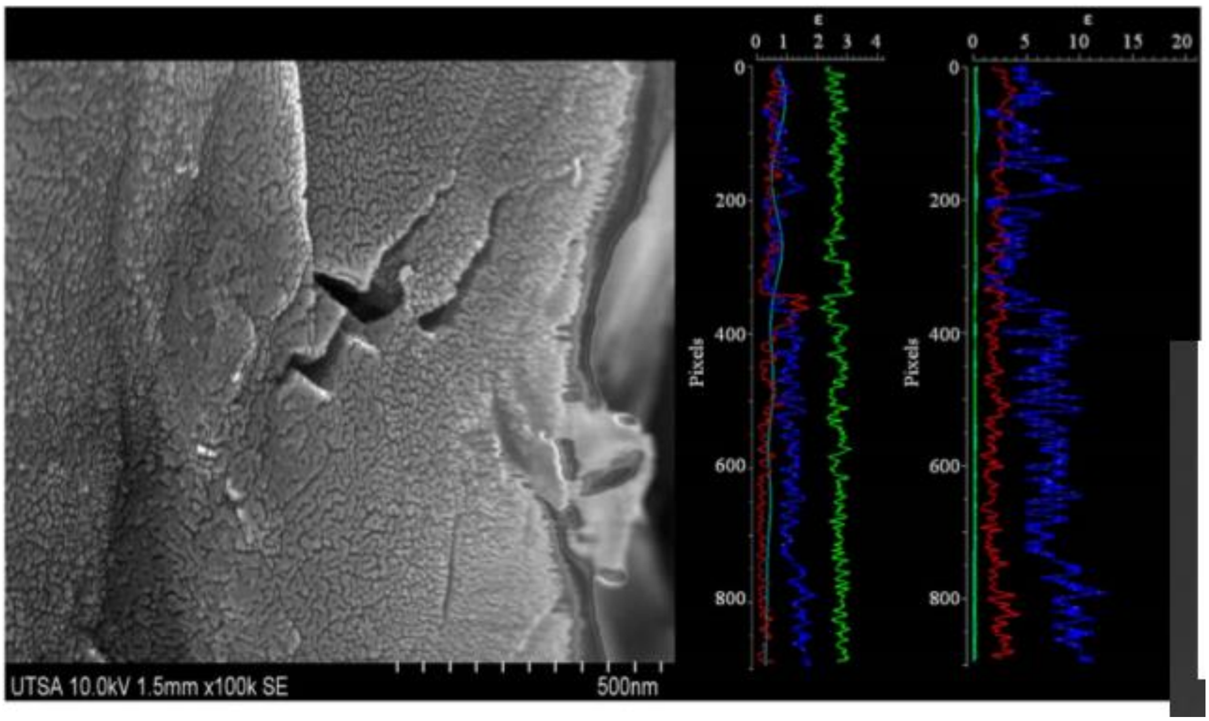


Fig.21. EM wave-propagation modeling with the *EMSoil-2.0*, Maxwell image-exploration program. Permittivity is assumed to be proportional to gray-scale value of the image.

EXCURSUS 3. MULTIPLE WAVE SCATTERING FROM FRACTAL AGGREGATES[90]

In the previous Section (3.1.D.3.2.) I described a mathematical model to relate the fractal dimension of the *GPR* record measured over a soil layer to the dimension of the self-similar pore structure of the soil. The signals returning from the fractal structure are self-affine functions of time, and their *Hurst exponent H* was found simply related to the mass-

[89] Samarskii, A.A.,1989. *The Theory of Difference Schemes*. (In Russian.), Nauka, Moscow.
[90] Korvin, G. & Oleschko, K. 'Multiple wave scattering from fractal aggregates'. *Chaos, Solitons and Fractals* 19(2)2004: 421-425.

fractal dimension D of the scatterers. To prove this mathematically for the case of the *GPR*, the scattered wave field was considered as a generalized *Weierstrass function*

$A(t) \propto \sum_{j=1}^{N\gg1} I_j\left(q_j\right)n_j\left(q_j\right)\exp[iq_jct]$ (Eq. 108), we assumed a hierarchic grain-size- and pore-size distribution and applied *Hunt's theorem* to arrive at a relation between $H$ and *D*. A relation between $H$ and $D$ was indeed derived but multiple scattering had to be neglected because of the difficulties of its analytic treatment. Also in literature, both the conventional *Fourier framework treatment* of fractal scattering[91] and the *time-domain approach*[92] neglect multiple scattering. We studied[93] the general problem, to see how multiples affect the fractal dimension of the wave field and found a probabilistic estimate for the spectral contribution of waves multiply scattered by the fractal structure (Eqs. 4.9 and 4.11 of Korvin & Oleschko 2004). These equations show that for extended fractal media with strong scattering cross-section, multiple scattering affects the value of the fractal dimension of the scattered wave field: it decreases the wavefield's Hausdorff dimension. It was also found (Eq. 4.8 of Korvin & Oleschko 2004) that multiply scattered waves in the fractal medium create *spurious resonance(s)* in the high-frequency ("blue") part of the received wavefield's spectrum.

## 3.2. ENTROPY

### 3.2. A. SHALE COMPACTION MAXIMIZES ENTROPY[94]

EXCURSUS 4. THE MAXIMUM ENTROPY METHOD Suppose a measurable rock property $\lambda$ can assume values belonging to $L$ distinct ranges $\Lambda_1, \ldots, \Lambda_L$. If we measure $\lambda$ on a large number $N$ of samples, we will find $N_1$ values in range $\Lambda_1, \ldots, N_L$ values in range $\Lambda_L$. Letting $N = \sum_{i=1}^{L} N_i$ , $p_i = \frac{N_i}{N}$, the set of numbers

$$\{p_1, p_2, \cdots, p_L\}, \quad p_i \geq 0, \sum_{i=1}^{L} p_i = 1 \qquad \text{(Eq. 113)}$$

constitute a *discrete probability distribution*. It can represent different degrees of randomness: the distribution $p_1 = 1, p_2 = p_3 = \cdots = p_L = 0$ is *not random*; the distribution

[91] Radlinski,A.P. *et al.* Fractal geometry of rocks. *Phys. Rev. Lett.* 1999;82:3078–81; Allain, C. & Cloitre, M. Optical Fourier transforms of fractals. *In*: Pietronero L, & Tosatti E, (eds). *Fractals in Physics*. Amsterdam: Elsevier; 1986: 61–64; Guerin C. *et al.* Electromagnetic scattering from multi-scale rough surfaces. *Wave Random Media* 1997;7:331–49.
[92] Guerin, C.A. & Holschneider, M. Time-dependent scattering on fractal measures. *J Math Phys* 1998;39(8):4165–94; Guerin, C.A. &, Holschneider, M. Scattering on fractal measures. *J Phys A: Math Gen* 1996; 29:7651–67.
[93] Korvin & Oleschko 2004.
[94] Korvin, G. 'Shale compaction and statistical physics'. *Geophysical Journal – Royal Astronomical Society* 78 (1)1984: 35-50.; Korvin, G. 2020d. 'Statistical Rock Physics' *In*: B. S. Daya Sagar, Quiming Cheng, Jennifer McKinley and Frits Agterberg (Eds.) Earth Sciences Series. *Encyclopedia of Mathematical Geosciences*. Springer (In Press).

$p_1 = \frac{1}{2}, p_2 = \frac{1}{2}, p_3 = 0, \cdots, p_L = 0$ is *not too random*, the distribution where all lithologies are equally possible, $p_1 = p_2 = p_3 = \cdots = p_L = \frac{1}{L}$ is as *random as posible*. To characterize quantitatively the "randomness" of the distribution $\{p_1, p_2, \cdots, p_L\}$, count how many ways one can classify the N samples such that $N_1 = p_1 N$ belongs to $\Lambda_1$, $N_2 = p_2 N$ to $\Lambda_2$, …, $N_L = p_L N$ to $\Lambda_L$. The number of such classifications is given by $\Pi = \frac{N!}{N_1! N_2! \cdots N_L!}$ (Eq. 114). The larger is Π, the more random the distribution. Instead of Π it is easier to estimate log Π ("log" always means natural logarithm in this *Dissertation*), $log\Pi = logN! - logN_1! - \cdots - logN_L$ (Eq. 115). If n>>1 we have the approximate Stirling's formula $\log(n!) = \log(1 \cdot 2 \cdot 3 \cdots n) = log1 + log2 + log3 + \cdots + logn$

$\approx \int_1^n logxdx = nlogn - n \sim nlogn$ (Eq. 116). Using this approximation in Eq. (115): $log\Pi \sim NlogN - \sum_{i=1}^{L} N_i \, logN_i = -\sum_{i=1}^{L} N_i \, log\frac{N_i}{n} = -N\sum_{i=1}^{L} \frac{N_i}{N} log\frac{N_i}{n}$

$= -N\sum_{i=1}^{L} p_i \, logp_i = N \cdot S(p_1, p_2, \cdots, p_L)$ (Eq. 117)

where $S(p_1, p_2, \cdots, p_L) = -\sum_{i=1}^{L} p_i \, logp_i$ is the *Shannon entropy* of the probability distribution $(p_1, p_2, \cdots, p_L)$.

In Rock Physics we frequently have to solve an *over-determined* system of equations

$$\left.\begin{array}{ccc} F_1(\xi_1, \xi_2, \cdots, \xi_L) & = & y^{(1)}_{measured} \\ \vdots & \vdots & \vdots \\ F_M(\xi_1, \xi_2, \cdots, \xi_L) & = & y^{(M)}_{measured} \end{array}\right\} \quad (L \gg M) \qquad \text{(Eq. 118)}$$

In the *Maximum Entropy (ME) Technique* we accept that particular solution of this system whose *Shannon entropy is maximal*.

### 3.2.A.1. A THEORETICAL DERIVATION OF ATHY'S LAW

By Athy's law[95] (Athy 1930) in thick pure shale porosity decreases with depth as
$\Phi(z) = \Phi_0 \exp(-kz)$ (Eq. 119)

where $\Phi(z)$ is porosity at depth $z$, $\Phi_0$ porosity at the surface, and $k$ a constant. Assuming all pores have the same volume, the porosity of a rock is proportional to the number of pores in a unit volume of the rock. Athy 's rule states in this case that the pores in compacted shales are distributed in such a manner that their number in a unit volume of rock exponentially decreases with depth. There are several analogies of this rule in *Statistical Physics*. The most familiar is the *barometric equation* of Boltzmann expressing the density $\rho(z)$ of the air at altitude z as $n\rho(z) = \rho(0) \cdot exp\left[-\frac{mgz}{kT}\right]$ (Eq. 120), where *m* is the mass of a single gas molecule, *g* gravity acceleration, *k* Boltzmann's constant, *T* absolute temperature. In *Statistical Physics*[96] Boltzmann's barometric equation is derived from the assumptions that the gas particles move

---

[95] Athy, L.., 1930. Compaction and oil migration. *Bull. Am. Ass. Petrol. Geol.* 14: 25-35.
[96] Landau, L.D. & Lifshitz, E.M.,1980. *Statistical Physics*. Pt.1. (Vol. 5 of *Course of Theoretical Physics*). Pergamon Press: Oxford, pp. 106-114.

independently of each other and the system tends toward its most probable (*maximum entropy*) state.

During compaction of shale, water is expulsed and clay particles rearrange themselves towards a more dense system of packing. In Korvin (1981) I adopted Litwiniszyn's model[97] and considered shale compaction history as an *upward migration of pores*. Take a rectangular prism *P* of the present-day shale of unit cross-section reaching down to the basement at depth $Z_0$ , and suppose its *mean porosity* is $\Phi$ i.e. it contains a fractional volume $\Phi Z_0$ of fluid and a volume $(1-\Phi)Z_0$ of solid clay particles. Assume that the compaction process is *ergodic*, i.e. it tends towards the *maximum-entropy final state*. Neglecting the actual depositional history we assume for time *t = 0* an initial condition where a prism of water of unit cross-section, height $\Phi Z_0$ and density $\rho_1$ had been overlain by solid clay of height $(1-\Phi)Z_0$ and density $\rho_2, \rho_1 < \rho_2$ (Fig. 22).

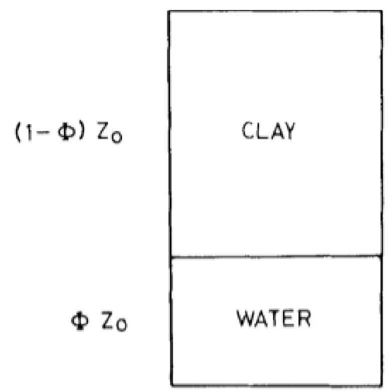


Fig. 22. The initial stage of deposition.

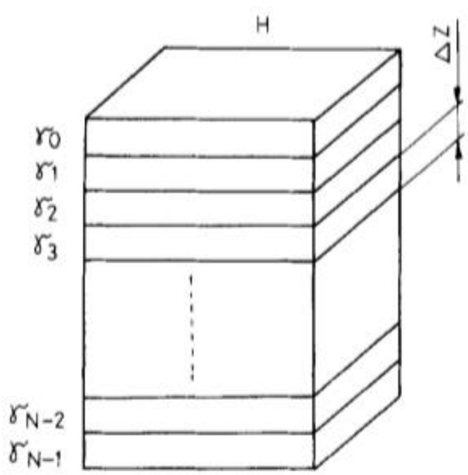


Fig. 23. Definition of the macroscopic states

[97] Litwiniszyn, J. 1974. *Stochastic Methods in the Mechanics of Granular Bodies*. International Centre for Mechanical Sciences. Courses and Lecture Notes no. 93. Springer-Verlag:Wien.

Divide the prism of water into $\mathfrak{N}$ "particles" (water-filled pores), each of volume $\Delta V$ , which at time *t = 0* started to migrate upwards independently of each other, until the final (*maximum entropy*) state had been reached. The initial potential energy of the system had been

$$E = \mathfrak{N} \cdot \Delta V \cdot g(\rho_2 - \rho_1)(1 - \Phi)Z_0 \;, \qquad \text{(Eq. 121)}$$

where initial porosity and particle number are connected by $\mathfrak{N} = \frac{Z_0 \Phi}{\Delta V}$ . Divide the prism *P* into *N* equal slabs of thickness $\Delta z = Z_0/\Delta z$ , denote the $i^{\text{th}}$ slab by $\gamma_i$ $(i = 0, 1, \cdots, N-1)$ , and divide the prism *P* into $N^* = Z_0/\Delta V$ non-overlapping small cubes (Fig. 23). We have $\mathfrak{N} \ll N^*$ if $\Phi$ is sufficiently small. We rank the *N** possible positions, called "states", of a pore into *N* groups: a pore is said to belong to the group $\gamma_i$ if and only if its centre (*x*, *y*, *z*) lies within the slab $\gamma_i$. This implies every group $\gamma_i$ contains $G = \Delta z/\Delta V$ states. Suppose that $N_i$ pores are found in state $\gamma_i$ . The numbers $N_i$ satisfy two constraints, the *conservation of pore-particle number*, and the *conservation of total potential energy*:

$$\textstyle\sum_{i=0}^{N-1} N_i = \mathfrak{N} \qquad \text{(Eq. 122a)}$$

$$\textstyle\sum_{i=0}^{N-1} \varepsilon_i N_i = E \qquad \text{(Eq. 122b)}$$

where E is the total energy (see Eq. 121); $\varepsilon_i$ is the potential energy of a single pore particle in group $\gamma_i$, due to buoyancy:

$$\varepsilon_i = \mathrm{g}(\rho_2 - \rho_1) \cdot \Delta V \cdot i \cdot \Delta z \qquad \text{(Eq. 123)}$$

The set of numbers $\{N_i\}$ determine the *macroscopic* distribution of pores inside the prism *P*. Apart from a constant factor, the entropy of the distribution is

$$S = \textstyle\sum_{i=1}^{N-1} N_i log \frac{eG}{N_i} \qquad \text{(Eq. 124)}$$

Denote the average number of pore particles in group $\gamma_i$ by $\bar{n}_i$ , then $\bar{n}_i = N_i/G$ ,

$S = G \sum_{i=1}^{N-1} \bar{n}_i log \frac{e}{\bar{n}_i}$ (Eq. 125) and the constraints (122a, b) become

$$G \cdot \textstyle\sum_{i=0}^{N-1} \bar{n}_i = \mathfrak{N} \;,\; G \cdot \sum_{i=0}^{N-1} \bar{n}_i \varepsilon_i = E \qquad \text{(Eq. 126a, b)}$$

The pore particles will migrate to such a position where the entropy (Eq. 124) is maximal. To maximize the entropy subject to the constraints (126a, b), we introduce *Lagrange multipliers* $\alpha, \beta$ , and assume that

$\frac{\partial}{\partial \bar{n}_i}\left(S + \alpha \frac{\mathfrak{N}}{G} + \beta \frac{E}{G}\right) = 0 \;\; (i = 0,1,\cdots,N-1)$ , that is $\bar{n}_i = exp(\alpha + \beta\varepsilon_i)$ , wherefrom $exp\, \alpha = \frac{\Phi}{1-\phi}$ , $\beta = -\frac{1}{E}$ and $\Phi(\mathrm{z}) = \frac{\Phi}{1-\phi} \cdot exp\left[-\frac{z}{(1-\phi)Z_0}\right]$ (Eq. 127)

Identifying the first factor in Eq. (127) with surface porosity $\Phi_0$ , the equation becomes

$\Phi(\mathrm{z}) = \Phi_0 \cdot exp\left[-\frac{(1+\Phi_0)z}{Z_0}\right]$ (Eq. 128). an equation that reproduces Athy's compaction law.

## 3.2.B. APPLICATIONS OF ENTROPY

### 3.2.B.1. ENTROPY AS PORE DETECTOR[98]

In a later study, Shannon entropy occurred in a very different context, namely as the *entropy of shortest distance* (*ESD*) between geographic elements ("elliptical intrusions", "lineaments", "points") on a map, or between "vugs", "fractures" and "pores" in the microscopic image of rocks. The procedure is applicable at all scales, from micrographs to aerial photos.

In the probabilistic treatment of irregularly placed points the *distances to nearest neighbor,* and their probability distribution, have become standard tool to characterize spatial relationships in populations[99]. It was first proved by Hertz[100], that if $N \gg 1$ points are distributed on the plane with density ρ, and for every point $P_i, i = 1, \cdots, N$ its distance to the nearest neighbor is $r_i, i = 1, \cdots, N$ then the expected value of $r_i$ is

$$\langle r \rangle = \lim_{N \to \infty} \frac{\sum_1^N r_i}{N} = \frac{1}{2\sqrt{\rho}} \qquad \text{(Eq. 129)}$$

For a regular square lattice, all distances $\{r_i\}$ are equal, and the Shannon entropy of the distance-to-nearest-neighbor distribution is 0. The more irregular is the lattice, the larger will be the range of the values in the set $\{r_i\}$, and consequently, the larger will be its Shannon entropy. If, for a randomly selected point $P_i$, we define $p_i = \min\{dist(r_i, r_j) | j \neq i\}$ where *dist* is the Euclidean distance, then $H = -\sum_{i=1}^{W} p_i \ln p_i$ is a measure of the irregularity of the point distribution. And, (because $H$ only depends on the probabilities, but not on the actual distances) this measure is *scale-free*.

The "*shortest distance to neighboring element*" idea was first studied in the *PhD Thesis* (in Economic Geology) of B. Sterligov[101]. Later, our group realized that by associating his three geographic elements "ellipses", "lineaments", "points" with the microscopically observable "vugs", "fractures" and "pores" of triple-porosity naturally fractured vuggy carbonates, we get a powerful new tool for the digital processing, analysis, and classification of the void space in carbonates, and other reservoir rocks. The procedure is applicable at all scales, from micrographs to aerial photos.

---

[98] Korvin, G., Sterligov, B., Oleschko, K. & Cherkasov, S. ‘Entropy of shortest distance (*ESD*) as pore detector and pore-shape classifier’. *Entropy* 15 (6)2013: 2384-2397;
[99] P.J. Clark & F.C. Evans, 1954: Distance to nearest neighbor as a measure of spatial relationships in populations. *Ecology*, 35(4): 445-453.
[100] P. Hertz, 1909: Über den gegenseitigen durchschnittlichen Abstand von Punkten, die mit bekannter mittlerer Dichte im Raume angeordnet sind. *Math. Annalen* 64: 387-398.
[101] B. Sterligov, 2010: *Analyse probabiliste des relations spatiales entre les gisements aurifères et les structures crustales: developpement méthodologique et applications à l'Yennisei Ridge (Russie)*. Ph.D. Thesis, Lomonosov State University, Moscow & Institut des Sciences de la Terre d'Orleáns.

Out of the many possible applications of the *ESD* concept, only the *sliding window entropy filtering for pore boundary enhancement* will be discussed. Using standard notations of geometry[102], if $A$ and $B$ are sets in the *n*-dimensional Euclidean space $R^n$ of finite measure $\mu(A) < \infty, \mu(B) < \infty$, then their *Minkowski sum* is defined as $A \oplus B = \bigcup_{x \in A; y \in B} (x + y)$ (Eq. 130)

In the special case when B is an *n*-dimensional hypersphere, we call $S(r; A) = A \oplus B$ the *extended sphere of radius r around A*. In the 2-dimensional (planar) case, assuming that the set *A* is convex, and denoting the length of its circumference by *c(A)*, by *Tomiczková's Theorem*[103] the area of the extended sphere $S(r; A)$ is a monotone increasing quadratic function of the radius *r*:

$$\mu\{S(r; A)\} = \mu(A) + \mu(B) + rc(A) = \mu(A) + r^2\pi + rc(A) \qquad \text{(Eq. 131)}$$

Consider now a "pore" *A* in the digital image, suppose the distance of *A* from the nearest pore is *D*. Let Δ denote pixel size, select a reasonable large $(d\Delta \times d\Delta)$-size (say $10 \times 10$ pixels) window *W*, where $d\Delta$ is less than half the distance of *A* from the closest pore, i.e. $d\Delta \le \frac{D}{2} = N\Delta$. The "pore" in the image is distinguished with a separate color, or a distinct range of values of gray scale. The boundary of the pore is generally *diffuse,* not clearly defined. For its better definition we introduce the following sequence of planar sets (see Fig. 24):

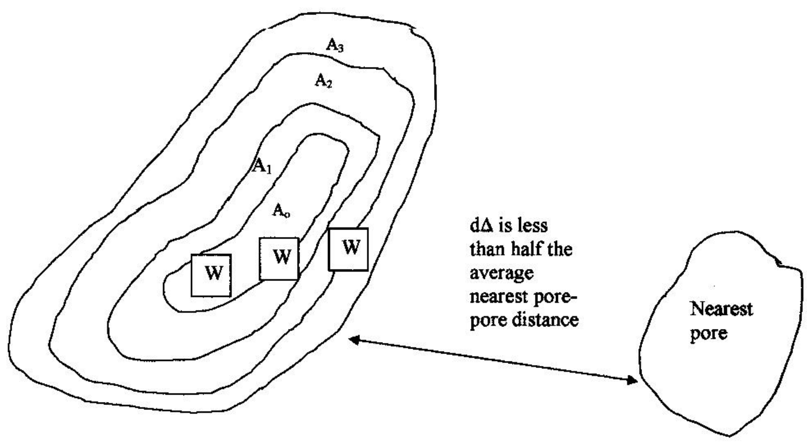


Fig. 24.Illustration of the *sliding window entropy* technique for a better definition of the boundary of the pore $A_0$.

---

[102] Mark de Berg, Marc van Kreveld, Mark Overmars & Otfried Schwarzkopf, 1997: *Computational Geometry. Algorithms and Applications*. Springer Verlag, Berlin; Mark Berman, 1977: Distance distributions associated with Poisson processes of geometric figures. *J. Appl. Prob*. 14:195-199.

[103] Světlana Tomiczková, 2005: Area of the Minkowski sum of two convex sets. *Proc. 25$^{th}$ Conf. on Geometry & Computer Graphics*, Sept. 12-16, 2005, Prague:255-260.

The sliding window W, which moves out of $A_0$, has a size less than half the distance to the nearest pore. The sequence $A_0 \subset A_1 \subset \cdots \subset A_N$ is strictly increasing, the difference sets $\rho_k = A_k \setminus A_{k-1}$ $(k = 1, \cdots, N)$ form one-pixel-wide "rings" or "halos" around $A_0$.

$$\begin{aligned} A_0 &= A = S(0; A) \\ A_1 &= S(\Delta; A) \\ A_2 &= S(2\Delta; A) \\ &\vdots \\ A_N &= S(N\Delta; A) = S(D/2; A) \end{aligned} \qquad \text{(Eq. 132)}$$

The sequence of these sets satisfies (where in the 2-D case the measure μ is *area*)
$A = A_0 \subset A_1 \subset \cdots \subset A_N$ and $\mu(A) < \mu(A_1) < \cdots < \mu(A_N)$. (Eq. 133a, b)
Taking set-theoretical differences between successive extended spheres around $A$ of respective radii $k\Delta$ and $(k-1)\Delta$ we get a sequence of rings $\rho_1, \cdots, \rho_N$ $(k = 1; 2, \cdots, N)$ around the pore $A$ defined as: $\rho_k = A_k \setminus A_{k-1}$ $(k = 1, \cdots, N)$. If the moving window $W$ is closer to the pore $A$ than *D/2* then $W = (W \cap A) \cup (W \cap \rho_1) \cup \cdots \cup (W \cap \rho_N)$ (Eq. 134)
and, consequently, (because the rings are distinct):

$$\mu(W) = \mu(W \cap A) + \sum_{i=1}^{N} \mu(W \cap \rho_i)\ . \qquad \text{(Eq. 135)}$$

Suppose the square-shaped window W moves, without rotation, staying parallel to its original position, along a linear path as shown in Fig. 24. In the figure, W starts to move from a position where it is fully inside *A*, $W \subset A$, then it passes through intermediate positions when only a part of W is inside the pore: $W \cap A \neq \emptyset$, $W \cap A \subset W$; up to a final position when W is fully outside the pore and it is covered by M successive rings: $A \subset \bigcup_{i=k}^{k+M} \rho_i; k \geq 1$.

In any position of the moving window, the altogether $d^2$ pixels in $W$ define the set of distances $\{\delta_{11}, \cdots \delta_{1d}, \cdots, \delta_{d1}, \cdots, \delta_{dd}\}$ where $\delta_{ij}$ is the shortest distance (with the precision of pixel-size Δ) between the pixel $p_{ij} \in W$ and the pore *A*, $i, j = 1, 2, \cdots, d$. Considering these distances as *random variables*, we can compute their empirical probability distribution $\{p_0, p_1, \cdots, p_k, \cdots, p_N\}$ where

$$p_k = \#\{\delta_{ij} \mid \delta_{ij} = k\Delta\} / d^2, \qquad \text{(Eq. 136)}$$

and the *Shannon entropy* of this distribution $H = -\sum_{k=1}^{N} p_k \ln p_k$. Consider the three possible positions of the window *W*. If *W* is fully inside *A*, $W \subset A$, then all distances $\delta_{ij}$ are 0, so that $\{p_0 = 1, p_1 = \cdots = p_N = 0\}$ and $H = 0$. If *W* is fully outside *A* but still inside the extended sphere of radius $N\Delta$ around A, then in a typical case it will have non-empty intersections with *d* consecutive rings:

$W \cap \rho_i \neq \emptyset$ for $i = k, k+1, \cdots, k+d-1; 1 \leq k \leq N+1-d$, (Eq. 137) in such a way that each intersection contains about $d$ pixels, and in the set $W \cap \rho_i$ all distances are equal to some $\delta_i$. In this case, the typical probability distribution will be

$$\{p_i = d/d^2 = 1/d \quad for \quad k \leq i \leq k+d-1 \quad and \quad p_i = 0 \quad otherwise\}. \qquad \text{(Eq. 138).}$$

The corresponding Shannon entropy is $H = -\sum_{i=0}^{d-1} \frac{1}{d} \ln \frac{1}{d} = \ln d$. (Eq. 139)

Consider now when part of the window W lies inside pore $A$, the rest of it is outside in such a way that it has non-empty intersections with the first $l$ rings: $W \cap A \neq \emptyset$, $W \cap \rho_i \neq \emptyset$ for $i = 1, 2, \cdots, l$ where $l < d$. In a typical case each intersection with the rings contains about $d$ pixels, and in the set $W \cap \rho_i$ all distances are equal to $\delta_i$. In this case the probability distribution is

$$\left\{ p_0 = \frac{d^2 - dl}{d^2}; p_1 = \cdots = p_l = \frac{1}{d} \quad and \quad p_i = 0 \quad otherwise \right\} \qquad \text{(Eq. 140)}$$

which yields the entropy $H = -\left(1 - \frac{l}{d}\right) \ln\left(1 - \frac{l}{d}\right) + \frac{l}{d} \ln d$. (Eq. 141)

Figure 25 shows, for the case when W consists of $10 \times 10$ pixels, how the Shannon entropy (Eq. 141) increases as W gradually moves out from the pore.

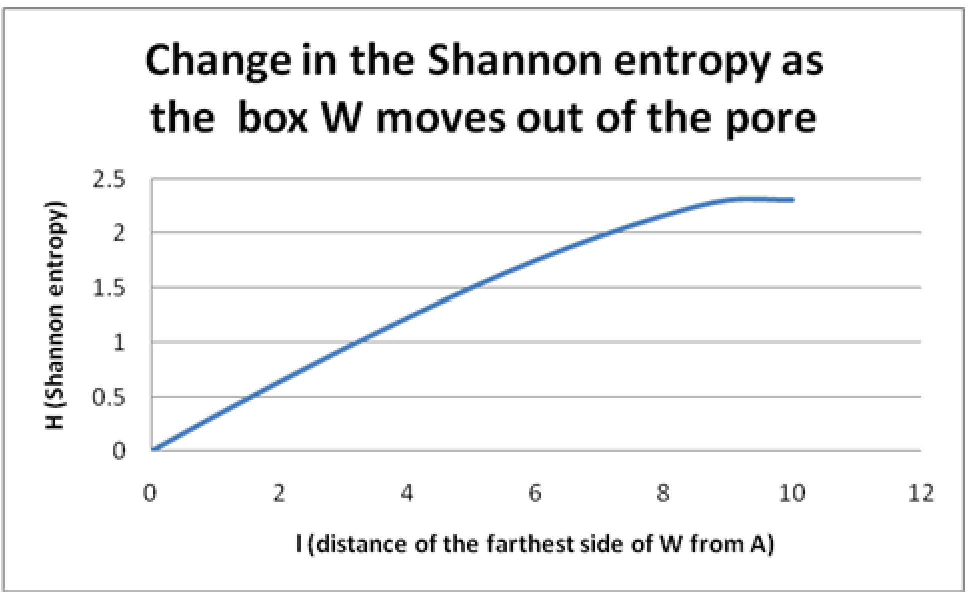


Fig. 25. Change of the Shannon entropy (Eq. 141).

As seen from this graph, we can define the boundary $\partial A$ of the pore A with the following algorithm: Select the size of $W$ less than the half distance between nearest pores. In any position of the moving window $W$ compute the distances $\{\delta_{11}, \cdots \delta_{1d}, \cdots, \delta_{d1}, \cdots, \delta_{dd}\}$ of its $d^2$ pixels from the nearest pore with the precision of pixel-size $\Delta$. Define the probability distribution $\{p_0, p_1, \cdots, p_k, \cdots, p_N\}$ where $p_k = \#\{\delta_{ij} | \delta_{ij} = k\Delta\} / d^2$ (see Eq. 136), and calculate the Shannon entropy $H=-\sum_{k=1}^{N} p_k \ln p_k$ . When $W$ is fully inside a pore, then $H=0$, when $W$ is moving out of the pore, step by step, the entropy of distances from the nearest pore will increase to $\ln d$ (according to Eq. 141). The maximal possible entropy of the distribution of distances $\{\delta_{11},\cdots\delta_{1d},\cdots,\delta_{d1},\cdots,\delta_{dd}\}$ would occur when all $\delta_{ij}$ are different, and this would be twice as large as $H$ in Eq. (139):

$$H_{\max}=-\sum_{i=1}^{d}\sum_{j=1}^{d}\frac{1}{d^2}\ln\frac{1}{d^2}=2\ln d \qquad (142)$$

If we select $W$ as $(10\times10)$ pixels, in Eq, (139) $\ln d=\ln 10=2.303$, and it is reasonable to define the *interior of the pore* with the inequality $H=-\sum_{k=1}^{N} p_k \ln p_k \leq 2$ . The boundary obtained in this way can be further smoothed using some *2-D filtering*, or *shaping* algorithm.

### 3.2.B.2. RELATIVE ENTROPY TRIANGLE IN AGROECOMETRY[104]

Some 20 years ago I was asked by a Mexican partner to find an algorithm to plot the *well-being function* of a country, state, or any other complex *Economic-Social-Ecologic System* on an *ECON-SOC-ECOL* ternary diagram. The main problem had been that the economic, social and ecologic variables are sometimes fuzzy concepts, semantic variables, and even if all three can be expressed in numbers, then not in *commensurable units* (as e.g. *ECON* = Gross National Income [US$], *SOC* = Life Expectancy [Years], *ECOL*= Per capita CO2 emission per year [Megaton]).
I recalled the famous "*how to keep the forecaster honest*" paradigm[105] from the early years of *Information Theory*, which asked how to design a payoff system which would force the forecaster to give an unbiased prediction of an unknown distribution of probabilities. It had been proved mathematically[106] that the way to do this is intimately connected with *Shannon entropy*.

Let the probability of the $i^{\text{th}}$ possible event be $p_i, i=1,\cdots,N$ and suppose the forecaster gets a payoff $f(p_i), i=1,\cdots,N$ if he predicts this event, that is his expected payoff is $\sum p_i f(p_i)$. If we want to keep the forecaster honest, we must select a function $f(p_i)$ such that for any other probability distribution $q_i, i=1,\cdots,N$ one has

---

[104] Klavdia Oleschko, Benjamin Figuerora-Sandoval, Gabor Korvin & Maria Martinez Menes. ‘Agroecometry: a toolbox for the design of virtual agriculture’. *Agricultura, sociedad y desarollo* 1(4)2004: 53-71 (In English & Spanish).

[105] I.J.Good, 1952: Rational decisions. *J. Roy. Stat. Soc. Ser. B*. 14: 107-114; I.J. Good, 1954: *Uncertainty and Business Decisions*. Liverpool University Press, Liverpool; J. McCarthy, 1956: Measures of the value of information. *Proc. Nat'l. Acad. Sci.* 10, 1956: 42(9): 654-655.

[106] P. Fischer, 1972: On the inequality $\sum p_i f(p_i) \geq \sum p_i f(q_i)$ . *Metrika* 18, 199-208; J. Aczél & Z. Daróczy, 1957: *On Measures of Information and their Characterization*. Academic Press, New York.

$$\sum p_i f(p_i) \geq \sum p_i f(q_i) \qquad \text{(Eq. 143)}$$

that is, the expected payoff is maximal if the forecaster predicts the events according to their correct probability. In a brilliant paper, my childhood friend and university school-mate Pál Fischer proved[107] that the only function satisfying Inequality (143) is $f(p) = const \cdot \log(p)$ that is – apart from a constant factor – the expected payoff is the Shannon entropy $H = -\sum p_i \log(p_i)$. Putting aside the "forecaster" analogy, we can say that *the only reasonable and unbiased quantitative "value" what we can associate with the information about a probability distribution* $p_i, i = 1, \cdots, N$ *is its entropy,* $H = -\sum p_i \log(p_i)$.

This consideration had been one of the motivations for our group to introduce the *TRISA relative-entropy triangle* to analyze and conveniently plot the joint development and mutual dependency of three variables, measured in incommensurable units[108].

In order to solve the problem, one has to transform the economy, social, and ecology variables to dimensionless variables $p_{econ}, p_{soc}, p_{ecol}$ between [0,1] such that $p_{econ} + p_{soc} + p_{ecol} = 1$, because otherwise we cannot work with a $(p_{econ}, p_{soc}, p_{ecol})$ ternary diagram. I present the method that I worked out in case of *countries of the world*. Any other *complex economic-social-ecologic system* could be treated along the same lines.The algorithm consists of seven steps.

**Step 1)** Design a number $N_{econ} \approx 15-20$ of possible classes of economy where the economy of any country can belong: $ECON_1, ECON_2, \cdots, ECON_{N_{econ}}$ .

The classes $ECON_1, ECON_2, \cdots, ECON_{N_{econ}}$ should be arranged in increasing order of merit, so that according to some plausable criterion $ECON_2$ is ”better” than $ECON_1$, etc. In a similar way the possible social indicators for the countries should be divided to a number $N_{soc} \approx 15-20$ possible classes $SOC_1, SOC_2, \cdots, SOC_{N_{soc}}$ arranged in increasing order of merit; and the possible ecologic measuress should be classified to a number $N_{ecol} \approx 15-20$ groups $ECOL_1, ECOL_2, \cdots, ECOL_{N_{ecol}}$ arranged in increasing order of merit.

**Step 2)** Use published statistics of *N* (*N* about 100 or more) countries for the last few years and prepare empirical histograms for the distribution of the variables ECON, SOC, ECOL among the classes defined in Step 1.

**Step 3)** Find a meaningful and objective *well-being function W* to characterize the stage of development of a country (for instance *Gross National Product* in US $ /population, or *Gross Agricultural Product/area of cultivated land*, etc.). Let the well-being function of the *i*-th country be $W_i (i = 1, 2, \cdots, N)$. If country *i* belongs to economy class $ECON_j$, social class $SOC_k$, ecology class $ECOL_l$, then define

[107] Fischer *op. cit.*
[108] Oleschko et al. 2004. TRISA is acronym for *Triangle of Sustainability of Agroecosystems*.

$$econ_i = \frac{j}{N_{econ}}; 0 \le econ_i \le 1$$
$$soc_i = \frac{k}{N_{soc}}; 0 \le soc_i \le 1 \qquad \text{(Eq. 144a)}$$
$$ecol_i = \frac{l}{N_{ecol}}; 0 \le ecol_i \le 1$$

**Step 4)** Fit *W* linearly as

$$W_i \approx \lambda \cdot econ_i + \mu \cdot soc_i + \upsilon \cdot ecol_i \qquad \text{(Eq. 144b)}$$

where the coefficients $\lambda, \mu, \nu$ are optimal in the least mean squares sense:

$$\sum_{i=1}^{N} (W_i - \lambda \cdot econ_i - \mu \cdot soc_i - \upsilon \cdot ecol_i)^2 = min \qquad \text{(Eq. 144c)}$$

**Step 5)** The histograms constructed in Step 2 define three probability distributions. For the case of *economy*, for example (as there are $N$ countries and $N_{econ}$ economic clases), if there are $N_1^{(econ)}, N_2^{(econ)}, \cdots$ countries in classes $ECON_1, ECON_2, \cdots$, such that $\sum_{j=1}^{N_{econ}} N_j^{(econ)} = 1$, denoting

$p_j^{(econ)} = \frac{N_j^{(econ)}}{N}$ (Eq. 145a), we get a complete probability distribution $\left\{ p_j^{(econ)}, j = 1, \cdots, N_{econ}, \sum_{j=1}^{N_{econ}} p_j^{(econ)} = 1 \right\}$. We similarly define the other two complete probability distributions

$$\left\{ p_k^{(soc)} = \frac{N_k^{(soc)}}{N}, k = 1, \cdots, N_{soc}; \sum_{k=1}^{N_{soc}} p_k^{(soc)} = 1 \right\} \qquad \text{(Eq. 145b)}$$

and

$$\left\{ p_k^{(ecol)} = \frac{N_k^{(ecol)}}{N}, k = 1, \cdots, N_{ecol}; \sum_{k=1}^{N_{eecol}} p_k^{(ecol)} = 1 \right\} \qquad \text{(Eq. 145c)}$$

The set of probabilities $p_j^{(econ)} \cdot p_k^{(soc)} \cdot p_l^{(ecol)}$, corresponding to the event that a given country falls to the *j*-th economic, *k*-th social and *l*-th ecologic class, also form a complete distribution $\sum_{j=1}^{N_{econ}} \sum_{k=1}^{N_{soc}} \sum_{l=1}^{N_{ecol}} p_j^{econ} p_k^{soc} p_l^{ecol} = 1.$

**Step 6)** The total Shannon entropy of the complete probability distribution $\{ p_j^{(econ)} \cdot p_k^{(soc)} \cdot p_l^{(ecol)} \}_{j,k,l}$ is

$$H_{total} = -\sum_{j=1}^{N_{econ}} \sum_{k=1}^{N_{soc}} \sum_{l=1}^{N_{ecol}} p_j^{(econ)} \cdot p_k^{(soc)} \cdot p_l^{(ecol)} \cdot \log\left( p_j^{(econ)} \cdot p_k^{(soc)} \cdot p_l^{(ecol)} \right)$$
$$= -\sum_{j=1}^{N_{econ}} \sum_{k=1}^{N_{soc}} \sum_{l=1}^{N_{ecol}} p_j^{(econ)} \cdot p_k^{(soc)} \cdot p_l^{(ecol)} \cdot \left( \log p_j^{(econ)} + \log p_k^{(soc)} + p_l^{(ecol)} \right). \qquad \text{(Eq. 146)}$$

If we observe a new "event" (another country) $A=\{ECON_j, SOC_k, ECOL_l\}$, this contributes a *partial entropy*

$$H_{jkl}\left( p_j^{(econ)}\cdot p_k^{(soc)}\cdot p_l^{(ecol)} \right)=-\, p_j^{(econ)}\cdot p_k^{(soc)}\cdot p_l^{(ecol)}\cdot\log\left( p_j^{(econ)}\cdot p_k^{(soc)}\cdot p_l^{(ecol)} \right) \qquad \text{(Eq. 147)}$$

to the total entropy $H_{total}$. The relative weights of information which the economic, social, and ecologic variables contribute to $H_{jkl}$ are as follows:

$$h_{j,relative}^{(econ)} \stackrel{def.}{=} \frac{-\, p_j^{(econ)}\cdot p_k^{(soc)}\cdot p_l^{(ecol)}\cdot\log p_j^{(econ)}}{-\, p_j^{(econ)}\cdot p_k^{(soc)}\cdot p_l^{(ecol)}\cdot\left[\log p_j^{(econ)}+\log p_k^{(soc)}+\log p_l^{(ecol)}\right]}$$
$$=\frac{\log p_j^{(econ)}}{\log p_j^{(econ)}+\log p_k^{(soc)}+\log p_l^{(ecol)}} \qquad \text{(Eq. 148a)}$$

and, similarly,

$$h_{k,relative}^{(soc)}=\frac{\log p_k^{(soc)}}{\log p_j^{(econ)}+\log p_k^{(soc)}+\log p_l^{(ecol)}} \qquad \text{(Eq. 148b)}$$

$$h_{l,relative}^{(ecol)}=\frac{\log p_l^{(ecol)}}{\log p_j^{(econ)}+\log p_k^{(soc)}+\log p_l^{(ecol)}} \qquad \text{(Eq. 148c)}$$

These relative weights of information are dimensionless, between 0 and 1, and their sum is 1:

$$h_{j,rel}^{(econ)}+h_{k,rel}^{(soc)}+h_{l,rel}^{(ecol)}=1. \qquad \text{(Eq. 149)}$$

Consequently, *these variables can be used as coordinates along the sides of the ECON-SOC-ECOL* equilateral triangle (instead of the original, incommensurable variables *ECON*, *SOC*, and *ECOL)* to plot the isoline representation of any function *F(ECON,SOC,ECOL)* of the original variables inside the triangle $\left\{ h_{j,rel}^{(econ)}, h_{k,rel}^{(soc)}, h_{l,rel}^{(ecol)} \right\}$.

**Step 7 (Final step):** Finally, we shall construct two ternary plots, one for the *relative entropy dynamics*, one for the *well-being function dynamics*. As there are $N_{econ}$ possible economy classes, $N_{soc}$ possible social classes, $N_{eecol}$ possible ecology classes, altogether $N_{econ}\cdot N_{soc}\cdot N_{ecol}$ points are to be plotted inside both ternary diagrams. The combination of variables $\{ECON\in ECON_j; SOC\in SOC_k; ECOL\in ECOL_l\}$ will correspond to the ternary coordinates $\left\{ h_{j,rel}^{(econ)}, h_{k,rel}^{(soc)}, h_{l,rel}^{(ecol)} \right\}$ along the sides of the triangle, where $h_{j,rel}^{(econ)}, h_{k,rel}^{(soc)}, h_{l,rel}^{(ecol)}$ can be computed using Eqs. (145a-c, 148a-c). In the *ternary diagram for entropy* we plot the relative entropy of the event $A=\{ECON_j, SOC_k, ECOL_l\}$ with respect to the total entropy:

$$H_{rel}=\{ECON_j, SOC_k, ECOL_l\}=\frac{-\, p_j^{(econ)}\cdot p_k^{(soc)}\cdot p_l^{(ecol)}}{H_{total}} \qquad \text{(Eq. 150)},$$

where $H_{total}$ is given by Eq. (146). In the *ternary diagram for well-being function*, if for the *i*-th country the parameters are $\{ECON_j, SOC_k, ECOL_l\}$ we plot, at the point $\left\{ h_{j,rel}^{(econ)}, h_{k,rel}^{(soc)}, h_{l,rel}^{(ecol)} \right\}$ inside the triangle, instead of the original $W_i$, the *smoothed value*

$W_{smoothed} \approx \lambda \cdot \frac{j}{N_{econ}} + \mu \cdot \frac{k}{N_{soc}} + \upsilon \cdot \frac{l}{N_{ecol}}$ (cf. Eqs. 144a-1c) instead of the original $W_i$, to eliminate random fluctuations. An example[109], for such a triangle is shown below:

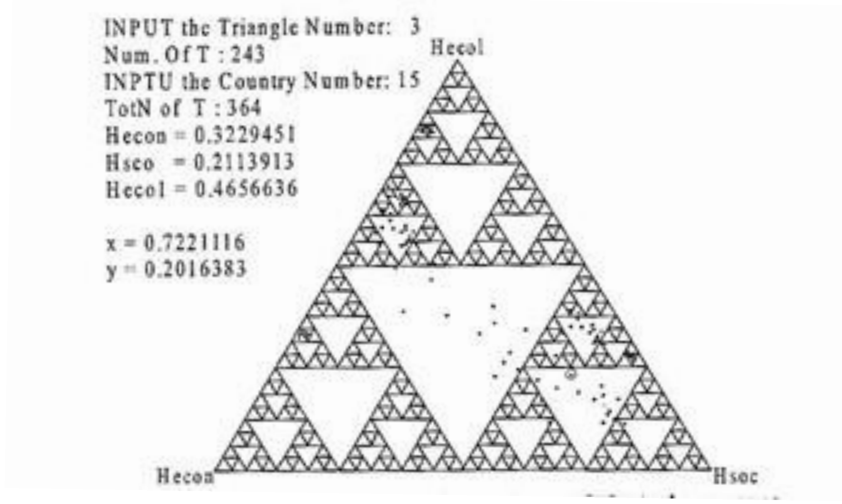


Fig. 26. Experimental points in the *TRISA* triangle. To see with increased accuracy the clustering of points, the triangle is divided fractally, as in a *Sierpinski gasket*[110]. Any sub-triangle can be zoomed, and studied separately.

## 3.3. MEAN-FIELD ROCK PHYSICS[111]

The question of generalized mean values has occupied me through my career, from an early paper with my friend Gyula Katona (1966) on mean values defined on directed graphs, to my latest review paper (2020) where I devote a chapter to “mean field theories”.

### 3.3.A. GENERALIZED MEAN VALUES FOR SEISMIC VELOCITIES

Suppose we are given a composite material consisting of two phases of respective volume fractions $P$, $Q$; $P + Q = 1$, and suppose these constituents are uniformly distributed within the total volume. Suppose g is some physically measurable property that assumes the values

---

[109] Oleschko et al. 2004: Fig. 3.

[110] Korvin, G. 1992a. *Fractal Models in the Earth Sciences*. Amsterdam: Elsevier: 93.

[111] G. Katona & Korvin, G. ‘Functions defined on a directed graph’. *Theory of Graphs. Proc. Symp.Tihany, Hung*., Sept. 1966: 209-213; G. Korvin. & Lux, I. ‘An analysis of the propagation of sound waves in porous media by means of the Monte Carlo method’. *Geophysical Transactions* 21(3-4)1972: 91-106; Korvin, G. 1978c. ‘The hierarchy of velocity formulae: Generalized mean value theorems.’*Acta Geod. Geoph. et Mont. Acad. Sci. Hung*. 13(1-2)1978: 211-222; Korvin, G. 1982a.‘Axiomatic characterization of the general mixture rule’. *Geoexploration* 19(4): 267-276; Korvin, G. ‘A few unsolved problems of applied geophysics’. *Geophysical Transactions* 31(4)1985:373-389; Korvin, G. ‘Bounds for the resistivity anisotropy in thinly-laminated sand-shale’. *Petrophysics* 53(1)2012: 14-21; 4. Korvin, G. 2020d. ‘Statistical Rock Physics’ in B. S. Daya Sagar, Quiming Cheng, Jennifer McKinley and Frits Agterberg (Eds.) Earth Sciences Series. *Encyclopedia of Mathematical Geosciences*. Springer (In Press).

$g_1$ & $g_2$ , respectively, for the two constituents, and a value g for the composite. Suppose, further, that the value of $g$ is unambiguously determined by the volume fractions $P$, $Q$ and the specific properties $g_1$ & $g_2$: $g = M(g_1, g_2, P, Q)$ (Eq. 151). In Korvin [1982a] it is shown that, if a set of physically plausible conditions are met, the only possible functional form of $M(g_1, g_2, P, Q)$ is the "*general mixture rule*"

$M_t(g_1, g_2, P, Q) = \{\Phi g_1^t + (1-\Phi) g_2^t\}^{1/t}$ (Eq. 152)

for some real $t, t \neq 0$ , or $M_{t=0}(g_1, g_2, P, Q) = g_1^{\Phi} g_2^{1-\Phi}$ (Eq. 153) which follows from Eq. (152) by *l'Hospital's rule* for t → 0. Here, $\Phi$ is *porosity*, defined as $\Phi = \mathrm{P}/(P+Q)$.
The general mean values have the important property[112] that for $g_1$ & $g_2 > 0, g_1 \neq g_2$. $\Phi \neq 0, \Phi \neq 1$ the expression $\{\Phi g_1^t + (1-\Phi) g_2^t\}^{1/t}$ is a strictly monotonously increasing function of *t* in $(-\infty, \infty)$ . In case of sound speeds in fluid-filled sedimentary rocks the general rules (152-153), contain, in particular, the following widely used *velocity formulae*: for *t* = -2 the "approximate Wood equation"[113]; for *t* = - 1 the "time-average" equation[114]; for *t* = 0 the "vugular carbonate" formula[115]; for t = 1 the average velocity formula[116]]. Tegland's method of sand-shale ratio determination[117] also assumes a "t = - 1"- type time average equation; Mateker's [1971] effective attenuation factor[118] in an alternating sequence of thick sand-shale layers is a linear weighted (i.e. "t = 1") combination of the specific attenuations, further examples from different fields of geophysics are listed in Korvin (1978c, 1982 a). The functional forms (152-153) were derived in Korvin (1982a) from the following set of conditions. (The derivation was based on the *Theory of Functional Equations*, particularly on the results of Aczél[119].)
*Condition 1*. Reflexivity: $M(g_1, g_1, P, Q) = g_1$ for all $\mathrm{P, Q, (P+\ Q\ >\ 0)}$ ;
*Condition 2*. Idempotency: $M(g_1, g_2, P, 0) = g_1$for all $\mathrm{P} > 0$; $M(g_1, g_2, 0, Q) = g_2$for all $\mathrm{Q} > 0$;
*Condition 3*. Homogeneity (of 0th order) with respect to the volume fractions:
$M(g_1, g_2, P, Q) = M(g_1, g_2, \lambda P, \lambda Q)$ for all P, Q such that $P + Q > 0, \lambda > 0$ ;
*Condition 4*. Internity. The property $g$ measured on the composite lies between the specific values $g_1$ & $g_2$ of the constituents; if $g_1 < g_2$, say, then for $P + Q > 0$:
$M(g_1, g_2, 1,0) \leq M(g_1, g_2, P, Q) \leq M(g_1, g_2, 0,1)$;

---

112 Beckenbach E. F.& Bellman R. 1961: *Inequalities*. Springer Verlag, Berlin-Göttingen-Heidelberg. § 1.16.
113 Waterman P. C. S. & Truell R. 1961 : Multiple scattering of waves. *J. Math. Phys*., 2, 4: 512-537; Korvin 1977, 1978c.

114 Wyllie M. R. J., Gregory A. R., Gardner L. W. 1956: Elastic wave velocities in heterogeneous and porous media. *Geophysics*, 21, 1: 41-70.
115 Meese A. D., Walther H. C. 1967: An investigation of sonic velocities in vugular carbonates. *8th SPWLA Symp*., Denver.
116 Berry J. E. 1959: Acoustic velocity in porous media. *J. Pet. Technol*, II, 10: 262-270.
117 Tegland E. R. 1970: Sand-shale ratio determination from seismic interval velocity. *23rd Ann. Midwestern Mtg., SEG*, AAPG, Dallas.
118 Mateker E. J. Jr. 1971: Lithologic predictions from seismic reflections. *Oil and Gas J.* (Nov. 8, 1971): 96-100.
119 Aczél. J. 1946: The notion of mean values. *Nor. Vidensk. Selsk. Forh.*, 19: 83-86; Aczél J: 1961: *Vorlesungen über Funktionalgleichungen und ihre Anwendungen*. VEB Deutscher Verlag der Wissenschaften. Berlin.

*Condition 5*. Bi-symmetry: Given two composites, the first consisting of $P_1$ & $Q_1$ parts of materials of $g_1$ & $g_2$ properties; the second of $P_2$ & $Q_2$ parts of materials of $G_1$ & $G_2$ properties, then the following two expressions for the measured property $g$ of the four- component aggregate must be equal:

$M[M(g_1, g_2, P_1, Q_1); M(G_1, G_2, P_2, Q_2); P_1 + Q_1; P_2 + Q_2] =$

$M[M(g_1, G_1, P_1, P_2); M(g_2, G_2, Q_1, Q_2); P_1 + P_2; Q_1 + Q_2]$ ;

*Condition 6*. Monotonicity with respect to the volume fractions:

If $g_1 < g_2$ say, $P + Q_1 > 0, Q_2 > Q_1$ then $M(g_1, g_2, P, Q_1) < M(g_1, g_2, P, Q_2)$ ;

*Condition 7*. Monotonicity with respect to the physical properties: If $P + Q > 0$ , $g_2 < g_3$ then $M(g_1, g_2, P, Q) < M(g_1, g_3, P, Q)$;

*Condition 8.* Homogeneity (of first order) with respect to the physical properties:

$M(\lambda g_1, \lambda g_2, P, Q) = \lambda M(g_1, g_2, P, Q)$ for all $P. Q, \lambda$ such that $P + Q > 0, \lambda > 0$ .

I proved[120] *that if the function $M(g_1, g_2, P, Q)$ , defining the effective physical property $g_{eff}$ of a two-component material, satisfies Conditions 1-8 then it must be of the form*

*$g_{eff} = M(g_1, g_2, P, Q) = \{\Phi g_1^t + (1 - \Phi) g_2^t\}^{1/t}$ for some real $t \neq 0$, or $g_{eff} = g_1^{\Phi} g_2^{1-\Phi}$ where $\Phi = P/(P + Q)$.*

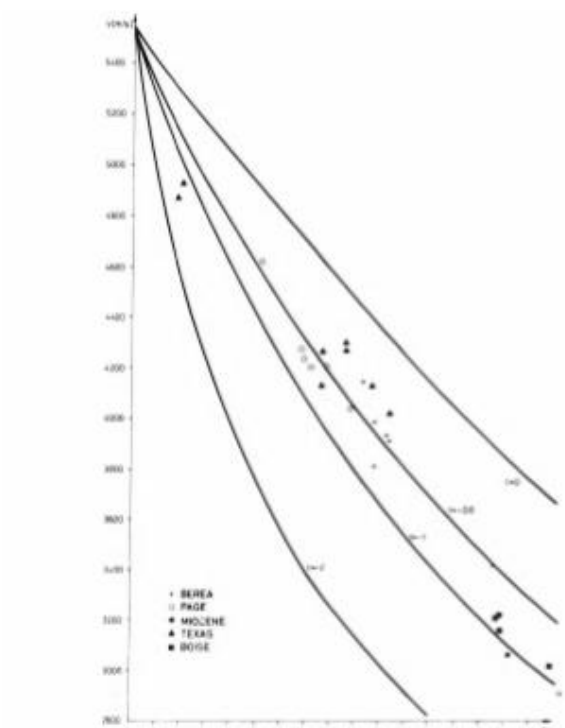


Fig. 27. Porosity-velocity master curves for sandstone (from Korvin 1978c).

---

[120] Korvin 1982a .

Figure 27 shows porosity-velocity curves for sandstone, for different values of the parameter *t* ($g_1 = v_{fluid}$ =1545 m/s; $g_2 = v_{matrix}$ =5542 m/s)[121]. The sandstone data are best fitted by a t = -0.6 curve, i.e. by the formula $v_{eff} = \{\Phi v_{fluid}^{-0.6} + (1-\Phi) v_{matrix}^{-0.6}\}^{1/(-0.6)}$ (Eq, 154).
In 1985, I posed the problem, what is the physical meaning (if any) of the parameter *t* in Eq. (152). Does t = - 0.6 have any particular significance for sandstone? There exists another, *variational* , approach for the determination of the effective properties of composite materials, culminating in the celebrated HS (Hashin – Shtrikman) bounds on the effective properties in terms of the specific ones[122]. In my 1985 paper I also asked, is it possible to reconcile the *functional equation approach* (of K o r v in 1978c, 1982a, discussed here) with the HS *variational approach,* or at least to use HS bounds to derive non-trivial bounds for parameter *t*.

## 3.3.B. RESISTIVITY ANISOTROPY IN THINLY-LAMINATED SAND-SHALE

In this research[123], awarded by *SPWLA* (*Society of Well Log Analysts*) the *Best Technical Paper of the Year 2012,* I studied the *electric resistivity anisotropy* of thinly laminated sand-shale formations, for the case when both sandstone and shale are electrically anisotropic, and derived simple upper- and lower bounds for the possible maximal and minimal values for the coefficient of resistivity anisotropy in such formations.

The introduction of induction logging tools with multi-directional coils[124] has made possible to independently measure horizontal and vertical effective resistivities $\rho_h$ and $\rho_v$ in wells and to derive from them vertical and horizontal shale resistivities $\rho_{sh\_v}$ and $\rho_{sh\_h}$, and a single resistivity value $\rho_{sd}$ for the sandstone which is considered isotropic. In this study I dealt with the more general case when both sandstone and shale are electrically anisotropic.
Suppose we have a horizontal stack of inherently anisotropic shale layers of horizontal resistivity $\rho_{sh\_h}$ and vertical resistivity $\rho_{sh\_v}$ alternating with anisotropic sandstone layers of horizontal resistivity $\rho_{sd\_h}$ and vertical resistivity $\rho_{sd\_v}$. The volume fractions of shale and sand, respectively, are $V_{sh}$ and $V_{sd}$ with $0 \le V_{sh} \le 1$, $0 \le V_{sd} \le 1$; in the absence of any further lithology $V_{sh} + V_{sd} = 1$. The two volume fractions are assumed as known, because they can be estimated from Gamma Ray log, SP log, or porosity crossplots.

---

[121] The *Berea, Boise, Miocene, Page* sandstone data are taken from Meese A.D.& Walther H.C.1967: An investigation of sonic velocities in vugular carbonates. *8th SPWLA Symp*., Denver; the *Texas* data are from Hicks W. G. & Berry J. E. 1956: Application of continuous velocity logs to determination of fluid saturation of reservoir rocks. *Geophysics*, 21, 3: 739-754.
[122] Hashin Z. & Shtrikman S. 1963: A variational approach to the theory of the elastic behaviour of multiphase materials. *J. Mech. Phys. Solids*. 11: 127-140; Hashin Z. 1964: Theory of mechanical behaviour of heterogeneous media. *Appl. Mech. Rev*. 17, No. 1: 1-9.
[123] Korvin, G. 'Bounds for the resistivity anisotropy in thinly-laminated sand-shale'. *Petrophysics* 53(1)2012: 14-21.
[124] Kriegshäuser, B., Fanini, O., Forgang, S., Itskovich, G., Rabinovich, M., Tabarovsky, L., Yu, L., Epov, M. & V.D. Horst J., 2000: "A new multicomponent induction logging tool to resolve anisotropic formations", *SPWLA 40th Logging Symp*.; Clavaud, J.-B., R. Nelson, U. K. Guru & H. Wang, 2005: "Field example of enhanced hydrocarbon estimation in thinly laminated formation with a triaxial array induction tool: A laminated sand-shale analysis with anisotropic shale," *SPWLA Annual Logging Symp*., New Orleans, Louisiana.

My assumption, that both sand and shale are electrically anisotropic, generalizes the model of Klein et al. (1997) who assumed isotropy for both sand and shale, and it also improves upon published models[125] where only the shale is taken as anisotropic but sand is assumed isotropic. The *Klein equations*[126] , which are based on Kirchoff's laws for laminated composites[127], express the effective horizontal resistivity $\rho_h$ and effective vertical resistivity $\rho_v$ of the whole stack of sand-shale layers in terms of specific resistivities:

$$\left.\begin{array}{ccccc} V_{sh}\rho_{sh} & + & V_{sd}\rho_{sd} & = & \rho_v \\ \dfrac{V_{sh}}{\rho_{sh}} & + & \dfrac{V_{sd}}{\rho_{sd}} & = & \dfrac{1}{\rho_h} \end{array}\right\} \quad \text{Eqs. (155a and b)}$$

From (155a), $\rho_{sh} = \dfrac{\rho_v - V_{sd}\rho_{sd}}{V_{sh}}$ Eq. (156), where the sand resistivity $\rho_{sd}$ is obtained by solving the quadratic equation $A\rho_{sd}^2 + B\rho_{sd} + C = 0$ Eq. (157), with

$$\begin{array}{lcl} A & = & V_{sd} \\ B & = & \rho_h\left(V_{sh}^2 - V_{sd}^2 - \dfrac{\rho_v}{\rho_h}\right) = \rho_h\left(V_{sh}^2 - V_{sd}^2 - \lambda^2\right) \\ C & = & \rho_h\rho_v V_{sd} \end{array} \quad \text{Eq. (158. a-c)}$$

Here $\lambda = \sqrt{\rho_v / \rho_h}$ (which is always greater than 1) is the *anisotropy coefficient* of the layered structure. Clavaud et al. (2005) assumed that the sand is isotropic with resistivity $\rho_{sd}$, but the shale layers are inherently anisotropic with two different resistivities $\rho_{sh\_v}$ and $\rho_{sh\_h}$. (Fig. 28).

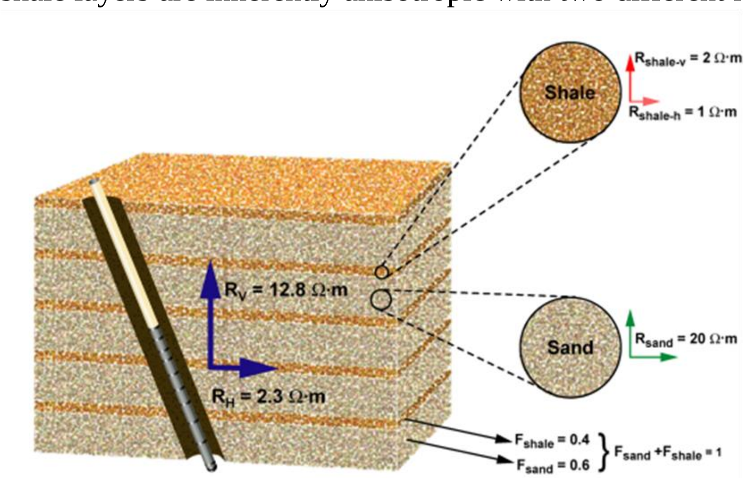


Fig. 28. The model for isotropic sand, anisotropic shale. (From Clavaud et al., 2005)

---

[125] Clavaud et al. *op. cit*.; Minh, Ch.C.,, J.-B. Clavaud, P. Sundararaman, S. Froment, E. Caroli, O. Billon, G. Davis & R. Fairbairn, 2007: "Graphical analysis of laminated sand-shale formations in the presence of anisotropic shales", *World Oil*. 228 No. 9.

[126] Klein, J.D., Martin, P.R. & Allen, D.F.1997. “The petrophysics of electrically anisotropic reservoirs”, *The Log Analyst*, 38, No. 3.

[127] Maxwell, James Clerk, 1891: *A Treatise on Electricity and Magnetism*. Clarendon, London (Repr. edn. by Dover, New York, 1954); Grant, F.S., & West, G.F., 1965: *Interpretation Theory in Applied Geophysics*. McGraw-Hill Book Co., New York; Mei, Chiand. C. & Bogdan Vernescu, 2010: *Homogenization Methods for Multiscale Mechanics*. World Scientific, Singapore.

In this case Kirchoff 's rules give $\left.\begin{array}{ccccc} V_{sh}\rho_{sh\_v} & + & V_{sd}\rho_{sd} & = & \rho_v \\ \dfrac{V_{sh}}{\rho_{sh\_h}} & + & \dfrac{V_{sd}}{\rho_{sd}} & = & \dfrac{1}{\rho_h} \end{array}\right\}$ Eqs. (159a and b)

As $\lambda_{sh} = \sqrt{\rho_{sh\_v} / \rho_{sh\_h}}$ is known from some independent measurement, Eqs. (159a and b) can be written as

$\left.\begin{array}{ccccc} V_{sh}\lambda_{sh}^2\rho_{sh\_h} & + & V_{sd}\rho_{sd} & = & \rho_v \\ \dfrac{V_{sh}}{\rho_{sh\_h}} & + & \dfrac{V_{sd}}{\rho_{sd}} & = & \dfrac{1}{\rho_h} \end{array}\right\}$ Eqs. (160a and b), i.e. $\rho_{sh\_h} = \dfrac{\rho_v - V_{sd}\rho_{sd}}{V_{sh}\lambda_{sh}^2}$ Eq. (161),

$A\rho_{sd}^2 + B\rho_{sd} + C = 0$ Eq. (162), the coefficients are $\begin{array}{ccc} A & = & V_{sd} \\ B & = & \rho_h\left(V_{sh}^2\lambda_{sh}^2 - V_{sd}^2 - \lambda^2\right) \\ C & = & \rho_h\rho_v V_{sd} \end{array}$ Eqs.(163. a-c)

I considered the most general case. I realized that a reasonably strong ($\lambda_{sd} = \sqrt{\rho_{sd\_v} / \rho_{sd\_h}}$ between 1 and 2) inherent electrical anisotropy can develop in a shale-free sandstone, especially if it is hydrocarbon bearing[128]. In such cases sand anisotropy cannot be excluded, and a more general set of equations must be used than Clavaud's or Klein's:

$\left.\begin{array}{ccccc} V_{sh}\rho_{sh\_v} & + & V_{sd}\rho_{sd\_v} & = & \rho_v \\ \dfrac{V_{sh}}{\rho_{sh\_h}} & + & \dfrac{V_{sd}}{\rho_{sd\_h}} & = & \dfrac{1}{\rho_h} \end{array}\right\}$ Eqs. (164a and b)

Using *known anisotropy values* (measured on cores or obtained from logs in nearby thick shale and sand) $\lambda_{sh} = \sqrt{\rho_{sh\_v} / \rho_{sh\_h}}$ and $\lambda_{sd} = \sqrt{\rho_{sd\_v} / \rho_{sd\_h}}$, Eqs. (164a and b) become:

$\left.\begin{array}{ccccc} V_{sh}\lambda_{sh}^2\rho_{sh\_h} & + & V_{sd}\lambda_{sd}^2\rho_{sd\_h} & = & \rho_v \\ \dfrac{V_{sh}}{\rho_{sh\_h}} & + & \dfrac{V_{sd}}{\rho_{sd\_h}} & = & \dfrac{1}{\rho_h} \end{array}\right\}$ Eqs. (165a and b). From Eq. (165a):

$\rho_{sh\_h} = \dfrac{\rho_v - V_{sd}\lambda_{sd}^2\rho_{sd\_h}}{V_{sh}\lambda_{sh}^2}$ Eq. (166), $A\rho_{sd\_h}^2 + B\rho_{sd\_h} + C = 0$ Eq. (167a),

where from

$\rho_{sd\_h} = \dfrac{-B \pm \sqrt{B^2 - 4AC}}{2A}$ Eq. (167b), with $\begin{array}{ccc} A & = & V_{sd}\lambda_{sd}^2 \\ B & = & \rho_h\left(V_{sh}^2\lambda_{sh}^2 - V_{sd}^2 - \lambda^2\right) \\ C & = & \rho_h\rho_v V_{sd} \end{array}$ Eq.(168a-c)

---

[128] Anderson, B., I. Bryant, M. Lüling, Brian Spies, K. Helbig, 1994: "Oilfield anisotropy: Its origins and electrical characteristics", *Oilfield Review*, October 1994: 48-56; Jing. X.D., Al-Harthy, S. & King, S., 2002: "Petrophysical properties and anisotropy of sandstones under true-triaxial stress conditions". *Petrophysics* 43: 358-362; Kennedy, D. & Herrick, D., 2004: "Conductivity anisotropy in shale-free sandstone". *Petrophysics* 45: 38-58.

For $\lambda_{sd} = 1$, Eqs. (165a & b) reduce to Clavaud's equations, and when both $\lambda_{sd} = \lambda_{sh} = 1$ we get back Klein's equations. To recognize the pioneering role of these authors, I called Eqs. (165a, b) *Generalized Klein-Clavaud Equations*.

As seen from Eqs. (166 to 168), in the general case of parallel, intrinsically anisotropic sand and shale layers, the anisotropic sand- and shale resistivitivities can be obtained in three steps: (1) computing A, *B*, *C*; (2) solving the quadratic equation (Eq. 167 a) for $\rho_{sd\_h}$; (3) then computing $\rho_{sh\_h}$ using Eq. (166). The specific vertical resistivities are obtained as $\rho_{sh\_v} = \lambda^2_{sh}\rho_{sh\_h}$, $\rho_{sd\_v} = \lambda^2_{sd}\rho_{sd\_h}$ .

For these calculations we need the following input data:

- three values inferred from well log measurements: $V_{sh}$ (shale volume), $\rho_h$ (horizontal resistivity of the formation, parallel with the bedding), $\rho_v$ (vertical resistivity of the formation, perpendicular to the bedding);
- two computed values: $V_{sd} = 1 - V_{sh}$ (sand volume), and $\lambda = \sqrt{\rho_v / \rho_h}$ (formation anisotropy);
- core-derived or defaulted specific anisotropy values: $\lambda_{sd}$ and $\lambda_{sh}$.

The independent parameters which are needed in Eqs. (168 a-c) span a *5-dimensional space* ($V_{sh}$, $\rho_h$, $\rho_v$, $\lambda_{sd}$, $\lambda_{sh}$), where they satisfy the obvious contraints that $0 \le V_{sh} \le 1$; $\rho_h$ and $\rho_v$ are positive real numbers; and none of the specific anisotropies $\lambda_{sd}$ and $\lambda_{sh}$ is less than one. To see why specific anisotropies cannot be less than one, consider the two cases presented in Figs. 29 and 30.

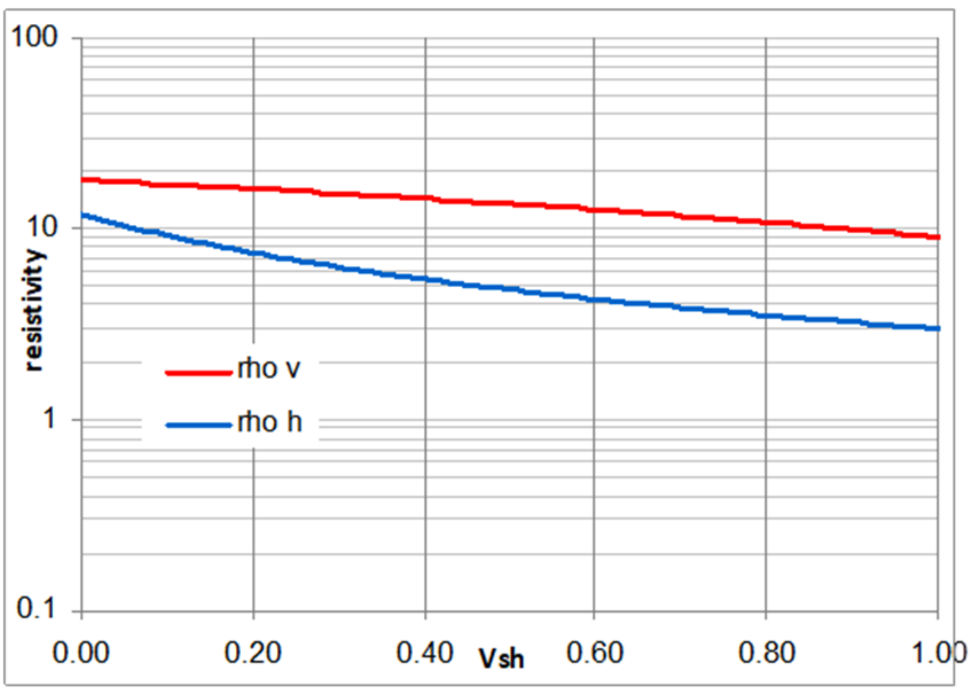


Figure 29. Example for a "physical" situation. (From Korvin 2012)

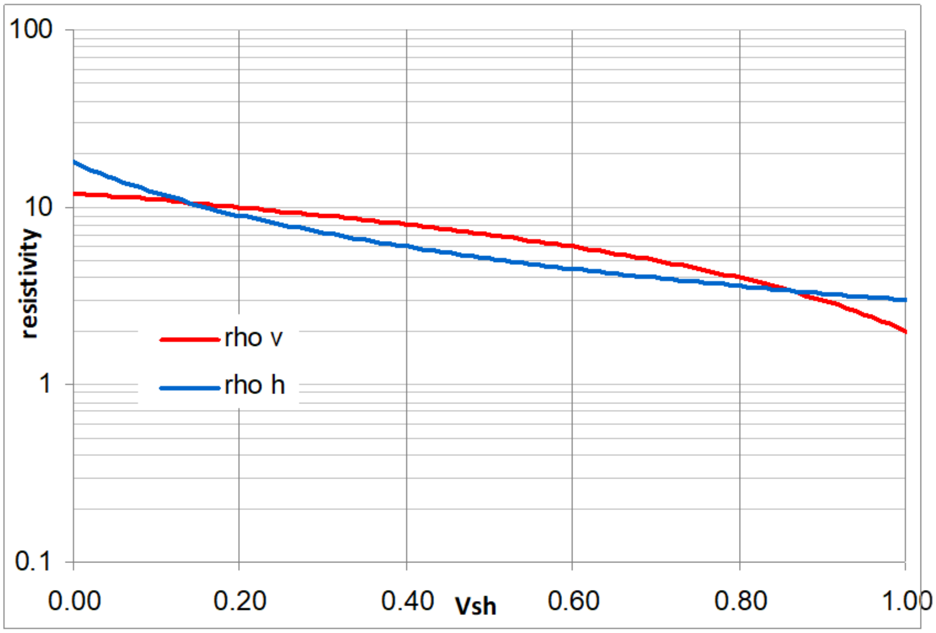


Fig. 30. A "nonphysical" case.

| Table 2. Parameters used for constructing Figs. 29 & 30 (From Korvin 2012) | | | | | | | |
|---|---|---|---|---|---|---|---|
| Fig. # | $V_{sh}$ | $\rho_{sd\_h}$ Ωm | $\rho_{sd\_v}$ Ωm | $\lambda_{sd}$ | $\rho_{sh\_h}$ Ωm | $\rho_{sh\_v}$ Ωm | $\lambda_{sh}$ |
| 2. | 0 to 1 | 12 | 18 | $\sqrt{1.5}$ =1.22 | 3 | 9 | $\sqrt{3}$ =1.73 |
| 3. | 0 to 1 | 3 | 2 | 0.82 | 18 | 12 | 0.82 |

Figure 29 shows the vertical and horizontal resistivities of a formation, computed by the *Generalized Klein-Clavaud Equations* (165a & b), as function of shale volume. The specific sand- and shale resistivities used for the calculation are contained in *Table 2*. The plot presents a reasonable situation: for all shale volumes one has $\rho_v > \rho_h$ that is $\lambda = \sqrt{\rho_v / \rho_h} > 1$, as it should be. In Fig. 30, on the other hand, for two ranges of $V_{sh}$ (very small and very large shale volumes) there arises a "nonphysical" case: $\rho_v < \rho_h$ that is $\lambda = \sqrt{\rho_v / \rho_h} < 1$. As seen in *Table 2*, in case of Fig. 29 both specific anisotropies are greater than one, while when constructing Fig.30, both were, *unphysically*, less than one.

A little algebra shows that the simultaneous fulfillment of

$$\frac{\rho_{sh\_v}}{\rho_{sh\_h}} = \lambda_{sh}^2 \geq 1; \; \frac{\rho_{sd\_v}}{\rho_{sd\_h}} = \lambda_{sd}^2 \geq 1 \quad \text{(Inequalities 169 a \& b)}$$

guarantees that if the solutions $\rho_v$ and $\rho_h$ of the *Generalized Klein-Clavaud Equations* are positive and real, then they satisfy $\lambda = \sqrt{\rho_v / \rho_h} > 1$. Indeed, from Eqs. (165a, b) and (169)

$$\frac{1}{\rho_h} = \frac{V_{sh}}{\rho_{sh\_h}} + \frac{V_{sd}}{\rho_{sd\_h}} > \frac{V_{sh}}{\rho_{sh\_v}} + \frac{V_{sd}}{\rho_{sd\_v}}, \text{ i.e. } \rho_h < \left\{ \frac{V_{sh}}{\rho_{sh\_v}} + \frac{V_{sd}}{\rho_{sd\_v}} \right\}^{-1} < V_{sh}\rho_{sh\_v} + V_{sd}\rho_{sd\_v} = \rho_v .$$

In the last step I used *Jensen's theorem*[129] according to which *for any two unequal positive numbers their weighted harmonic mean is less than their arithmetic mean*.

Some further numerical experimentation in the *parameter space* ($V_{sh}$, $\rho_h$, $\rho_v$, $\lambda_{sd}$, $\lambda_{sh}$) reveals that Conditions (169a & b), in themselves, still do not guarantee that the quadratic equation $A\rho_{sd\_h}^2 + B\rho_{sd\_h} + C = 0$ (where the coefficients are computed from Eqs. 168 a-c) would have a real positive solution for $\rho_{sd\_h}$. The question naturally arises: is there a way to characterize those points ($V_{sh}$, $\rho_h$, $\rho_v$, $\lambda_{sd}$, $\lambda_{sh}$) of the parameter space for which the *Generalized Klein-Clavaud Equations* have physically meaningful (real and positive) solutions for $\rho_{sd\_h}$ and $\rho_{sh\_h}$? I proved[130] the following two theorems:

*THEOREM 1. The overall anisotropy of the layered sand/shale formation satisfies the inequalities* $\left(V_{sh}\lambda_{sh} + V_{sd}\lambda_{sd}\right)^2 \le \lambda^2 \le V_{sh}^2\lambda_{sh}^2 + V_{sd}^2\lambda_{sd}^2 + 2V_{sh}V_{sd}\max\left(\lambda_{sd/sh}^2, \lambda_{sh/sd}^2\right)$ Eq. (170),

where $\lambda = \sqrt{\rho_v / \rho_h}$, $\lambda_{sh} = \sqrt{\rho_{sh\_v} / \rho_{sh\_h}}$, $\lambda_{sd} = \sqrt{\rho_{sd\_v} / \rho_{sd\_h}}$, and I introduced the *"cross-anisotropies"* $\lambda_{sh/sd} = \sqrt{\rho_{sh\_v} / \rho_{sd\_h}}$, $\lambda_{sd/sh} = \sqrt{\rho_{sd\_v} / \rho_{sh\_h}}$.

*THEOREM 2. If the parameters* ($V_{sh}$, $V_{sd}$, $\lambda$, $\lambda_{sd}$, $\lambda_{sh}$) *satisfy* $\left(V_{sh}\lambda_{sh} + V_{sd}\lambda_{sd}\right)^2 \le \lambda^2$ *Eq. (171) then the generalized Klein-Clavaud Equations (165a&b) have physically meaningful (real and positive) solutions* $\rho_{sh\_h}$, $\rho_{sh\_v}$, $\rho_{sd\_h}$, $\rho_{sd\_v}$ .

The lower bound in Inequality (170) *can be used in the numerical or graphical interpretation of triaxial induction logs to exclude such "nonphysical" cases when the graphical or numerical solutions would result in negative, or complex-valued specific resistivities, or in unrealistic formation anisotropies for which* $\lambda = \sqrt{\rho_v / \rho_h} < 1$.

## 3.4. FRACTALS[131]

---

[129] Beckenbach, E.F. & Bellman, R.,1961: *Inequalities*. Springer Verlag, Berlin-Göttingen-Heidelberg; Bullen, P.S., 2003: *Handbook of Means and Their Inequalities*. Kluwer Academic Publishers, Dordrecht-Boston-London.

[130] Details are in Korvin 2012.

[131] Korvin, G. 'Fractals in geophysics: A guided tour'. *ASEG-SEG Adelaide* 1988: 301-303; Korvin, G. 'Fractured but not fractal: Fragmentation of the Gulf of Suez basement'. *Pure and Applied Geophysics PAGEOPH* 131(1-2)1989: 289-305; Korvin, G., Boyd, D.M. & O'Dowd, R. 'Fractal characterization of the South Australian gravity station network'. *Geophysical Journal International* 100(3)1990: 535-539; Korvin, G. 1992a. *Fractal Models in the Earth Sciences*. Amsterdam: Elsevier; Korvin, G. 'The kurtosis of reflection coefficients in a fractal sequence of sedimentary layers'. *Fractals-Complex Geometry Patterns and Scaling in Nature and Society* 1(2)1993: 263-268; 55.Gabor Korvin. 'Book review: Fractals in reservoir engineering: H.H. Hardy and R.A. Beier, World Scientific, London, 1994, Hardcover, XIV + 359 pp., ISBN 981-02-2069-3'. *Journal of Hydrology* 03/1996; 176(1–4):290–

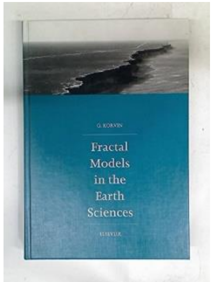


Fig. 31. My 1992 book. The book cover is not a computer-generated fractal, but photo of the Tertiary limestone cliffs, the Nullarbor karst, Australia. (Courtesy Dr. Yvonne Bone & Dr. Noel P. James)

---

293; Korvin, G., Mohiuddin, M.A. & Abdulraheem, A. 'Experimental investigation of the fractal dimension of the pore surface of sedimentary rocks under pressure'. Geophysical Transactions 44(1)2001: 3-19; Hassan, H.M., Korvin, G. & Abdulraheem, A. 'Fractal and genetic aspects of Khuff reservoir stylolites, Eastern Saudi Arabia.' *Arabian Journal for Science and Engineering* 27(1A)2002: 29-56; Masudul A. Choudhury, G. Korvin & Fazal Seyyed. 'Discovering micro level tradeoff in economic development and studying their fractal character'. *Indonesian Management & Accounting Research* 1(1)2002: 49-70; Oleschko, K., Korvin, G., Balankin, A.S., Khachaturov, R.V., Flores, L. Figueroa, B., Urrutia, J. & Brambila, F. 'Fractal scattering of microwaves from soils'. *Physical Review Letters* 89(18)2002: 188501/1-188501/4; Oleschko, K., Korvin, G., Figueroa, B., Vuelvas, M.A., Balankin, A.S., Flores, L., Carreón, D. 'Fractal radar scattering from soil'. *Physical Review E - Statistical, Nonlinear, and Soft Matter Physics* 67(41)2003: 41403/1-41403/13;Klavdia Oleschko, Benjamin Figuerora-Sandoval, Gabor Korvin & Maria Martinez Menes. 'Agroecometry: a toolbox for the design of virtual agriculture'. *Agricultura, sociedad y desarollo* 1(4)2004: 53-71 (In English & Spanish); Korvin, G. & Oleschko, K. 'Multiple wave scattering from fractal aggregates'. *Chaos, Solitons and Fractals* 19(2)2004: 421-425; Arizabalo, R.D., Oleschko, K., Korvin, G., Ronquillo, G. & Cedillo-Pardo, E. 'Fractal and cumulative trace analysis of wire-line logs from a well in a naturally fractured limestone reservoir in the Gulf of Mexico'. *Geofisica Internacional* 43(3)2004: 467-476; Korvin, G. 'Is the optical image of a non-Lambertian fractal surface fractal?' *IEEE Geoscience and Remote Sensing Letters* 2(4)2005:380-383; Nieto-Samaniego, A.F., Alaniz-Alvarez, S.A., Tolson, G., Oleschko, K., Korvin, G., Xu, S.S & Pérez-Venzor, J.A. 'Spatial distribution, scaling and self-similar behavior of fracture arrays in the Los Planes Fault, Baja California Sur, Mexico'. *Pure and Applied Geophysics* 162(5)2005: 805-826; Arizabalo, R.D., Oleschko, K., Korvin, G., Lozada, M., Castrejón, R. & Ronquillo, G. 'Lacunarity of geophysical well logs in the Cantarell oil field, Gulf of Mexico'. *Geofisica Internacional* 45 (2)2006: 99-113; 30. K. Oleschko, G. Korvin, A. Muñoz , J. Velazquez, M. E. Miranda, D. Carreon, L. Flores, M. Martinez, M. Velasquez-Valle, F. Brambila, , J.-F. Parrot & G. Ronquillo. 'Mapping soil fractal dimension in agricultural fields with GPR'. *Nonlinear Processes in Geophysics* 15(5)2008: 711-725; Velázquez-García, J., Oleschko, K., Muñoz-Villalobos, J.A., Velázquez-Valle, M., Menes, M.M., Parrot, J.-F., Korvin, G., Cerca, M. 'Land cover monitoring by fractal analysis of digital images'. *Geoderma* 160(1)2010: 83-92; Oleschko, K., Korvin, G., Flores, L., Brambila, F., Gaona, C., Parrot, J.-F., Ronquillo, G. & Zamora, S. 'Probability density function: A tool for simultaneous monitoring of pore/solid roughness and moisture content'. *Geoderma* 160(1)2010: 93-104; Torres-Argüelles, V., Oleschko, K.,Tarquis, A.M., Korvin, G., Gaona, C., Parrot, J.-F. & Ventura-Ramos, E. 'Fractal Metrology for biogeosystems analysis (Short & complete versions)'. *Biogeosciences* 7 (11)2011: 3799-3815 & *Biogeosciences Discussions* 7(2011): 4749-4799; Velásquez Valle, M.A., Medina García, G., Cohen, I.S., Oleschko, I.K., Ruiz Corral, J.A. & Korvin, G. 'Spatial variability of the Hurst exponent for the daily scale rainfall series in the state of Zacatecas, Mexico'. *Journal of Applied Meteorology and Climatology* 52(12)2013: 2771-2780; Arizabalo, R.D., González-Ávalos, E. & Korvin, G. 'Multifractal analysis of atmospheric sub-micron particle data'. *Atmospheric Research* 154(2015): 191-20; Gabor Korvin, Ruben V. Khachaturov, Klaudia Olechko. Gerardo Ronquillo, Maria de Jesus Correa Lopez & Juan-José Garcia. 'Computer simulation of microwave propagation in heterogeneous and fractal media'. *Computers & Geosciences* 100(2017): 156-165.
.

My research in fractals (which *started*, rather than reached its zenith, with my 1992 book) has been so much diversified, that I can only review three short topics to which I contributed, to illustrate the beauty and wide applicability of fractals.

## 3.4. A. SCALING OF TORTUOSITY IN SEDIMENTARY ROCKS[132]

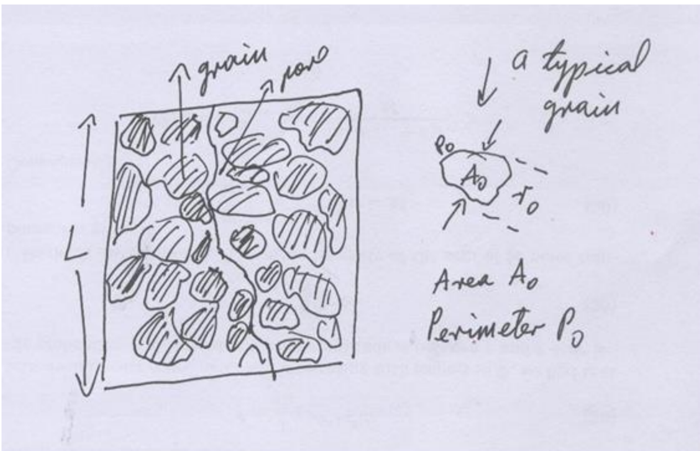


Fig. 32. Tortuosity scaling model

I developed a new model for the scaling of hydraulic tortuosity in a 2D cross-section of granular porous sedimentary rocks using heuristic arguments. Let (Fig. 32) $L$ be the vertical size of the section considered (hydraulic flow goes from top to bottom); Φ porosity (in fraction); τ *tortuosity* (= expected *hydraulic path length/Euclidean length* between two randomly selected points, $\tau \geq 1$); $r_0, P_0, A_0$ characteristic *size*, characteristic *perimeter*, characteristic *area* of the grains (in the *2D* section); $Z$ average number of pores adjacent to a grain (in the *2D* section). We shall denote by $D_{P/A}$ the exponent in the celebrated Mandelbrot's *perimeter-area law*[133] stated for the grains seen in 2D section:

$$P = P_0 \left(\frac{\sqrt{A_0}}{r_0}\right)^{D_{P/A}} \qquad \text{(Eq. 172)}$$

I proved the following: *The average hydraulic path of the flow from top to bottom is given by the equation* $\frac{L_{hydr}}{L} = \tau = \Phi + \frac{(1-\Phi)}{Z}\left(\frac{P_0}{r_0}\right)\left(\frac{\sqrt{A}}{r_o}\right)^{D_{P/A}}$ (Eq. 173)

---

[132] G. Korvin. 2016b. 'Permeability from Microscopy: Review of a Dream'.*Arabian J. of Science & Engineering* 41(6): 2045-2065; Korvin, G. 2020d. '*Statistical Rock Physics'* in B. S. Daya Sagar, Quiming Cheng, Jennifer McKinley and Frits Agterberg (eds.) Earth Sciences Series. *Encyclopedia of Mathematical Geosciences*. Springer (In Press); a similar model was used in: Naeem-Ur-Rehman Minhas, Bilal Saad, Maaruf Hussain & Gabor Korvin. 'Big Data hiding in small rocks: Case study of advanced microscopy and image processing to aid upstream asset development'. *Paper SPE-KSA*-233(2016).

[133] B. Mandelbrot, 1982. *The Fractal Geometry of Nature*. W.H. Freeman & Co., NY.; J. Feder, 1988. *Fractals*. Plenum, Plenum Press, NY.; G. Korvin, 1992: *Fractal Models in the Earth Sciences*. Elsevier, Amsterdam.

Note that for $\Phi = 1$ we have $\tau = 1$; for $\Phi = 0$ there are no pores at all, that is $Z = 0$ and consequently $\tau = \infty$ as it should be. Equation (173) can be derived with a *scaling argument*:
Along a randomly selected top-to-bottom vertical line of length $L$ by the *De-Lesse principle* of stereology[134] a total length $\Phi L$ of the line goes through pore space. Along such parts of the line the flow goes along a straight line. The remaining $(1-\Phi)L$ length of the vertical line is filled by grains, the fluid path would meet $\frac{(1-\Phi)L}{r_0}$ grains if it could flow along a straight vertical line. But it cannot proceed straight, as we see on Fig. 32. Every time the flow reaches a grain it changes direction and continues in a "throat" following the curvature of the grain's perimeter. By the definition of *the grain/pore coordination number Z*, the periphery $P$ of a grain is adjacent to Z grains, so that every individual "detour" adds a length $\left(\frac{P}{Z}\right)$ to the hydraulic path. This detour is, by Mandelbrot's Eq. (172) equal to $\left(\frac{P}{Z}\right) = \frac{P_0}{Z}\left(\frac{\sqrt{A}}{r_0}\right)^{D_{P/A}}$. As there are $\frac{(1-\Phi)L}{r_0}$ such detours, the total hydraulic length from top to bottom is $L_{hydr} = \Phi L + \frac{(1-\Phi)L}{Z}\left(\frac{P_0}{r_0}\right)\left(\frac{\sqrt{A}}{r_0}\right)^{D_{P/A}}$, what is the same as Eq. (173) to be proven.

I note that in most theoretical predictions of tortuosity, there is explicit or implicit dependence on porosity. In the *Lattice Gas* (LG) model of Koponen's group $\tau = 0.8(1-\Phi)+1$; in their percolation model $\tau = 1 + a\frac{(1-\Phi)}{(\Phi-\Phi_c)^m}$ (*a* and *m* are fitting parameters)[135]. Comiti and Renaud[136] used cube-shaped grains and got $\tau = 1 + P\ln\left(\frac{1}{\Phi}\right)$ (*P* is a fitting parameter). Yu's *2D* model[137] uses square-shaped grains, and yields the scaling law $\tau = \left(\frac{L}{\lambda_{\min}}\right)^{D_T-1}$ where the tortuosity dimension is $D_T = 1 + \frac{\ln\tau_{av}}{\ln\frac{L}{\lambda_{av}}}$ (the porosity dependence enters through the term "$\tau_{av}$" which is a complicated function of porosity (*op. cit*., Eq. (2)).

---

[134] K. Oleschko, 1988. Delesse principle and statistical fractal sets: 1. Dimensional equivalents. *Soil & Tillage Research*, 49: 255.
[135] A. Koponen, M. Kataja & J. Timonen, 1996, Tortuous flow in porous media. *Phys. Rev. E* 54: 406; A. Koponen, M. Kataja & J. Timonen, 1997, Permeability and effective porosity in porous media. *Phys. Rev. E* 56: 3319.
[136] J. Comiti, J. & M. Renaud, 1989. A New Model for Determining Mean Structure Parameters of Fixed Beds from Pressure Drop Measurements: Application to Beds Packed with Parallelepipedal Particles. *Chem. Eng. Sci.* 44(7):1539-1545.
[137] Bo-Ming Yu, 2005. Fractal character for tortuous streamtubes in porous media. *Chinese Phys. Lett*. 22(1): 158-160.

## 3.4. B. FRACTAL DISTRIBUTION OF THE SOUTH AUSTRALIAN GRAVITY STATION NETWORK[138]

In any country, the distribution of gravity stations is the result of a *multistage decision process*: in Australia, for example (i) the reconnaissance surveys totalling over 170, 000 stations have been completed by the *Bureau of Mineral Resources* using stations approximately 11 km apart (in South Australia and Tasmania 7 km apart), (ii) semi-regional surveys are usually read on a 0.5-2 km grid, according to the gravity response expected, and (iii) the detailed gravity surveys use stations with 100-500m spacing[139] . Because of the irregularity and sparsity of the stations there are interpolation errors, estimated[140] by Barlow with the formula $\varepsilon = 2k\sqrt{\Delta x}$ (where $k = 0.32 \pm 0.02$ and $\Delta x$ is interstation distance in km). Barlow concluded that $\varepsilon$ can be as high as 2.1 mgal for the Australian regional gravity survey, and 1.3 mgal where a more dense data coverage has been obtained.

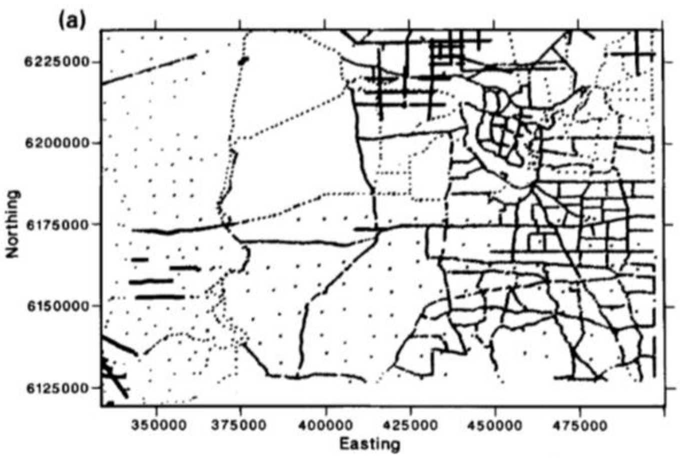


Fig. 33. A dense part of the South Australian gravity network: the Adelaide gravity stations. (From Korvin et al. 1990).

In 1986 Lovejoy and his group[141] proved that the *World Meteorological Station Network* is a 1.75-dimensional fractal set on the 2-D surface of the Earth, which is “highly regrettable” since

---

[138] Korvin, G., Boyd, D.M. & O'Dowd, R. ‘Fractal characterization of the South Australian gravity station network’. *Geophysical Journal International* 100(3)1990: 535-539.

[139] Fraser, A. R., Moss, F. J. & Turpie, A., 1976. Reconnaissance gravity survey of Australia, *Geophysics*, 41, 1337-1345; Lynch, A. M. & King, A. R.; 1983. A review of parameters affecting the accuracy and resolution of gravity surveys. *Bull. Aust. Soc. Expl. Geophys*., 14, 131-142.

[140] Barlow, B. C., 1977. Data limitations on model complexity; 2-D gravity modelling with desk-top calculators. *Bull. Austr. Soc. Expl. Geophys*., 8, 139-143; Sazhina, N. & Grushinsky, N., 1971. *Gravity Prospecting*, Mir Publishers, Moscow.

[141] Lovejoy, S. & Schertzer, D., 1986. Scale invariance, symmetries, fractals, and stochastic simulations of atmospheric phenomena, *Bull. Am. Meteor. Soc*., 67, 21-32. Lovejoy, S., Schertzer, D. & Ladoy, P., 1986a. Fractal characterization of inhomogeneous geophysical measuring networks, *Nature*, 319, 43-44. Lovejoy, S., Schertzer, D. & Ladoy, P., 1986b. Outlook brighter on weather forecasts, *Nature*, 320,401; Schertzer, D. & Lovejoy, S., 1985.

'to detect phenomena, not only must a network have sufficient spatial resolution, it must also have sufficient dimensional resolution. Whenever $D_f (= D_{fractal}) < D_e (= D_{Euclidean})$, sparsely distributed phenomena with dimension less than $D_e$-$D_f$ cannot be detected' (Lovejoy et al. 1986a). In our study, we determined the *fractal dimension* (more precisely, the *correlation dimension*) for the South Australian gravity station network.

EXCURSUS 5. CORRELATION DIMENSION OF FRACTAL POINT SETS[142]

> The standard (Mandelbrot's) method of estimating the fractal dimension of a planar point set is to divide a large square containing the set into $X^2$ equal squares and to count the number *N(X)* of those small squares containing points of the set. For fractal point sets $N(X) \propto X^{D_t}$ (Eq. 174a) , and $D_t$ $(0 < D_t < 2)$ is the corresponding fractal dimension. Another method consists of taking circles or squares of increasing size and counting how many points they contain. For fractal point sets the number of points in a circle of radius $X$ scales as $N(X) \propto X^{D_{t\prime}}$ (Eq.174b) where $D_t$ and $D_{t\prime}$ are not necessarily equal. Grassberger and Procaccia introduced the *density correlation function* of a point set A as $C(X) = \{Number\ of\ pairs\ of\ points\ such\ that\ X_i\ , X_j \in A, |X_i - X_j| = X\}$ (Eq.174c) and proved that for fractal sets $C(X) \propto X^{D_c}$ (Eq.174d) where the exponent $D_c$ is the same as $D_{t\prime}$ of (Eq.174b). They proved that Mandelbrot's fractal dimension $D_t$ (of Eq. 174a) and the correlation dimension $D_c$ are related by $D_c < D_t$ (Eq.174e). Since Inequality (Eq.174e) is quite tight in most cases, in most applications it is tacitly assumed that $D_c = D_t$ mainly because numerically[1] the determination of $D_c$, is much easier.

In order to determine the *correlation dimension* of the South Australian gravity network, we computed the correlation function by determining the cumulative frequency distribution (Eq.174c) of the interstation distances for a total number of 65, 049 stations. The distances were determined by spherical trigonometry, neglecting elevations. On double logarithmic plot (Fig. 34) the cumulative frequency distribution becomes a straight line over more than 2 decades of distance, proving the fractal character of the station distribution. The correlation dimension, determined from the slope of this straight line was surprisingly low: $D_c = 1.42$.

---

Generalised scale invariance in turbulent phenomena, *Phys.Chem. Hydrodyn*., 6, 623-635. Schertzer, D. & Lovejoy, S., 1986. Generalised scale invariance and anisotropic inhomogeneous fractals in turbulence, in: *Fractals in Physics*, pp. 457-460, Eds Pietronero, L. & Tosatti, E., North-Holland, Amsterdam; Korvin, G. 1992a. *Fractal Models in the Earth Sciences*. Amsterdam: Elsevier:120-126.

[142] B. Mandelbrot, 1982. *The Fractal Geometry of Nature*. W.H. Freeman & Co., NY; Grassberger, P. & Procaccia, I., 1983a. Measuring the strangeness of strange attractors, *Physica*, 9D, Nos 1 and 2, 189-208; Grassberger, P. & Procaccia, I., 1983b. Characterisation of strange attractors, *Phys. Rev. Lett.*, 50, 346-349.

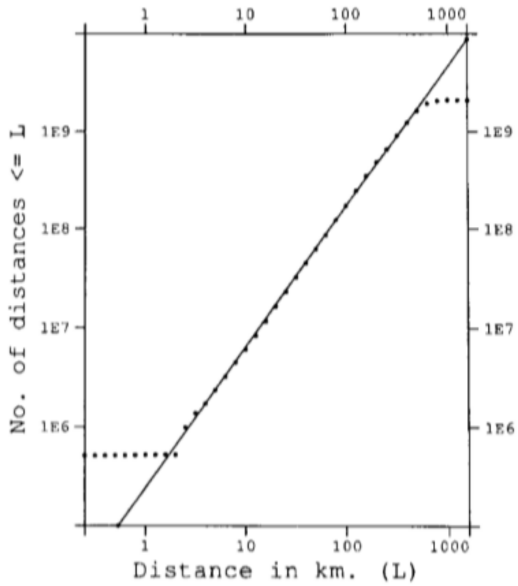


Fig. 34. Cumulative frequency distribution of the interstation distances for the South Australian gravity station network. (From Korvin et al. 1990).

The observable Bouguer gravity anomaly field is band-limited, i.e. there exists a geologically meaningful shortest wavelength $\lambda_{min}$ such that the power spectrum $B(k_x, k_y)$ of the Bouguer anomaly field is zero for wavenumbers $(k_x, k_y)$ for which $k_x^2 + k_y^2 \leq \frac{1}{\lambda_{min}^2}$ (Eq. 175).

If the region is a square of side $X$ then – by the 2-D form of *Shannon's sampling theorem*[143] – the gravity field can only be restored from its sampled values if at least $N = \pi \frac{X^2}{\lambda_{min}^2}$ (Eq. 176) samples are taken *along a regular grid*. For a fractal network of dimension d < 2, the number of stations within a square of side $X$ scales as $X^d$ rather than $X^2$ with increasing $X$, i.e. the network becomes more and more sparse and falls short of the Shannon condition (Eq. 176). Sampling along this low-dimensional *point set will preserve some aliasing frequencies and this will lead to spurious* anomalies if we interpolate onto a more dense regular grid. Though all wavenumbers will be affected, high-wavenumber (short-wavelength) information will be most seriously distorted. Such fractal analyses of sparse networks will be helpful in the optimal location of the necessary additional stations.

3.4. C. IS THE GULF OF SUEZ BASEMENT FRACTAL?[144]

[143] Brillouin, L., 1962. *Science and Information Theory*, 2nd edn, Academic Press, New York: Chapter 8.
[144] Korvin, G.'Fractured but not fractal: Fragmentation of the Gulf of Suez basement'. *Pure and Applied Geophysics PAGEOPH* 131(1-2)1989: 289-305; Korvin, G. 1992a. *Fractal Models in the Earth Sciences*. Amsterdam: Elsevier; Nieto-Samaniego, A.F., Alaniz-Alvarez, S.A., Tolson, G., Oleschko, K., Korvin, G., Xu, S.S & Pérez-Venzor, J.A.

Geophysical studies[145] revealed that the Palaeozoic basement of the *Gulf of Suez* consists of an enormous number of fault blocks whose network qualitatively resembles the contraction- crack polygons which can be found in nature in a wide variety of materials and on all scales (mud cracks, hardening concrete, age cracking in paintings, etc.[146]). The fault network of the Gulf of Suez basement forms a rather uniformly spaced polygonal pattern, most of the blocks are four-sided (Figs. 35, 36), the lengths of block sides parallel with the Gulf of Suez axis are exponentially distributed (Fig. 37a). By carefully analyzing the fault network, I found that a power-law size distribution associated with fractal (scale-free) fragmentation can be ruled out.

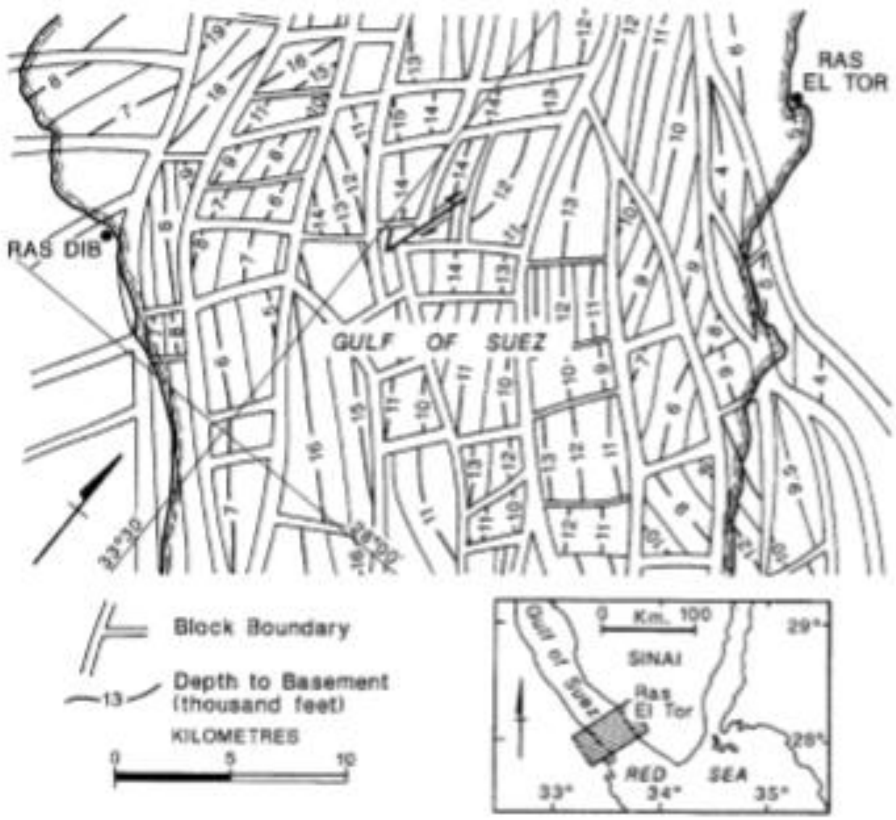


Fig. 35. A detail of the structural map of the Palaeozoic basement of the Gulf of Suez. Contour lines show depth to basement in thousand feet. (After Hammouda 1986).

---

'Spatial distribution, scaling and self-similar behavior of fracture arrays in the Los Planes Fault, Baja California Sur, Mexico'. *Pure and Applied Geophysics* 162(5)2005: 805-826.

[145] Hammouda, H. M. (1986), *Study and Interpretation of Basement Structural Configuration in the Southern Part of Gulf of Suez using Aeromagnetic and Gravity data*. Ph.D. Thesis, Faculty of Science, Cairo University.

[146] Korvin, G. 1992a. *Fractal Models in the Earth Sciences*. Amsterdam: Elsevier:

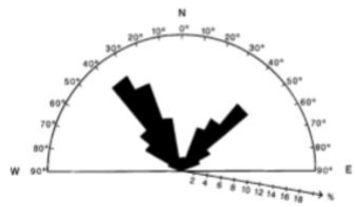

Fig.36. Rose diagram showing the directional distribution of the sides of fault blocks in the Gulf of Suez basement. The two main peaks correspond to the "Gulf of Suez" trend (N20-40$^{o}$W) and the "cross" trend (N40-50$^{o}$E structural directions). (From Korvin 1989).

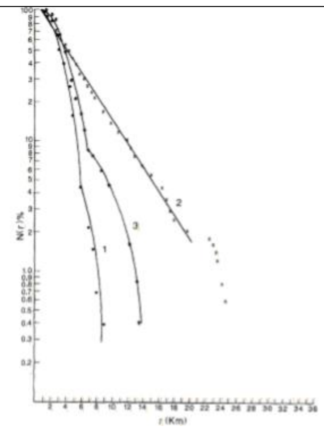

Fig. 37a.

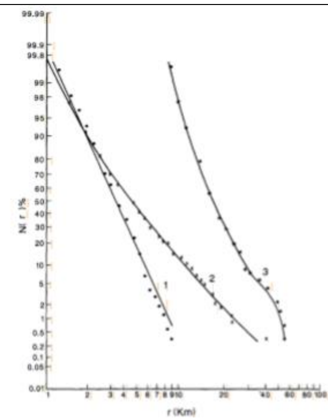

Fig. 37b

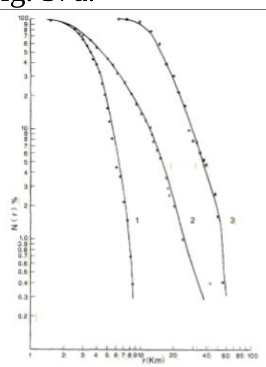

Fig.37c.

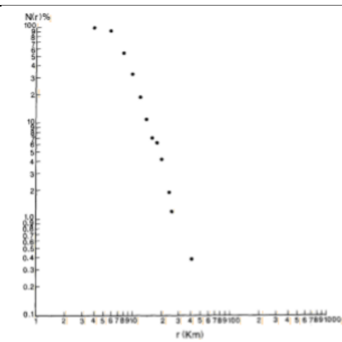

Fig. 38.

Figs. 37.a-c. Empirical cumulative frequency curves *N(r)* of the relative number of block sides greater than *r*. Curve 1: lengths of the "cross trend" sides (N40-50$^{o}$E); Curve 2: lengths of the "Gulf of Suez trend" sides (N20-40$^{o}$W); Curve 3: perimeter of the basement blocks in case of Figs. 37b and 37*c*, and quarter perimeters in Fig. 37a. Fig. 37*a* is *semilogorithmic plot*, Fig. 37b is a *lognormal probability plot*; Fig. 37*c* is *log-log plot*. Exponential distributions show up as straight lines on grid *a*, lognormal distributions on grid *b* and power-law (“fractal”) distributions on grid *c*. (From Korvin 1989).

Fig. 38. Log-log plot of the empirical cumulative frequency curve of the relative number *N(r)* of blocks whose *sieve diameter* (i.e., diameter of the smallest circumscribed circle) is larger than *r*. (From Korvin 1989).

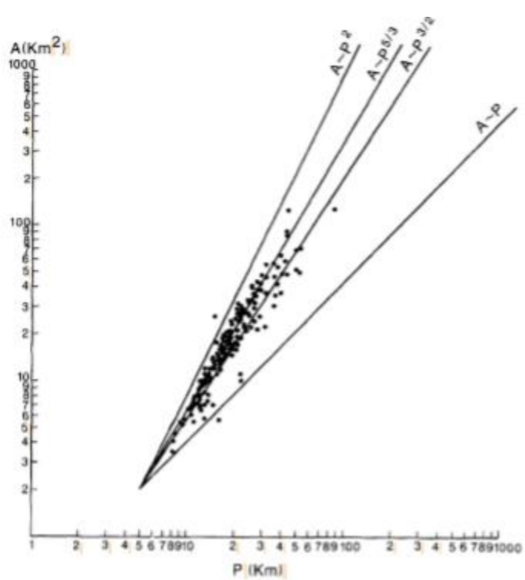


Fig. 39. Area-perimeter relation for the Gulf of Suez basement blocks. The lines $A \propto P^2$, $A \propto P^2, A \propto P^{5/3}, A \propto P^{\ 3/2}, A \propto P$ correspond, in turn, to the fractal dimensions D = 1; 6/5; 4/3 and 2. (From Korvin 1989).

The cumulative frequency distribution of fragment size is usually approximated by one of the following functions: (a) by an *exponential distribution*[147]: $N(r) \sim exp[-|r/r_0|^{\nu}]$ (Eq. 177a) where *N(r)* is number of fragments greater than $r$, $r_0$ and $\nu$ are constants; (b) by a *lognormal distribution*[148] : $N(r) \sim \int_r^{\infty} \frac{1}{\sigma(x-r_1)} \cdot exp\left[-\frac{1}{2\sigma^2}\left\{log\frac{r-r_1}{b}\right\}^2\right] dx$ ( Eq. 177b), where $\sigma$ , $r_1$ and $b$ are constants; and (c) by the *power-law* distribution[149]: $N(r) \sim (r/r_0)^{\alpha}$ $(\alpha < 0, r \neq 0)$ (Eq. 177c). In experimental studies the most commonly used measure of size is the "sieve diameter"[150]: for the particles passing through the sieve with opening diameter *r* their size is regarded as less than *r* . The distribution Eq. (177c) is exhibited by many geographical objects over a limited range of sizes. Korčak (1940) first described this distribution[151] for the areas of islands, Mandebrot[152] proved that Korčak law is the consequence of the repetitive subdivision of geometric figures and the exponent α is related to the *fractal dimension* of the objects which are usually self-similar, that is their arbitrarily small substructures look statistically similar to the whole object

---

[147] Brown,W.K.,Karp, R. R.& Grady, D. Z.1983. Fragmentation of the Universe, *Astrophys. and Space Science* 94: 401-412.
[148] Epstein, B. 1947. The Mathematical Description of Certain Breakage Mechanisms Leading to the Logarithmico-normal Distribution, *J. Franklin Inst*. 244: 471-477.
[149] Mandelbrot, B. B. 1982. *The Fractal Geometry of Nature*, Freeman, San Francisco; Rothrock, D. A. & Thorndike, A. S. 1984, Measuring the Sea Ice Floe Size Distribution. *J. Geophys. Res*. 89C: 6477-6486; Turcotte, D. L. 1986. Fractals and Fragmentation, *J. Geophys. Res*. 9IB:1921-1926.
[150] Epstein *op. cit.*
[151] Korčak, J. 1940, Deux types fondamentaux de distribution statistique, *Bull. Inst. Int. Stat*. 30, 295-299.
[152] Mandelbrot, B. B. 1975, Stochastic models for the Earth's Relief, the Shape and the Fractal Dimension of the Coastlines, and the Number-area Rule for Islands. *Proc. Nat. Acad. Sci. USA* 72:3825-3828.

under proper magnification. The power-law size distribution observed in the fragmentation of earth materials (rocks and sea ice) is consequence of the *scale invariance of the fragmentation mechanism*, that is the pre-existing zones or planes of weakness where breakage occurs, exist on all scales[153]. In fractal fragmentation theories it is assumed that the flaws leading to damage have a hierarchical structure, where a fracture at the macroscopic scale is caused by the accumulation of micro-fractures at lesser scales. The formalization of this principle has led to the *RNG* (*Renormalization Group*) methods of predicting rock failure[154].

The basement map (only a small part of it is shown in Fig. 35) contains 242 blocks. Most of them (220) are four-sided, eight are two-sided, seventeen are three-sided and fifteen are five-sided. As in the absence of asymmetrical tectonic forces the surface of a homogeneous medium will be criss-crossed by a hexagonal crack system[155], the predominance of four-sided blocks suggests *anistropic stress*. This is corroborated by the *rose diagram* of block sides (Fig. 36). There are two distinct directional sets: one parallel to the Gulf of Suez axis (N20-40$^o$W) and an almost perpendicular "cross trend" (N40-50$^o$E)[156] . Thus, the system is *oriented orthogonal*[157].

I separately studied the following size parameters (Figs. 37.a-c, & 38): length of the "cross trend" block sides (curve 1 in Figs. 37a-c); length of the "Gulf of Suez trend" sides (curve 2 in Figs. 37a-c); perimeters of the blocks (curve 3 in Figs. 37a-c, see also Fig. 39); "sieve diameter Fig. 38); and area of the blocks (Figure 39).

On the basis of Fig. (37c & 38), and by visually inspecting Fig. 35, which shows a uniform spacing between the fault lines (rather than a scale-free Apollonian gasket associated with fractal fragmentation[158]), , the power-law distribution of the size parameters can be ruled out. As a matter of fact, a power-law block-size distribution would correspond to *scale invariance*, while

---

[153] Matsushita, M. 1985. Fractal viewpoint of Fracture and Accretion, *J. Phys. Soc. Japan*. 54:857-860; Turcotte *op. cit*.

[154] Allègre C. J., Le MouelL, J. L., & Provost, A. 1982. Scaling Rules in Rock Fracture and Possible Implications for Earthquake Prediction, *Nature* 297: 4749; Madden, T. R. 1983. Microcrack Connectivity in Rocks: A Renormalisation Group Approach to the Critical Phenomena of Conduction and Failure in Crystalline Rocks. *J. Geophys. Res*. 88:585-592; Turcotte *op. cit*.; Korvin, G. 1992a. *Fractal Models in the Earth Sciences*. Amsterdam: Elsevier: 210-215; .Korvin, G. 2020d. ‘Statistical Rock Physics’ in: B. S. Daya Sagar, Quiming Cheng, Jennifer McKinley and Frits Agterberg (Eds.) Earth Sciences Series. *Encyclopedia of Mathematical Geosciences*. Springer (In Press).

[155] Thompson, D'Arcy W., *On Growth and Form*. Cambridge University Press, Cambridge 1942; Billings, M. P., *Structural Geology*. Prentice Hall, New York 1954.

[156] Also observed by Jarrige, J. J., D'estevou, P. O., Burollet, P. F., Thiriet, J. P., Icart, J. C., R1chert, J. P., Sehans, P., Montenat, C., and Prat, P. 1986. Inherited Discontinuities and Neogene Structure: The Gulf of Suez and the Northwestern Edge of the Red Sea, *Phil. Trans. R. Soc. Lond*. A317, 129-139.

[157] According to the classification of Lachenbruch, A. H. 1962. Mechanics of Thermal Contraction Cracks and Ice-wedge Polygons in Permafrost. *Geol. Soc. Am. Spec. Paper* 70, 69 pp.

[158] Rothrock, D. A., and Thorndike, A. S. 1984. Measuring the Sea Ice Floe Size Distribution, J. Geophys. Res. 89C: 6477-6486; MatsushitA, M. 1985. Fractal viewpoint of Fracture and Accretion. *J. Phys. Soc. Japan*. 54, 857-860.

contraction-crack polygons always have a *characteristic length* related to the elastic properties and thickness of the contracting layer[159].

The exponential distribution of the length of the (N20-40$^o$W) block sides reminds us of fragmentation processes leading to such size distribution. Griffith showed that if the energy consumed in breaking is proportional to the new surface formed, then (the Maxwell- Boltzmann) *energy partition law* leads to an exponential size distribution of the resulting particles. Gilvarry derived the exponential distribution of fragment size in processes where the breakage proceeds along pre-existing Poisson-distributed flaws. Within the framework of Gilvarry's theory the value of $r_0$ = 4.66 km figuring in the size distribution $N(r)\sim exp[-r/r_0]$ of curve 2 in Fig. (37a) equals the mean spacing between pre-existing Poisson-distributed flaws. The Poisson distribution of flaws prior to fragmentation is also in concord with the finding that most of the blocks are four-sided, as we know from *Statistical Geometry* that if a plane is dissected by *Poisson-distributed random straight lines*, the expected number of sides of the resulting polygons will be four[160].The *lognormal distribution* of the length of the (N40-50$^o$E) block sides calls for a reconsideration of the work of Epstein who explained the *lognormal size distribution of fragments* assuming a scale-invariant and iterative breaking process[161].

As Fig. (39) shows, there is a fair correlation between the area of the blocks and a power of their perimeter with an exponent slightly less than two. It is well-known that for a set of random planar figures bounded by irregular curves of fractal dimension D, the area and perimeter are related by Mandelbrot's rule $P \propto \left(\sqrt{A}\right)^D$ (Eq. 178, same as Eq. 172 above ). Thus, the exponents 2, 5/3, 3/2, 1 indicated in Fig. (39) correspond, in turn, to perimeters of fractal dimension D = 1, D = 6/5, D = 4/3, D = 2. As most of the points in Fig. (39) cluster in the range 1.2 < D < 1.33 of low fractal dimensions, this is a further indication that the *fragmentation of the Gulf of Suez basement is not fractal*.

In an attempt to model the fractal relief of the earth, Mandelbrot[162] started out from *Poisson-distributed* random straight lines dissecting a plane, in each case subjected the two sides to random vertical displacements in order to create "cliffs" and repeated this process *ad infinitum*. The fault network, and the vertical displacement of the blocks, observed in the Gulf of Suez

[159] Neal, J. T., Langer, A. M., & Kerr, P. F. 1968. Giant Desiccation Polygons of Great Basin Playas. *Geol. Soc. Amer. Bull.* 79, 69-70.
[160] Kendall, M. G., and Moran, P. A. P., *Geometrical Probability*. Griffin and Co., London, 1963.
[161] Epstein, B. 1947. The Mathematical Description of Certain Breakage Mechanisms Leading to the Logarithmico-normal Distribution, *J. Franklin Inst*. 244, 471-477; Gilvarry, J. J. 1964. Fracture of Brittle Solids. Distribution Function for Fragment Size in Single Fracture. (Theoretical). *J. Appl. Phys*. 32, 391-399; Griffith, L. 1943. A Theory of the Size Distribution of Particles in a Comminuted System. *Can. J. Research* 21A: 57-64.
[162] Mandelbrot, B. B. 1975. Stochastic models for the Earth's Relief, the Shape and the Fractal Dimension of the Coastlines, and the Number-Area Rule for Islands. *Proc. Nat. Acad. Sci. USA* 72: 3825-3828.

Palaeozoic Basement, resemble *an early stage of this random geomorphological process*. Using modern terminology, they resemble a *prefractal*.[163]

## 3.5. PETROPHYSICS OF POROUS ROCKS[164]

### 3.5.A. PERMEABILITY OF KAOLINITE-BEARING SANDSTONES

#### EXCURSUS 6. PERCOLATION THEORY[165]

*Percolation Theory* was invented by S. R. Broadbent who worked on the design of gas masks for use in coal mines. The masks contained porous carbon granules into which the gas could penetrate. Broadbent found that if the pores were large enough and sufficiently well connected, the gas could permeate the interior of the granules; but if the pores were

---

[163] Prefractals are sets that are only fractal in a *limited range of scales*. That is, *their iterative generation stopped after some finite steps*. See e.g. Behzad Ghanbarian-Alavijeh, Humberto Millán & Guanhua Huang 2010. A review of fractal, prefractal and pore-solid-fractal models for parameterizing the soil water retention curve. *Canadian Journal of Soil Science* 91(1): 1-14.

[164] Korvin, G. 2020d. 'Statistical Rock Physics' in B. S. Daya Sagar, Quiming Cheng, Jennifer McKinley and Frits Agterberg (eds.) Earth Sciences Series. *Encyclopedia of Mathematical Geosciences*. Springer (In Press); Islam el-Deek, Osman Abdullatif & Gabor Korvin, 'Heterogeneity analysis of reservoir porosity and permeability in the late Ordovician glacio-fluvial Sarah formation paleovalleys, central Saud Arabia. *Arab. J. Geosci*. 10(2017): 400-417; G. Korvin. 2016b. 'Permeability from Microscopy: Review of a Dream'.*Arabian J. of Science & Engineering* 41(6)2016: 2045-2065; Naeem-Ur-Rehman Minhas, Bilal Saad, Maaruf Hussain & Gabor Korvin. 'Big Data hiding in small rocks: Case study of advanced microscopy and image processing to aid upstream asset development'. Paper SPE-KSA-233(2016); Abdlmutalib, A., Abdullatif, O., Korvin, G. & Abdulraheem, A. 'The relationship between lithological and geomechanical properties of tight carbonate rocks from Upper Jubaila and Arab-D Member outcrop analog, Central Saudi Arabia'. *Arabian Journal of Geosciences* 8(12)2015: 1031–1048; Korvin, G., Oleschko, K. & Abdulraheem, A. 'A simple geometric model of sedimentary rock to connect transfer and acoustic properties'. *Arabian Journal of Geosciences* 7(3)2014: 1127-1138; Korvin, G., Sterligov, B., Oleschko, K. & Cherkasov, S. 'Entropy of shortest distance (ESD) as pore detector and pore-shape classifier'. *Entropy* 15 (6)2013: 2384-2397; Korvin, G. 'Bounds for the resistivity anisotropy in thinly-laminated sand-shale'. *Petrophysics* 53(1)2012: 14-21; Oleschko, K., Korvin, G., Flores, L., Brambila, F., Gaona, C., Parrot, J.-F., Ronquillo, G. & Zamora, S. 'Probability density function: A tool for simultaneous monitoring of pore/solid roughness and moisture content'. *Geoderma* 160(1)2010: 93-104; A. Abdulraheem, E. Sabakki, M. Ahmed, A. Ventala, I. Raharja, & G. Korvin. 'Estimation of permeability from wireline logs in a Middle Eastern Carbonate Reservoir using fuzzy logics'. *Paper SPE-10535*0(2007); Korvin, G., Mohiuddin, M.A. & Abdulraheem, A. 'Experimental investigation of the fractal dimension of the pore surface of sedimentary rocks under pressure'. *Geophysical Transactions* 44(1)2001: 3-19; Korvin, G. 1992b 'A percolation model for the permeability of kaolinite-bearing sandstones'. *Geophysical Transactions* 37(2-3): 177-209; Korvin, G. 1982a.'Axiomatic characterization of the general mixture rule'. *Geoexploration* 19(4): 267-276; 70.Korvin, G. 'Effect of random porosity on elastic wave attenuation'. *Geophysical Transactions* 26(1980): 43-56; Korvin, G. 1978c. 'The hierarchy of velocity formulae: Generalized mean value theorems.'*Acta Geod. Geoph. et Mont. Acad. Sci. Hung*. 13(1-2)1978: 211-222; G. Korvin. & Lux, I. 'An analysis of the propagation of sound waves in porous media by means of the Monte Carlo method'. *Geophysical Transactions* 21(3-4)1972: 91-106.

[165] Broadbent S. R. 1954: Discussion on Symposium on Monte Carlo Methods. *J. Roy. Statistic. Soc*. B. 68 p.; Hammersley J. M. 1983: Origins of percolation theory. *In*: Deutscher G., Zallen R. and Adler J. (Eds.) *Percolation Structures and Processes. Ann. Israel Phys. Soc*. 5, pp. 48-57; Zallen R. 1983: *Introduction to percolation: A model for all seasons. In*: Deutscher G., Zallen R. and Adler J. (Eds.) *Percolation Structures and Processes. Ann. Israel Phys. Soc.* 5, pp. 4-16; Ziman J. M. 1979*: Models of Disorder*. Cambridge U. Press, Cambridge.

too small or inadequately connected, the gas would not get beyond the granules' surface. There was a *critical* porosity and pore interconnectedness, above which the mask worked well and below which it was ineffective. Thresholds of this sort are typical of *percolation processes*. In the *bond- percolation* problem we assume that a fraction *1-p* ( $0 < p < 1$) of the bonds of a regular grid are randomly cut and a fraction *p* are left uncut.

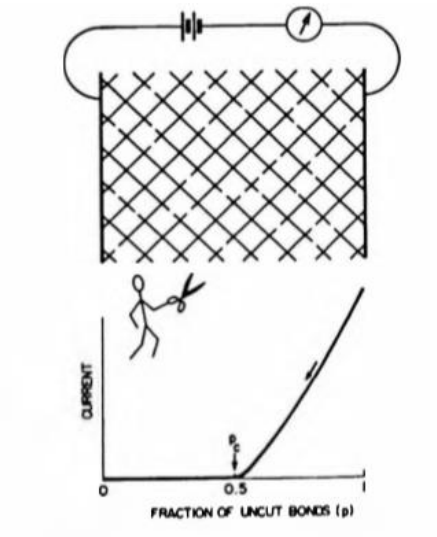


Fig. 40. Randomly cut electric network as example for percolation (after Zallen 1983)

Then there exists a critical fraction $p_c$ (called *percolation threshold*) such that there is no continuous connection along the bonds of the network between the opposite faces for $p < p_c$ , and there exists a connection with probability 1 for $> p_c$ . For the 2-dimensional square lattice the percolation threshold is 0.5. In the more general case the percolation threshold depends on the dimensionality of the network, *d*, and on its coordination number *Z* (the average number of bonds connected to any node of the network), but *it is independent of the detailed structure of the network.* Table 2 lists coordination numbers and percolation thresholds for some common networks. In *d*-dimensions, the percolation thresholds and coordination numbers conform closely to the empirical rule: $Zp_c = d/(d-1)$ .

Table 2. Lattices with their Percolation Probabilities (From Korvin 1992: 22; 1992a)

| Lattice | Dimension | Coordination number $Z$ | $p_c$ |
|---|---|---|---|
| Honeycomb | 2 | 3 | 0.6527 |
| Square | 2 | 4 | 0.5 |
| Triangular | 2 | 6 | 0.3473 |
| Tetrahedral (diamond) | 2 | 4 | 0.39 |
| Simple Cubic | 3 | 6 | 0.25 |
| Body Centered Cubic | 3 | 8 | 0.18 |
| Face Centered Cubic | 3 | 12 | 0.12 |
| Hexagonal Close Packing | 3 | 12 | 0.12 |

Close to the percolation threshold ( $p > p_c$ ) the nodes which are connected with each other by continuous paths form large clusters of average size $\xi$ , called the *correlation length*. The correlation length diverges for $p \to p_c, p > p_c$ as $\xi \propto (p - p_c)^{-\nu}$ , for 3-dimensional networks $\upsilon = 0.83$ , independently of the coordination number. Percolation between two opposite nodes of a cluster, a distance $\xi$ apart, takes place along tortuous zig-zag paths. Near the percolation threshold the length $L(\xi)$ of a typical flow path will grow as a power of $\xi$ : $L(\xi) \propto (p - p_c)^{\alpha}$ for $p \to p_c, p > p_c$ . As the correlation length $\xi$ is the natural length scale in percolation problems, we define the *tortuosity* of the percolation path as: $\tau = L(\xi)/\xi \propto \xi^{\alpha-1} =:= (p - p_c)^{-\gamma}$ where, for different models of the percolation path the tortuosity exponents $\gamma$ are compiled in Table 3.

Table 3. Tortuosity Exponents (after Korvin 1992: 29, 1992a)

| Model of the percolation path | $\gamma$ | Note |
|---|---|---|
| Straight line through the correlation length $\xi$ | 0 | 3D percolation |
| Minimum path | 0.25 | 3D percolation |
| Conductive path | 0.29 | 3D percolation-conduction |
| Self-avoiding random walk on uncut bonds | 0.58 | 3D percolation |
| Brownian motion in 3D | 0.83 | |
| Brownian motion on a $d_f$-dimensional fractal | $0.83(1.5d_f - 1)$ | By the “Alexander-Orbach conjecture” $\alpha = \left(\frac{3}{2}\right).d_f$ (Korvin 1992a: 29 |

I applied[166] *Percolation Theory* to explain a set of controversial *permeability vs. porosity measurements*[167] (Fig. 41) on 638 cylindrical kaolinite-bearing sandstone core plugs cut from Eromanga Basin[168], South Australia wells. (Kaolinite is a "discrete-particle" clay[169], it is preferentially deposited in the throats of the sandstone's pores, completely blocking them.). Absolute grain density and *Cation Exchange Capacity* (CEC) were determined on 246 plugs. Forty-seven samples were subject to X-ray diffraction analysis to find the distribution of the bulk mineralogy and the mineralogy of the < 2 $\mu$m fraction. Sixty samples were submitted for electrical properties determination, using simulated formation brines, twenty-one of these had repeat measurements of conductivity in NaCl brines of differing salinity. (Results are tabulated in Gravestock & Alexander *op. cit.*). Five grain-size categories were selected (see Fig. 41) by visual examination: coarse-, medium- and fine sandstone, siltstone and mudrock. Fine sandstone samples were further sub-divided into two sets: those with permeability of 100 md or more, and those with less than 100 md permeability

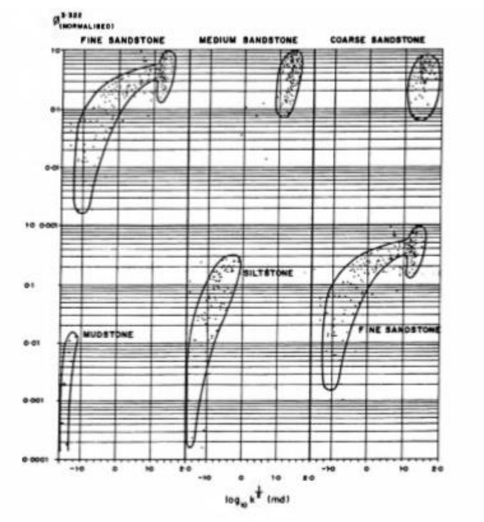


Fig. 41. Porosity—permeability trends by visual grain-size [from Gravestock & Alexander 1988]

---

[166] Korvin 1992: 28-33; 1992a.
[167] Gravestock D. I & Alexander E. M. 1986: Porosity and permeability of reservoirs and caprocks in the Eromanga Basin, South Australia. *The Australian Petroleum Exploration Association Journal* 26: 202-213.
[168] Eromanga Basin (Fig. 42) is Australia's largest onshore hydrocarbon province, covers an area approximately 1,000,000 km$^2$, within which up to 3,000 m of Jurassic to Late Cretaceous sediments are preserved. The sequence consists of a lower suite of continental deposits which unconformably overlie deeper Palaeozoic basins or older metamorphic and igneous rocks, and an upper suite of transgressive marine sediments which in turn are overlain by thick paralic to continental strata. Numerous oil and gas accumulations have been discovered in the lower suite.
[169] According to the classification of Neasham J. W. 1977. The morphology of dispersed clay in sandstone reservoirs and its effects on sandstone shaliness, pore space and fluid flow properties. *SPE Paper* 6858.

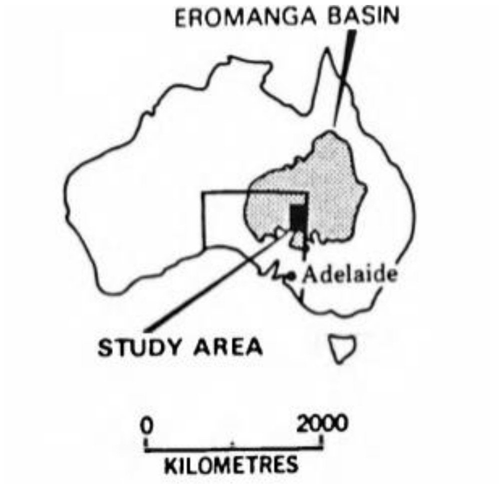


Fig. 42. Location map of the study area.

I realized that If the pore structure of a sedimentary rock is converted to a discrete lattice by letting *pores correspond to nodes, and throats to bonds,* then the continuous *Darcy flow* becomes a *lattice percolation*. For *kaolinite-bearing sandstones,* if a given throat is completely blocked by kaolinite the corresponding bond will be considered as 'cut'. If any throat is open with probability $p$ and blocked by kaolinite particles with probability $q = 1-p$ , then in the equivalent bond-percolation problem a fraction $q$ of the bonds are randomly cut. There exists a *percolation threshold* such that the fluid cannot flow through the sample for $p < p_c$ and percolation starts for $p > p_c$. At the onset of percolation the fluid particles follow zig-zag paths, the closer is $p$ to $p_c$, the greater will be the length $L(x)$ of a typical path between two nodes, which are geometrically a distance $x$ apart. (Fig. 43).

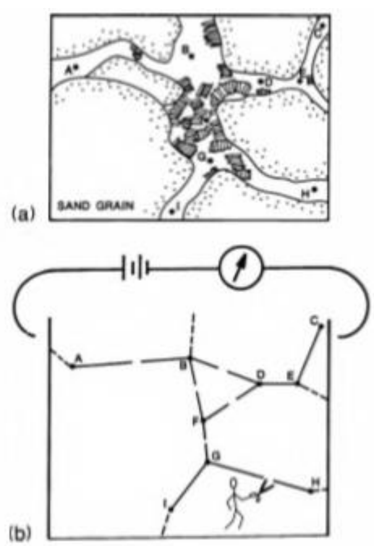


Fig. 43. Fluid transfer through kaolinite-bearing sandstone (a) and the corresponding lattice percolation model (b). Nodes correspond to pores, uncut bonds to open throats, cut bonds to throats blocked by kaolinite particles. The symbolic 'current' can be an arbitrary transfer process.

Express the *Kozeny-Carman* (*KC*) equation in terms of the hydraulic radius as

$k = \frac{R_{HYD}^2}{b} \cdot \Phi \cdot \frac{1}{\tau^2}$, (more precisely, $k[md] = \frac{(R_{HYD}[mm])^2}{b} \Phi \frac{1}{\tau^2} \cdot 10^9$), let $\lambda$ denote the volume fraction of kaolinite , $\Phi$ porosity, then the ratio of open pore space to the total space filled by pores or clays is $p = \frac{\Phi}{\Phi+(1-\Phi)\lambda}$ . The tortuosity tends to infinity with $p \to p_c, p > p_c$ as $\tau \propto (p-p_c)^{-\nu}$, that is $\frac{1}{\tau^2} \propto (p-p_c)^{2\nu}$. Define a percolation function PERC as

$$PERC = \begin{cases} 0 \quad if \quad p \leq p_c \\ C_0(p-p_c)^{2\nu} = C_0(p-p_c)^{PEX} \quad if \quad p > p_c \end{cases} \qquad \text{(Eq. 179)}$$

where $PEX = 2\nu$, the normalizing constant $C_0$ is chosen such as to make *PERC(1)=1*, that is $C_0 = 1/(1-p_c)^{PEX}$ . To find the *prefactor* in the asymptotic law $\frac{1}{\tau^2} \propto (p-p_c)^{2\nu}$ , we consider clean sand with $\lambda = 0$ kaolinite content, in which case $p$= *1* and PERC(1) = 1, that is for $\tau_0$ we can choose a reasonable average tortuosity for clean sands, say $\tau_0 = 4$ . Geometrical considerations give $R_{HYD} = \frac{1}{3} \cdot \frac{\Phi+(1-\Phi)\lambda}{(1-\Phi)(1-\lambda)} \cdot r\sqrt{p}$ (where $\Phi, \lambda \neq 1$ , $r$ is *mean grain radius*). The final expression for *k* becomes, as function of $\Phi, r, Z, \lambda$ (porosity, grain radius, coordination number, and kaolinite volume content):

$$k = \begin{cases} \frac{R_{HYD}^2}{b\tau_0^2} \cdot \Phi \cdot 10^9 \cdot \left(\frac{p-p_c}{1-p_c}\right)^{PEX} \quad p \geq p_c \\ 0 \quad p < p_c \end{cases} \qquad \text{(Eq. 180)}$$

with $b = 2, \tau_0 = 4, p_c = 1.5/Z$ ; $p = \frac{\Phi}{\Phi+(1-\Phi)\lambda}$ ; $R_{HYD} = R_{HYD} = \frac{1}{3} \cdot \frac{\Phi+(1-\Phi)\lambda}{(1-\Phi)(1-\lambda)} \cdot r\sqrt{p}$ .

There is a good correlation between measured permeabilities, and permeabilities computed with Eq. (180) using the parameters shown in Table 4 and Fig. 45:

Table 4. Summary of data used to construct Figure 44

| Lithology Number | Code | Name | Wentworth Size Range (mm) | $\bar{r}$ | No. of samples | $\Phi_{min}$ | $\Phi_{max}$ | $Z_{opt}$ | $PEX_{opt}$ |
|---|---|---|---|---|---|---|---|---|---|
| 1 | ❑ | Coarse sandstone | 1-0.5 | 0.375 | 31 | 0.11 | 0.24 | 2.5 | 1.5 |
| 2 | ❍ | Medium sandstone | 0.5-0.25 | 0.188 | 57 | 0.06 | 0.25 | 2.5 | 3.0 |
| 3 | ■ | High $k$ (clean) fine sandstone | 0.25-0.125 | 0.094 | 37 | 0.0 | 0.26 | - | 0 |
| 4 | △ | Low $k$ (shaly) fine sandstone | 0.25-0.125 | 0.094 | 74 | 0.0 | 0.26 | 6.0 | 5.5 |
| 5 | ▲ | Silstone | 0.0625-0.0039 | 0.02 | 30 | 0.0 | 0.18 | 6.0 | 2.0 |

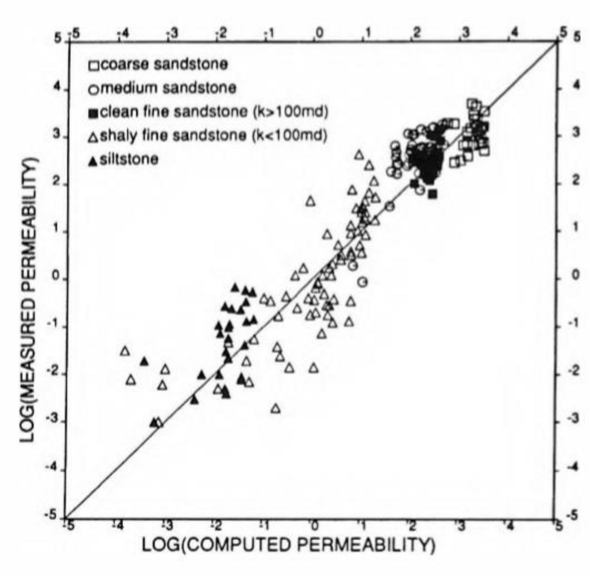


Fig. 44. Crossplot of measured vs. computed permeabilities

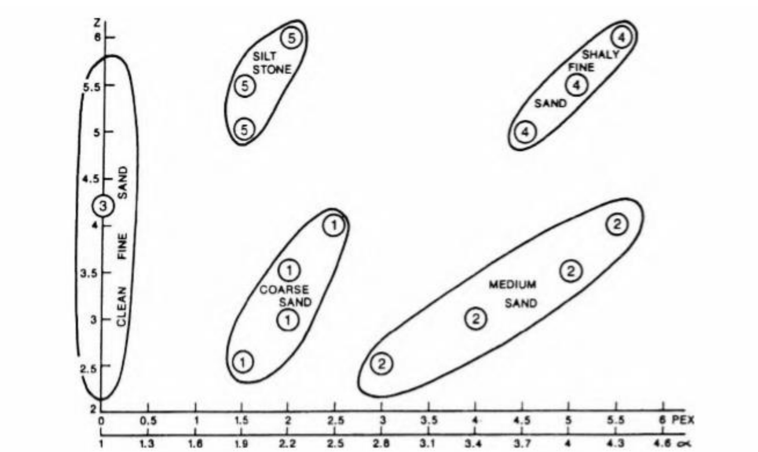


Fig. 45. Optimal percolation parameters $Z_{opt}$ and $PEX_{opt}$ for the five different lithologies . $Z$ = coordination number, $PEX$ = percolation exponent, $\alpha$ fractal dimension of the tortuous flow path.

Figure 45, showing the optimum percolation parameters ($Z_{opt}$, $PEX_{opt}$) for the different lithologies, has two horizontal scales: the percolation exponent $PEX$ and the fractal dimension $\alpha$ of the percolating fluid path. The two values are related by: $PEX = 1.66\ (\alpha - 1)$ for 3-dimensional percolation[170].

[170] Ritzenberger A. L.,& Cohen R. J. 1984. First passage percolation: Scaling and critical exponents. *Phys. Rev. B*. 30, 7: 4038-4040.

Equations (179-180) only apply for sandstones containing ‘discrete particle’ type clay[171], for example, kaolinite. In their derivation, I used an empirical equation which I established for the Eromanga Basin samples: $\lambda = 0.002\, CEC$ (Eq. 181), where *CEC* is in *meq /100 g*, and $\lambda$ is the weight proportion of the clay size ($< 2\ \mu$m ) fraction, determined from semiquantitative *XRD*. For any other region a new calibration should be found between kaolinite content and *CEC*.

The most important finding of the study had been that the *vanishing permeability at and below the percolation threshold can be ascribed to the divergence of tortuosity. I expect this conclusion to remain valid for other clay morphologies, though different percolation models would describe the effect of pore-lining (chlorite) and pore-bridging (illite) clays*. Mixed clay morphologies (as e.g. Permian sandstones from the Cooper Basin, South Australia, where the illite/kaolinite ratio has been found[172] to depend on the grain-size of the host rock) pose an intriguing, if not intractable, challenge.

### 3.5.B. A NEW GEOMETRIC MODEL OF SEDIMENTARY ROCK[173]

Apart from living organism, rocks are the most complicated structures in the world:

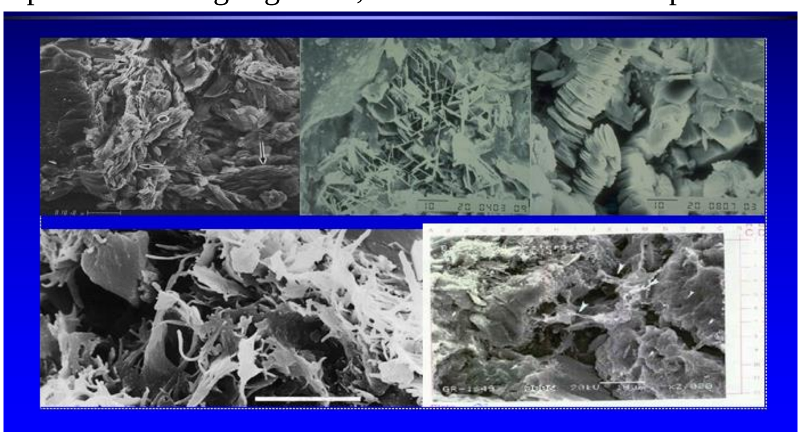

Fig. 46a. Sedimentary rocks under the *SEM*.

---

[171] Neasham J. W. 1977. The morphology of dispersed clay in sandstone reservoirs and its effects on sandstone shaliness, pore space and fluid flow properties. SPE Paper 6858.
[172] Schulz-Rojahn J. P. & Phillips S. E. 1989: Diagenetic alteration of Permian reservoir sandstones in the Nappameri Trough and adjacent areas, southern Cooper Basin. *Proc. of the Cooper and Eromanga Basins Conf.*, Adelaide: 629-645.
[173] Korvin, G., Oleschko, K. & Abdulraheem, A. ‘A simple geometric model of sedimentary rock to connect transfer and acoustic properties’. Arabian Journal of Geosciences 7(3)2014: 1127-1138.


Fig. 46b. Turbidite sandstone core from Campos Basin, Brazil (From: Grochau & Gurevich, *Geophysics* 73(2)2008: E59-E65).

Between 2010-2015, I worked on the following research problem, raised[174] by dr. Nabil Akbar of Saudi Aramco, Dhahran, Saudi Arabia: *Suppose we are given the measured porosity Φ, permeability k, and cementation exponent m of a sedimentary rock. Find an equivalent rock model characterized by the following three geometric, and one topological properties:*

- *r (average pore radius)*
- *d (average distance between two nearest pores)*
- *δ (average throat diameter)*
- *Z (average coordination number[175] of a pore)*

*The model should be derivable from values of k, m, Φ measured at atmospheric pressure, and it should exactly reproduce the measured values.*

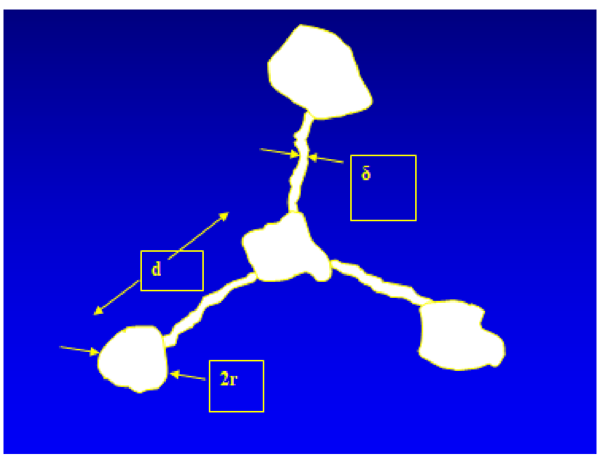


Fig. 47. The parameters r, d, δ, Z . (Z=3 in this case).

---

[174] Akbar, N.A. (1993). Seismic signatures of reservoir transport properties and pore fluid distribution. *Ph. D. Thesis*, Stanford University, Stanford; N. A. Akbar, Mavko G, Nur A, Dvorkin J. 1994. Seismic signatures of reservoir properties and pore fluid distribution. *Geophysics* 59(8):1222–1236.

[175] The coordination number Z is the average number of throats emerging from one pore.

(Here: *porosity* $\Phi$ =*volume of empty space*/*total volume*; *permeability* $\kappa$ is in Darcy units in the Equation $V_x = -\frac{\kappa}{\eta}\frac{\partial P}{\partial x}$ where $V_x$ is fluid-flow rate in the *x*-direction, $\eta$ is viscosity, *P* fluid pressure; *cementation exponent m* is the exponent in Archie's Law $\varrho = \Phi^{-m}\rho_{fluid}$ ).

EXCURSUS 7. ROCK INVERSION THEORY – WHY 3 PARAMETERS?

Consider a rock whose pores are fluid-filled ellipsoids with semi-axes (*a, b, c*), a pore is connected to *Z* nearby pores with throats which have a length *l* and an elliptic cross-section with semi axes ($r_1$, $r_2$ ).

We measure *M* bulk data $B_1$, ,…,$B_M$ such as density, porosity, permeability, $V_P$, $V_S$ etc, for

*N* pressure steps {$P_1, …, P_N$}. *Elasticity*- and *Transport Theory* yield equations for how geometric parameters {*a, b, c, l,* $r_1$, $r_2$, *Z*} change as functions of pressure and how the bulk properties depend on pressure.

Each geometric rock property *a, b, c, l,* $r_1$, $r_2$, *Z* has a probability distribution. For example "*a*" can take different values $a_i$ with *Prob*$(a=a_i) = p(a)_i$ where $\Sigma p(a)_i$=1. {$p(a)_i$} is called the s*pectrum* of *a*. The procedure ROCK PHYSICS ⇛ROCK TEXTURE INVERSION involves finding the spectra of *geometric parameters from the M bulk properties* measured at *N pressure* steps. There are three cases:

CASE a) # of unknowns = # of equations (*Direct nonlinear inversion*, analytical solution only exists in special cases)

CASE b) # of unknowns < # of equations (*Gauss' Least Mean Squares approach*)

CASE c) # of unknowns > # of equations (Out of the ∞ number of possible solutions we either accept (c1) the MOST UNIFORM one (*Tikhonov Regularization*), or (c2) the MOST HETEROGENEOUS one (*Maximum Entropy Method*).)

But why do we use *only three* parameters? Because *four* are way too much! By Neumann's famous saying: *Give me four parameters, and I will fit an elephant, give me a fifth, and I will make it wiggle its trunk*. (Actually,[176] the contours of an elephant can be fit using 30 real coefficients, or 4 complex ones in the parametric Fourier representation $x(t) = \sum_{k=0}^{\infty}(A_k^x coskt + B_k^x sinkt)\,, y(t) = \sum_{k=0}^{\infty}\left(A_k^y coskt + B_k^y sinkt\right)$.

[176] J. Wei, "Least Square Fitting of an Elephant," *CHEMTECH* 5(2), 1975:128–129; Jügen Mayer, Khaled Khairy and Jonathon Howard. Drawing an elephant with four complex parameters, *American Journal of Physics* 78(2010): 648-649.

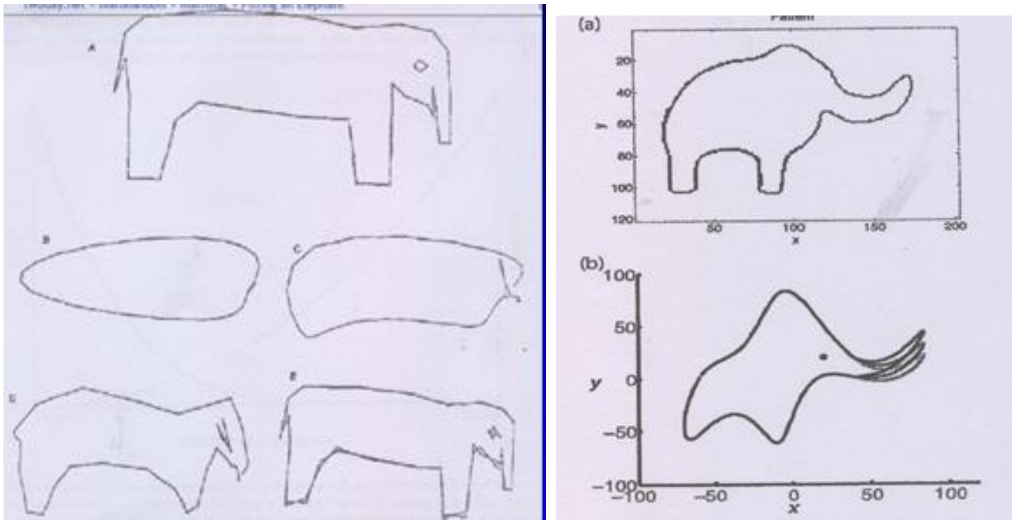


Fig. 48. Fitting an elephant: LHS: (Wei, 1975) sketch of an elephant, fitting with 5, 10, 20 and 30 sine coefficients; RHS: (Mayer et al., 2010) (a) four complex coeficients, (b) five complex coefficients make it wiggle its trunk.

We recall, that many times in *Rock Physics* three parameters can describe a complex rock-physical process, as for example, in the *Cole-Cole model* of *IP* (*Induced Potential*) in metal-bearing rocks. Figure 49 shows the *equivalent circuit model* of the IP effect:

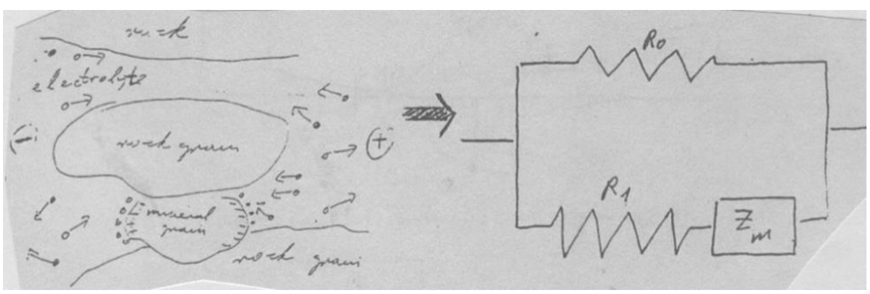


Fig. 49.

$R_0$ is resistance of host rock, $R_1$ resistance of the pore-filler liquid, $Z_m$ is complex impedance for the metallic grains. In the Cole-Cole model

$Z(\omega) = R_0\left[1 - M\left(1 - \frac{1}{1+(j\omega\tau)^c}\right)\right]$ (Eq. 181), governed by *three parameters* $M, \tau,$ c.

Historically, out of the three inversion approaches, my group used *LMS inversion* to find *pore surface fractal dimension* from porosity vs. pressure, and permeability vs. pressure data, for sandstones and carbonates[177]. Apparently, *Tikhonov Regularization* has not been used yet for rock inversion – though promising. Doyen[178] found with *ME-inversion* the

[177] Korvin, G., Mohiuddin, M.A. & Abdulraheem, A.'Experimental investigation of the fractal dimension of the pore surface of sedimentary rocks under pressure'. *Geophysical Transactions* 44(1)2001: 3-19.

[178] Doyen, P. E.,1987. Crack geometry of igneous rocks: a maximum entropy inversion of elastic and transport properties. *J. Geophys. Res*. 92 (B8): 8169-8181. Also discussed in Korvin, G. 2020d. 'Statistical Rock Physics' *in*

spectrum of crack shape for Westerly granite from porosity-, compressibility-, resistivity-, and permeability data at different pressures. Our study, discussed here, has been the first *direct inversion*!

As compared to Doyen's *ME* model, we simplified the rock-model as follows:

Table 5. Simplified assumptions

| Assumptions of Doyen's Max Entropy model | Our simplified assumptions |
|---|---|
| The pores are fluid-filled ellipsoids with semi axes ($a$, $b$, $c$), each pore is connected to $Z$ nearby pores with throats of length $l$ and elliptic cross-section with semi axes ($r_1$, $r_2$). | The pores are fluid-filled spheres with radius $r$, each pore is connected to $Z$ nearby pores with throats of length $d$ and circular cross-section with diameter $\delta$. |
| One measures $M$ bulk data $B_1, \ldots, B_M$ for $N$ pressure steps $\{P_1, \ldots, P_N\}$ | We measure *three* bulk data $\Phi$, $k$, $m$ for a *single* pressure step only. |

We made the following *theoretical assumptions*: (a) $Z = 2m/(m-1)$ (from *effective medium theory of granular materials*[179]); (b) $\kappa = \frac{1}{b} \cdot \Phi^3 . \frac{1}{S^2} . \frac{1}{\tau^2}$ (Kozeny-Carman Equation[180]); (c) $\tau = 1/\Phi^{m-1}$ (non standard assumption, it follows from a work of Peres-Rosales and Archie's Law), where $Z$ is coordination number, $m$ cementation exponent, $S$ specific surface, $\Phi$ porosity, $\tau$ tortuosity, $\kappa$ permeability. We obtained the following, exact and easily computable, mathematical solution:

$$r = 10^{-4} \cdot \sqrt[3]{\frac{3\left(\Phi - \Phi^{m}\right)}{4\pi}} \cdot \frac{2\pi \cdot \sqrt{2k}}{\Phi^{m} \cdot \sqrt{10\Phi}} \cdot \left[ 2 \cdot \left\{ \frac{3\left(\Phi - \Phi^{m}\right)}{4\pi} \right\}^{2/3} + \sqrt{\frac{1}{\pi} \cdot \frac{m}{m-1} \cdot \Phi} \right]$$

$$\delta = 10^{-4} \sqrt{\frac{m-1}{m} \cdot \frac{\Phi^{2m-1}}{\pi}} \cdot \frac{2\pi \cdot \sqrt{2k}}{\Phi^{m} \cdot \sqrt{10\Phi}} \cdot \left[ 2 \cdot \left\{ \frac{3\left(\Phi - \Phi^{m}\right)}{4\pi} \right\}^{2/3} + \sqrt{\frac{1}{\pi} \cdot \frac{m}{m-1} \cdot \Phi} \right]$$

$$d = 10^{-4} \cdot \frac{2\pi \cdot \sqrt{2k}}{\Phi^{m} \cdot \sqrt{10\Phi}} \cdot \left[ 2 \cdot \left\{ \frac{3\left(\Phi - \Phi^{m}\right)}{4\pi} \right\}^{2/3} + \sqrt{\frac{1}{\pi} \cdot \frac{m}{m-1} \cdot \Phi} \right]$$

(Eqs. 182.a-c)

Results for a typical carbonate sample (*Khuff limestone*, red color indicates pore space are shown in Fig. 50.

---

B. S. Daya Sagar, Quiming Cheng, Jennifer McKinley and Frits Agterberg (Eds.) Earth Sciences Series. *Encyclopedia of Mathematical Geosciences*. Springer (In Press)

[179] Yonezawa, F. & Cohen, M.H. 1983. Granular effective medium approximation. *J Appl Phys.*54:2895–2899.

[180] Walsh, J.B.& Brace, W.F.1984.The effect of pressure on porosity and the transport property of rock. *J Geophys Res* 89B(11):9425–9431.

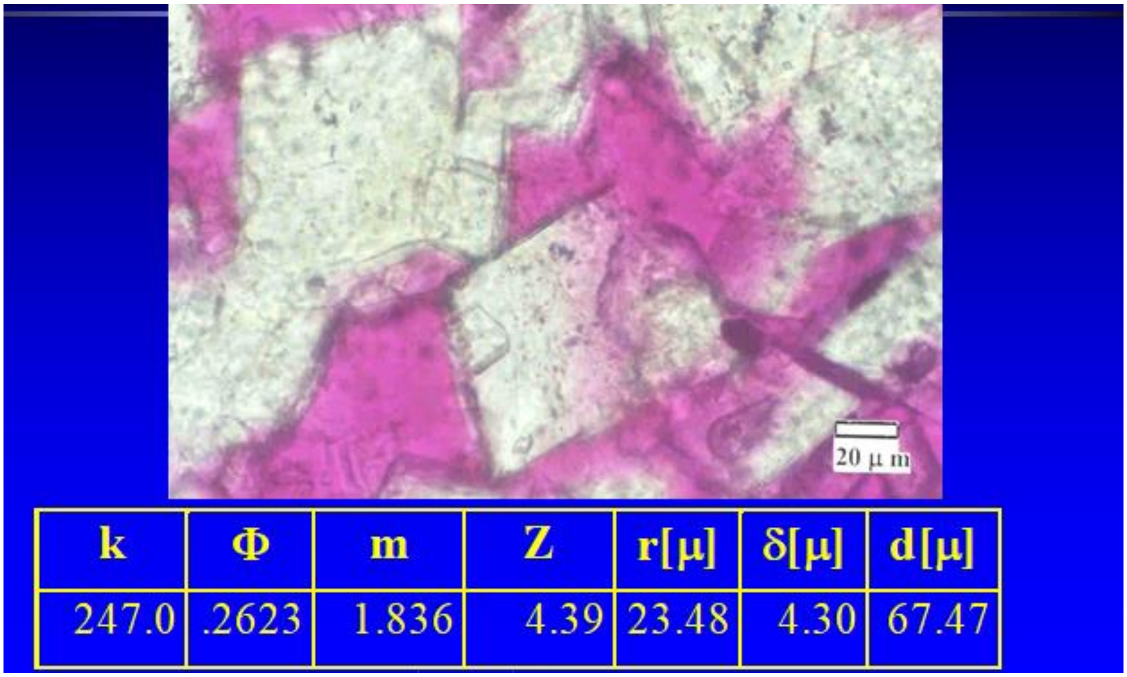


| k | Φ | m | Z | r[μ] | δ[μ] | d[μ] |
|---|---|---|---|---|---|---|
| 247.0 | .2623 | 1.836 | 4.39 | 23.48 | 4.30 | 67.47 |

Fig. 50. The geometrical properties $Z, r, \delta, d$ computed from $k, \Phi, m, Z$ using Eqs. (182.a-c).

The proposed *equivalent geometric model of sedimentary rocks belongs to the family of effective medium models*[181], the parameters (*Z*, *r*, δ, and *d*) can be easily derived from a few measured rock properties (*k, Φ*, and *m*). The converse is also true: from the values (*Z, r, δ*, and *d*), one can easily calculate the bulk rock properties (*k, Φ*, and *m*). If the specific matrix- and fluid properties are also known, the elastic constants and the P- and S-velocities can be calculated both for fully saturated and partially saturated rocks. The *dc* resistivity can be computed from (*Z, r, δ, d*) in case of complete saturation by Archie's law, but for partial saturation, we need a further rock property, the saturation exponent *n*. In our model, we could not derive the saturation exponent *n* in terms of (Z, r, δ, d) or ( k, Φ, and m) using physical arguments. Also, we have not succeeded to describe relative permeabilities for two-phase flow. The geometric model works well for sandstones; for carbonates, the resulting pore parameters are not physically impossible, but they show only order-of-magnitude agreement with the microscopic rock structure. The model assumed *statistical homogeneity and isotropy* of the rock volume, which might be true for a small cutting, less true for plug-sized samples, and certainly not valid on reservoir scale. Issues of upscaling the model to reservoir scale, making it heterogeneous and anisotropic, are among the further tasks to be solved – I leave this to the next generation.

---

[181] Kachanov M (1994). Elastic solids with many cracks and related problems. *Adv Appl Mech* 30:259–345; Sayers CM, Kachanov M (1995). Microcrack induced elastic wave anisotropy of brittle rocks. *J. Geophys. Res.* 100:4149–4156; Schubnel A, Guéguen Y (2003). Dispersion and anisotropy in cracked rocks. *J. Geophys. Res.* 108:2001; Fortin J, Schnubnel A, Guéguen Y (2005). Elastic wave velocities and permeability evolution during compaction of Bleuswiller sandstone. *Int.J .Rock. Mech. Min. Sci.* 42:873–889.

# APPENDICES

## APPENDIX 1. SHORT BIO OF DR. GABOR KORVIN

Professor Gábor Korvin, Applied Mathematician, Geophysicist, Petrophysicist, Historian. He was born in Hungary (1942), has M. Sc. In Applied Mathematics (1966, Univ. Nat. Sciences, Budapest, Hungary); *C.Sc.* & *Dr. Techn*. in Geophysics (1978 , Univ. Heavy Industries, Miskolc,Hungary); Graduate Diploma in Islamic Studies (1998, Univ. New England, Armidale, Australia).

Between1966-1985 he was exploration seismologist and software developer in the Hungarian Geophysical Institute, Budapest; in 1986-1991 Senior Lecturer, University of Adelaide, Australia; 1994 – 2016 (when he retired) Professor of Geophysics, King Fahd University of Petroleum and Minerals (KFUPM), Dhahran, Saudi Arabia.

At KFUPM he was Coordinator of the *Reservoir Characterization Research Group*.
As Professor, he taught *Reservoir Characterization, Seismic Stratigraphy, Petrophysics & Well logging, Solid Earth Geophysics, Geoelectric Exploration, Reflection Seismology, Inverse Problems, Geostatistics. Reservoir Characterization*.

He has 90 published works. His book *Fractal Models in the Earth Sciences* (Amsterdam, Elsevier, 1992) was internationally acclaimed. His publication on resistivity anisotropy in thinly-laminated sand-shale received the *Best Petrophysics Paper in 2012 Award*.
His main research interest lies in finding stochastic mathematical and physical models to describe sedimentary rocks. He used the most diverse tools of mathematics and physics to solve petrophysical problems, such as: Gaussian random fields, effective field theory; fractals; Percolation Theory. In 2014 he worked out a new rock model to connect different petrophysical properties.
For some twenty years he was Earth Sciences Editor of the *Arabian Journal of Science and Engineering* (*AJSE*, Dhahran, Saudi Arabia). On the occasion of his retirement (2016) he wrote a Review Paper for this Journal on his dreams about the stochastic approach to Petrophysics. He also publishes in Theoretical Mathematics (Number Theory, Combinatorics) and on Linguistics, Cultural and Religious History.

APPENDIX 2. PUBLICATIONS OF GÁBOR KORVIN, 1966-2020

2020

1. Gabor Korvin 2020a. The Song is Jacob’s, the Letters are Esau’s: Urdu Ghazals in Hindi Script. *Acta Orientalia* (submitted).
2. Gabor Korvin 2020b. Koran in the Saddle Bag: How Camel Drivers Brought Islam to Australia’. *Journal of the Pakistan Historical Society* (In Press).
3. Gabor Korvin 2020c. Ali Baba in Australia: Tale of a Semantic Shift. *ETC: A Review of General Semantics* 75(3-4) (In Press).
4. Korvin, G. 2020d. Statistical Rock Physics. *In*: B. S. Daya Sagar, Quiming Cheng, Jennifer McKinley and Frits Agterberg (Eds.) *Earth Sciences Series*. Encyclopedia of Mathematical Geosciences. Springer (In Press).

2019

5. Gabor Korvin (Ed.). ‘The memoirs of Khawājah Muhammad Bux (Australian Businessman)’. *Journal of the Pakistan Historical Society* Pt. VII 67(1-2)2019: 195-225; Pt. VIII 67(3)2019: 85-112.

2018

6. Gabor Korvin (Ed.) 2018a. The memoirs of Khawājah Muhammad Bux (Australian Businessman). *Journal of the Pakistan Historical Society* Pt. V 66(4)2018: 225-249; Pt. VI 66(3-4): 209-234.
7. Korvin Gabor 2018b. Abu Huraira’s cat in Goethe’s Paradise. *Hamdard Islamicus* 41(3-4): 7-15.
8. Korvin Gábor, 2018c. Nyelvcsúfoló – egy Kmoskó-idézet ürügyén. *Keletkutatás* (Tavasz): 141-146.

2017

9. Islam el-Deek, Osman Abdullatif and Gabor Korvin 2017. Heterogeneity analysis of reservoir porosity and permeability in the late Ordovician glacio-fluvial Sarah formation paleovalleys, central Saud Arabia. *Arab. J. Geosci*. 10(2017): 400-417.
10. Jarrah Mohammed Ahmed Babiker, Mustafa Hariri, Osman Abdullatif and Gabor Korvin 2017. Types and nature of fracture associated with Late Ordovician paleochannels of glaciofluvial Sarah formation, Qasim region, central Saudi Arabia. *Arab. J. Geosci.* 10(6)2017: 1 -12.
11. Gabor Korvin, Ruben V. Khachaturov, Klaudia Olechko. Gerardo Ronquillo, Maria de Jesus Correa Lopez and Juan-José Garcia 2017. Computer simulation of microwave propagation in heterogeneous and fractal media. *Computers & Geosciences* 100: 156-165.

2016

12. Gabor Korvin (Ed.). 2016a. The memoirs of Khawājah Muhammad Bux (Australian Businessman)’. *Journal of the Pakistan Historical Society* Pt. I: 64(1)2016: 67-91; Pt. II 64(4)2016: 95-111; Pt. III 65(3)2017:77-94; Pt. IV 65(4)2017: 109-123;

13. G. Korvin. 2016b. Permeability from Microscopy: Review of a Dream. *Arabian J. of Science & Engineering* 41(6): 2045-2065.
14. G. Korvin. 2016c. Abuhuraira's Cat in Goethe's Paradise. *ISAA Review* (Canberra) 5(1)20: 23-28 & 76.
15. Naeem-Ur-Rehman Minhas, Bilal Saad, Maaruf Hussain and Gabor Korvin 2016. Big Data hiding in small rocks: Case study of advanced microscopy and image processing to aid upstream asset development'. *Paper SPE-KSA*-233.

2015

16. Abdlmutalib, A., Abdullatif, O., Korvin, G. and Abdulraheem, A. 2015. The relationship between lithological and geomechanical properties of tight carbonate rocks from Upper Jubaila and Arab-D Member outcrop analog, Central Saudi Arabia. *Arabian Journal of Geosciences* 8(12): 1031–1048.
17. Arizabalo, R.D., González-Ávalos, E. and Korvin, G. 2015. Multifractal analysis of atmospheric sub-micron particle data. *Atmospheric Research* 154: 191-203.

2014

18. Korvin, G., Oleschko, K. and Abdulraheem, A. 2014. A simple geometric model of sedimentary rock to connect transfer and acoustic properties. *Arabian Journal of Geosciences* 7(3)2014: 1127-1138.
19. G. Korvin 2014. 'Short Note: Every Large Set of Integers Contains a Three Term Arithmetic Progression'. *arXiv*:1404.1557 [math.NT].

2013

20. Velásquez Valle, M.A., Medina García, G., Cohen, I.S., Oleschko, I.K., Ruiz Corral, J.A. and Korvin, G. 2013. Spatial variability of the Hurst exponent for the daily scale rainfall series in the state of Zacatecas, Mexico. *Journal of Applied Meteorology and Climatology* 52(12): 2771-2780.
21. Korvin, G., Sterligov, B., Oleschko, K. and Cherkasov, S. 2013. Entropy of shortest distance (ESD) as pore detector and pore-shape classifier. *Entropy* 15 (6): 2384-2397.

2012

22. Korvin, G. 2012. Bounds for the resistivity anisotropy in thinly-laminated sand-shale. *Petrophysics* 53(1): 14-21. (Received from *SPWLA – Society of Well Log Analysts –* The *Best Technical Paper of the Year Award*)

2011

23. Torres-Argüelles, V., Oleschko, K.,Tarquis, A.M., Korvin, G., Gaona, C., Parrot, J.-F. & Ventura-Ramos, E. 2011. Fractal Metrology for biogeosystems analysis (Short & complete versions)'. *Biogeosciences* 7 (11): 3799-3815 & *Biogeosciences Discussions* 7: 4749-4799.

2010

24. Velázquez-García, J., Oleschko, K., Muñoz-Villalobos, J.A., Velázquez-Valle, M., Menes, M.M., Parrot, J.-F., Korvin, G., Cerca, M. 2010. Land cover monitoring by fractal analysis of digital images. *Geoderma* 160(1): 83-92.
25. Oleschko, K., Korvin, G., Flores, L., Brambila, F., Gaona, C., Parrot, J.-F., Ronquillo, G. & and Zamora, S. 2010. Probability density function: A tool for simultaneous monitoring of pore/solid roughness and moisture content. *Geoderma* 160(1): 93-104.

2009

26. Aslam Chaudhry and Gabor Korvin 2009. 'The asymptotic representation of some series and the Riemann hypothesis'. *arXiv*:0903.3007 [math.NT].
27. Gabor Korvin 2009. Fractal Subseries of the Harmonic Series. *arXiv*:0903.2141 [math.NT].

2008

28. Adetunji, A.Q., Al-Shuhail, A. and Korvin, G. 2008. Mapping the internal structure of sand dunes with *GPR*: A case history from the Jafurah sand sea of eastern Saudi Arabia. *Leading Edge* (Tulsa, OK) 27(11):1446-1452.
29. Hariri, Mustafa M., Korvin, G. and Ahmed, Zulfiqar (Eds.) 2008. *Theme Issue on Arabian Plate Basement Rocks and Mineral Deposits. Arabian Journal for Science and Engineering* 33(1C).
30. K. Oleschko, G. Korvin, A. Muñoz , J. Velazquez, M. E. Miranda, D. Carreon, L. Flores, M. Martinez, M. Velasquez-Valle, F. Brambila, , J.-F. Parrot and G. Ronquillo 2008. Mapping soil fractal dimension in agricultural fields with *GPR*. *Nonlinear Processes in Geophysics* 15(5): 711-725.

2007

31. Abdulazeez Abdulraheem, E. Sabakki, M. Ahmed, A. Ventala, I. Raharja, and G. Korvin 2007. Estimation of permeability from wireline logs in a Middle Eastern Carbonate Reservoir using fuzzy logics. *Paper SPE*-105350.

2006

32. Arizabalo, R.D., Oleschko, K., Korvin, G., Lozada, M., Castrejón, R. & Ronquillo, G. 2006. Lacunarity of geophysical well logs in the Cantarell oil field, Gulf of Mexico. *Geofisica Internacional* 45 (2): 99-113.

2005

33. Korvin, G. 2005. Is the optical image of a non-Lambertian fractal surface fractal? *IEEE Geoscience and Remote Sensing Letters* 2(4): 380-383.
34. Nieto-Samaniego, A.F., Alaniz-Alvarez, S.A., Tolson, G., Oleschko, K., Korvin, G., Xu, S.S and Pérez-Venzor, J.A. 2005. Spatial distribution, scaling and self-similar behavior of fracture arrays in the Los Planes Fault, Baja California Sur, Mexico. *Pure and Applied Geophysics* 162(5): 805-826.

2004

35. Arizabalo, R.D., Oleschko, K., Korvin, G., Ronquillo, G. & Cedillo-Pardo, E. 2004. Fractal and cumulative trace analysis of wire-line logs from a well in a naturally fractured limestone reservoir in the Gulf of Mexico. *Geofisica Internacional* 43(3): 467-476.
36. G. Korvin 2004. Adventures of a Kashmiri Merchant in Australia – An Unknown Urdu Travelogue. *Journal of the Pakistan Historical Society* 52(1): 21-39.
37. Korvin, G. and Oleschko, K. 2004. Multiple wave scattering from fractal aggregates. *Chaos, Solitons and Fractals* 19(2): 421-425.
38. Cerone Pietro, Chaudhry Aslam, Korvin, G. and Qadir Asghar 2004. New Inequalities Involving the Zeta Function. *JIPAM. Journal of Inequalities in Pure & Applied Mathematics* [electronic only] 5.2 (2004): Paper No. 43, 17 p., <http://eudml.org/doc/12504.
39. Klavdia Oleschko, Benjamin Figuerora-Sandoval, Gabor Korvin and Maria Martinez Menes 2004. Agroecometry: a toolbox for the design of virtual agriculture. *Agricultura, sociedad y desarollo* 1(4): 53-71 (In English & Spanish).

2003

40. Siddiqi, A.H., Korvin, G., Mosco, U., Dahlke, S. and Frieden, W. (Eds.) 2003. *Theme Issue on Wavelet and Fractal Methods in Science and Engineering: Parts I & II. Arabian Journal for Science and Engineering* 28(2C)2003 & 29(2C)2004.
41. Al-Ali, M., Hastings-James, R., Makkawi, M. and Korvin, G. 2003. Vibrator attribute leading velocity estimation. *Leading Edge* (Tulsa, OK) 22(5): 400, 402-405.
42. Oleschko, K., Korvin, G., Figueroa, B., Vuelvas, M.A., Balankin, A.S., Flores, L. and Carreón, D. 2003. Fractal radar scattering from soil. *Physical Review E - Statistical, Nonlinear, and Soft Matter Physics* 67(41): 41403/1-41403/13.
43. Korvin, G. 2003a. Paternal influence on mtDNA?: A case from Western Australian history. *ISAA Review* (Canberra) 2(5): 30-31.
44. Korvin, G. 2003b. Afghan and South-Asian pioneers of Australia (1830–1930): A biographical study (Parts 1 & 2). *Journal of the Pakistan Historical Society* 51(1) 2003: 49-90 & 51(2) 2003: 45-97.

2002

45. Oleschko, K., Korvin, G., Balankin, A.S., Khachaturov, R.V., Flores, L. Figueroa, B., Urrutia, J. and Brambila, F. 2002. Fractal scattering of microwaves from soils. *Physical Review Letters* 89(18): 188501/1-188501/4.
46. Choudhury, M.A. and Korvin, G. 2002. Simulation versus optimization in knowledge-induced fields. *Kybernetes* 31(1): 44-60.
47. Hassan, H.M., Korvin, G. and Abdulraheem, A. 2002. Fractal and genetic aspects of Khuff reservoir stylolites, Eastern Saudi Arabia. *Arabian Journal for Science and Engineering* 27(1A): 29-56.

48. Masudul A. Choudhury, G. Korvin and Fazal Seyyed 2002. Discovering micro level tradeoff in economic development and studying their fractal character. *Indonesian Management & Accounting Research* 1(1): 49-70.

2001

49. Korvin, G., Mohiuddin, M.A. and Abdulraheem, A. 2001. Experimental investigation of the fractal dimension of the pore surface of sedimentary rocks under pressure. *Geophysical Transactions* 44(1): 3-19.
50. Masudul Alam Choudhury and Gabor Korvin 2001. Sustainability in knowledge-centered socio-scientific systems. *International Journal of Sustainability in Higher Education* 2(3): 257-266.
51. M.A.Mohiuddin, G. Korvin, A. Abdulrahim and K. Khan 2001. Attenuation characteristics of Saudi Arabian Reservoir sandstone and limestone cores. *SCA (Society of Core Analysts) Paper* 2001-57: 1-5.

2000

52. Gabor Korvin. 2000a. The Value of Information in the Interactive, Integrative and Evolutionary World Model: A Case Study. *Humanomics* 16(1):15-24.
53. Gabor Korvin. 2000b. Jokes of the Prophet: In search of a lost book. *ISAA Rev.* (Canberra) 1(2): 28-31.

1999

54. Gabor Korvin 1999.'Women's Leadership through the History of Islam'. *Hamdard Islamicus* 22(3): 17-50 and *Journal of the Pakistan Historical Society* 48(1): 29-63.

1996

55. Gabor Korvin 1996. Book review: *Fractals in reservoir engineering*: H.H. Hardy and R.A. Beier, World Scientific, London, 1994, Hardcover, XIV + 359 pp., ISBN 981-02-2069-3. *Journal of Hydrology* 03/1996; 176(s 1–4):290–293.

1993

56. Korvin, G. 1993. The kurtosis of reflection coefficients in a fractal sequence of sedimentary layers. *Fractals-Complex Geometry Patterns and Scaling in Nature and Society* 1(2): 263-268.

1992

57. Korvin, G. 1992a. *Fractal Models in the Earth Sciences*. Amsterdam: Elsevier.
58. Korvin, G. 1992b. A percolation model for the permeability of kaolinite-bearing sandstones'. *Geophysical Transactions* 37(2-3): 177-209.

1990

59. Korvin, G., Boyd, D.M. and O'Dowd, R. 1990. Fractal characterization of the South Australian gravity station network. *Geophysical Journal International* 100(3): 535-539.

1989

60. Korvin, G. 1989. Fractured but not fractal: Fragmentation of the Gulf of Suez basement. *Pure and Applied Geophysics PAGEOPH* 131(1-2): 289-305.

1988

61. Korvin, G. 1988. Fractals in geophysics: A guided tour. *ASEG-SEG Adelaide* 1988: 301-303.

1985

62. Miller, J.I., Lee, M.W., Kilényi, É, Petrovics, I., Braun, L. and Korvin, G. 1985. Seismic modeling in a complex tectonic environment. *Geophysical Transactions* 31(1-3): 213-255.
63. Korvin, G. 1985. A few unsolved problems of applied geophysics'. *Geophysical Transactions* 31(4): 373-389.

1984

64. Korvin, G. 1984. Shale compaction and statistical physics. *Geophysical Journal – Royal Astronomical Society* 78 (1): 35-50.

1983

65. Korvin, G. 1983a. Megjegyzés Bodri Bertalan és Bodriné Cvetkova Lujza "A Pannónia medence kéreg kivékonyodásának kapcsolata a térség geotermikájával" c. dolgozatához. *Magyar Geofizika* 24(1): 33-35.
66. Korvin, G. 1983b. 'General theorem on mean wave attenuation'. *Geophysical Transactions* 29(3):191-202. (Received the *Best Technical Paper of the Year Award* from the Hungarian Geophysicists' Association).

1982

67. Korvin, G. 1982a. Axiomatic characterization of the general mixture rule. *Geoexploration* 19(4): 267-276.
68. Korvin, G. 1982b. Certain problems of seismic and ultrasonic wave propagation in a medium with inhomogeneities of random distribution. III. Statistics of the diffuse reflection shadow following a rough reflecting boundary. *Geophysical Transactions* 28(1): 8-19.

1981

69. Korvin, G. and Armstrong, B.H. 1981. Discussion of "Frequency-independent background internal-friction in heterogeneous solids". *Geophysics* 46(9): 1314-1315.

1980

70. Korvin, G. 1980. Effect of random porosity on elastic wave attenuation. *Geophysical Transactions* 26: 43-56.

1978

71. Korvin, G. 1978a. Some notes on a problem of Treitel and Wang. *Geophysical Transactions* 21(8): 53-58.
72. Korvin, G. 1978b. Correlation properties of source-generated random noise, scattered on velocity inhomogeneities. *Acta Geod. Geoph. et Mont. Acad. Sci. Hung.*13(1-2): 201-210.
73. Korvin, G. 1978c. The hierarchy of velocity formulae: Generalized mean value theorems. *Acta Geod. Geoph. et Mont. Acad. Sci. Hung*. 13(1-2): 211-222.
74. Korvin, G. 1977-1978. Két tanulmány a véletlen közegekben terjedő szeizmikus hullámok elméletéről. I.rész: Elnyelődés többkomponensű közegekben, az elnyelődési együttható és a heterogeneitás (kőzetentrópia) kapcsolata. *Magyar Geof*. 18(3)1977: 106-116; II. rész A közeg inhomogeneitásának becslése a szeizmikus jelek fluktuációja alapján. (Esettanulmány). *Magyar Geof*. 18(4)1978: 134-149. 1977

75.

76. Korvin, G. 1977. Certain problems of seismic and ultrasonic wave propagation in a medium with inhomogeneities of random distribution. II. Wave attenuation and scattering on random inhomogeneities. *Geophysical Transactions* 24(Supplement 2): 1-38.

1976

77. Korvin, G. and Ilona Petrovics 1976. 'Kisérletek reflexiós szeizmikus adatok csökkentett bitszámú feldolgozására. *Magyar Geofizika* 17(1): 15-23.

1975

78. Petrovics Ilona, Jánvári J., Korvin, G. and Sipos, J. 1975. Reflexiós szintek korrelációjának vizsgálata digitális szűrés, energiaanalízis, abszorpció számitás felhasználásával. *Magyar Geofizika* 16(3): 98-105.
79. Korvin, G. and Petrovics, I. 1975. Seismic data processing using a reduced number of bits. *Geophysical Transactions* 23: 47-69 (English text); 71-83 (Hungarian text).

1973

80. Korvin, G. 1973. Certain problems of seismic and ultrasonic wave propagation in a medium with inhomogeneities of random distribution. *Geophysical Transactions* 21: 5-34.

1972

81. G. Korvin and Lux, I. 1972. An analysis of the propagation of sound waves in porous media by means of the Monte Carlo method. *Geophysical Transactions* 21(3-4): 91-106.

1971

82. Bodoky, T., Korvin, G., Liptai, I. and Sipos, J. 1971. An analysis of the initial seismic pulse near underground explosions. *Geophysical Transactions* 21(3-4): 7-26.
83. Posgay, K., Korvin, G. and Vincze, J. 1971. Concepts of seismic digital instrumental and methodological developments in the ELGI. *Geophysical Transactions* 20(1-2):9-16.

84. Gróh Edina, Karas, Gy., Korvin, G., Lendvai, K. and Sipos, J. 1971. Computation of synthetic seismograms from acoustic logs. *Geophysical Transactions* 20(1-2): 23-39 (In Russian).
85. Korvin Gábor 1971. Digitális szeizmikus kiértékelés kis elektronikus számítógéppel. *Magyar Geofizika* 12(2-3): 51-55.

1969

86. Korvin, G. 1969. Kisértetreflexiók eltávolitása és a logikai dekonvolúció elve. *Geophysical Transactions* 18(4): 63-68.

1968

87. Korvin Gábor 1968. Empirikus függvények differenciálásáról.*Magyar Geofizika* 9(4-5): 194-197.

1967

88. Korvin, G. 1967. Some combinatorial problems on complete directed graphs. *In*: *Theory of Graphs.* New York: Gordon & Breach, Paris: Dunod: 197-202.

1966

89. G. Katona and Korvin, G. 1966. Functions defined on a directed graph. *Theory of Graphs. Proc. Symp.* Tihany, Hung., Sept. 1966: 209-213.
90. Korvin, G. 1966. On a theorem of L. Rédei about complete oriented graphs. *Acta Sci. Math.* (Szeged) 27(1-2): 99-103.

## APPENDIX 3. COURSES TAUGHT BY PROF. G. KORVIN AT KFUPM

GEOPHYSICAL EXPLORATION
GEODYNAMICS
GEOPHYSICAL WELL LOGGING
INVERSE PROBLEMS
PETROPHYSICS
REFLECTION SEISMOLOGY
RESERVOIR CHARACTERIZATION
RESERVOIR GEOSTATISTICS
SEISMIC PROCESSING
SEISMIC STRATIGRAPHY
SEISMIC WAVES
SENIOR PROJECT
SOLID EARTH GEOPHYSICS
WELL LOG INTERPRETATION

APPENDIX 4. WORKS CO-ATHORED WITH GRADUATE STUDENTS

| Year | Author | Short title | Student(s) involved | Institution (ADELAIDE = U. of Adelaide, South Australia; UNAM = Universidad Nacional Autónoma de México; KFUPM = King Fahd University of Petroleum & Minerals. SaudiArabia) |
|---|---|---|---|---|
| 2017 | Islam el-Deek et al. | Heterogeneity analysis | Islam el-Deek | KFUPM |
| 2017 | Jarrah et al. | Types and nature of fracture | Jarrah | KFUPM |
| 2017 | Korvin et al. | Computer simulation of microwave | Lopez & Garcia | UNAM |
| 2015 | Abdlmutalib et al. | The relationship between lithological and geomechanical properties | Abdlmutalib | KFUPM |
| 2015 | Arizabalo et al. | Multifractal analysis of atmospheric | Arizabalo | UNAM |
| 2013 | Velásquez Valle et al. | Spatial variability of the Hurst exponent | Velásquez Valle | UNAM |
| 2011 | Torres-Argüelles et al. | Fractal metrology for biogeosystems | Torres-Argüelles | UNAM |
| 2010 | Velázquez-García et al. | Land cover monitoring | Velázquez-García | UNAM |
| 2010 | Oleschko et al. | Probability density function | Flores | UNAM |
| 2008 | Adetunji et al. | Mapping the internal structure | Adetunji | KFUPM |
| 2008 | Oleschko et al. | Mapping soil fractal dimension | Flores | UNAM |
| 2007 | Abdulraheem et al. | Estimation of permeability | Sabakki | KFUPM |
| 2006 | Arizabalo et al. | Lacunarity of geophysical well logs | Arizabalo | UNAM |
| 2004 | Arizabalo et al. | Fractal and cumulative trace analysis | Arizabalo | UNAM |
| 2004 | Oleschko et al. | Agroecometry: a toolbox | Maria Martinez Menes | UNAM |
| 2003 | Al-Ali et al. | Vibrator attribute | Al-Ali | KFUPM |
| 2003 | Oleschko | Fractal radar scattering | Flores | UNAM |

| | | | | |
|---|---|---|---|---|
| | et al. | | | |
| 2002 | Oleschko et al. | Fractal scattering of microwaves | Flores | UNAM |
| 1990 | Korvin et al. | Fractal characterization | O'Dowd | ADELAIDE |

APPENDIX 5. REFERENCES TO OTHER AUTHORS CITED


Doddy Abdassah and Iraj Ershaghi 1986. Triple-porosity systems for representing naturally fractured reservoirs. *SPE Formation Evaluation*, April 1986: 113-127.

Aczél. J. 1946. The notion of mean values. *Nor. Vidensk. Selsk. Forh*., 19: 83-86.

Aczél J. 1961. *Vorlesungen über Funktionalgleichungen und ihre Anwendungen*. VEB Deutscher Verlag der Wissenschaften. Berlin.

J. Aczél and Z. Daróczy 1957. *On Measures of Information and their Characterization*. Academic Press, New York.

Wayne M. Ahr 2008. *Geology of Carbonate Reservoirs. The Identification, Description, and Characterization of Hydrocarbon Reservoirs in Carbonate Rocks*. John Wiley & Sons, Inc., Hoboken, NJ.

Akbar N. A. 1993. *Seismic signatures of reservoir transport properties and pore fluid distribution*, Ph. D. Thesis, Stanford University, Stanford.

N. A.  Akbar N, Mavko G, Nur A and Dvorkin J (1994) Seismic signatures of reservoir properties and pore fluid distribution. Geophysics 59(8):1222-1236.

Aki, K. 1980: Attenuation of shear waves in the lithosphere for frequencies from 0.05 to 25 Hz. *Phys. Earth. Planet. Int*. 21, 1: 50-60.

Allain, C. and Cloitre M. 1986. Optical Fourier transforms of fractals. *In*: Pietronero L, Tosatti E, (Eds.) *Fractals in Physics*. Amsterdam: Elsevier: 61–64.

Allain, C., and Cloitre, M. 1991. Characterizing the lacunarity of random and deterministic fractal sets. *Phys. Rev. A*, 44, 6: 3552-3558.

Allègre C. J., Le MouelL, J. L., and Provost, A. 1982. Scaling Rules in Rock Fracture and Possible Implications for Earthquake Prediction.  *Nature* 297: 4749.

Ament, W. S. 1953. Sound propagation in gross mixtures. *Journal Ac. Soc. Am*. 25(4): 638-641.

Anderson, B., I. Bryant, M. Lüling, Brian Spies and  K. Helbig1994. Oilfield anisotropy: Its origins and electrical characteristics.  *Oilfield Review*, October 1994: 48-56.

Athy, L. I. 1930. Compaction and oil migration. *Bull. Am. Ass. Petrol. Geol*.14: 25-35.

Attewell, P. B. and Ramana, Y. W. 1966: Wave attenuation and internal friction as functions of frequency in rocks. *Geophysics* 31, 6: 1049-1056.

Azimi, Sh. A ., Kalinin, A. V ., Kalinin,V.V. and Pivovarov, B.L. 1968: Impulse and transient characteristics of media with linear and quadratic absorption laws. *Izv. Earth Phys*. No 2: 42-54.

P. Bak and R. Bruisma: One-dimensional Ising model and the complete Devil's staircase. *Phys. Rev. Let.*, 49 (1982: 249-251.

A.- L. Barabási and H. E. Stanley 1995. *Fractal Concepts in Surface Growth*. Cambridge University Press.

Barkhatov A. N. 1982: *Modelling of the propagation of sound waves in the oceans* (In Russian). Hydro-Meteoizdat, Leningrad.

Barkhatov A. N., Shmelev I. I. 1969: A study of the under-surface sound channel as communication channel, under model conditions (In Russian). *Akust. Zhurnal* 15, 2.

Barlow, B. C., 1977. Data limitations on model complexity; 2-D gravity modelling with desk-top calculators. *Bull. Austr. Soc. Expl. Geophys*., 8:139-143.

Barton C.C. 1995. Fractal Analysis of Scaling and Spatial Clustering of Fractures. *In*: Barton C.C., La Pointe P.R. (Eds.) *Fractals in the Earth Sciences*. Springer, Boston, MA.

Beckenbach E. F. and Bellman R. 1961. *Inequalities.* Springer Verlag, Berlin-Göttingen-Heidelberg.

Beckmann, P. 1965. Shadowing of random rough surfaces. *IEEE Trans. AP*-13 No. 3: 384-388.

Bellman, R. and Kalaba, R. 1956. On the Principle of Invariant Imbedding and Propagation Through Inhomogeneous Media. *Proceedings of the National Academy of Sciences USA*, 42: 625-637.

Beltzer A. 1978. The influence of random porosity on elastic wave propagation. *J. Sound Vibr*. 58, 2: 251-256.

Julius Bendat 1981. *Nonlinear System Analysis and Identification from Random Data*. New York: Wiley-Interscience.

Mark de Berg, Marc van Kreveld, Mark Overmars and Otfried Schwarzkopf 1997. *Computational Geometry. Algorithms and Applications*. Springer Verlag, Berlin.

Mark Berman 1977. Distance distributions associated with Poisson processes of geometric figures. *J. Appl. Prob*. 14: 195-199.

Berry J. E. 1959. Acoustic velocity in porous media. *J. Pet. Technol*, II, 10: 262-270.

M.V. Berry 1979. Diffractals. *Journal of Physics A: Mathematical and General* 12(6): 781-797.

Billings, M. P. 1954. *Structural Geology*. Prentice Hall, New York.

Bradley, J. J. and Fort, A. N. Jr. 1966. Internal friction in rocks. *In*: *Handbook of Physical Constants* (Ed. Clark, S. P. Jr). *Geol. Soc. Am. Memoir*, 97: 175-193.

Brillouin, L., 1962. *Science and Information Theory*, 2nd edn, Academic Press, New York.

Broadbent S. R. 1954. Discussion on Symposium on Monte Carlo Methods. J. *Roy. Statistic. Soc. B*. 68 p.

Brown, W. K., Karp, R. R., and Grady, D. Z. 1983. Fragmentation of the Universe, *Astrophys. and Space Science* 94:401-412.

Bullen, P.S., 2003. *Handbook of Means and Their Inequalities*. Kluwer Academic Publishers, Dordrecht-Boston-London.

Byryakovskiy, L. A. 1968: Entropy as criterion of heterogeneity of rocks. *Soviet Geol*. No 3: 135 - 138. (In Russian, English transl. in *Internat. Geol. Rev*. 10, No 7).

Chang, C., Zoback, M., and Khaksar, A. 2006. Empirical relations between rock strength and physical properties in sedimentary rocks. *J. Pet. Sci. Eng.* 51:223–237.

Chernov, L. A., 1960. *Wave Propagation in a Random Medium*. McGraw Hill, New York.

P.J. Clark and F.C. Evans 1954. Distance to nearest neighbor as a measure of spatial relationships in populations. *Ecology* 35(4): 445-453.

Clavaud, J.-B., R. Nelson, U. K. Guru & H. Wang 2005. Field example of enhanced hydrocarbon estimation in thinly laminated formation with a triaxial array induction tool: A laminated sand-shale analysis with anisotropic shale. *SPWLA Annual Logging Symposium*, New Orleans, Louisiana.

Cochran, M.D. 1973. Seismic signal detection using sign bits. *Geophysics* 38 (6): 1042–1052.

J. Comiti, J. and M. Renaud 1989, A New Model for Determining Mean Structure Parameters of Fixed Beds from Pressure Drop Measurements: Application to Beds Packed with Parallelepipedal Particles, *Chem. Eng. Sci*. 44(7):1539-1545.

Dainty, A. M. 1981. A scattering model to explain seismic *Q* observations in the lithosphere between 1 and 30 Hz. *Geoph. Res. Letters*, 8(11): 1126-1128.

Davis, A. M., and W. Wiscombe 1994. Wavelet-based multifractal analysis of non-stationary and/or intermittent geophysical signals. *In*: Wavelets in Geophysics, E. Foufoula-Georgiu and P. Kumar, Eds., Academic Press: 249–298.

Dolan, S. S., CH. J. Bean and B. Riollet 1998. The broad-band fractal nature of heterogeneity in the upper crust from petrophysical logs. *Geophys. J. Int*. 132: 489-507.

Dowds, J.P. 1969. Oil rocks: Information theory: Markov chains: Entropy. **Quart. Col. Sch. Mines** 64: 275-293.

Doyen, P. E. 1987. Crack geometry of igneous rocks: a maximum entropy inversion of elastic and transport properties. *J. Geophys. Res*. 92 (B8): 8169-8181.

Drummond, Carl N. and D.N. Sexton 1998: Fractal Structure of Stylolites. *Journal of Sedimentary Research* 68(1): 8-10.

F.A.L. Dullien 1979. *Porous Media: Fluid Transport and Pore Structure*. Acad. Press, NY.

Epstein, B. 1947. The Mathematical Description of Certain Breakage Mechanisms Leading to the Logarithmico-Normal Distribution. *J. Franklin Inst*. 244: 471-477.

Erdős, P. and Rényi, A. 1959. On Random Graphs. *Publicationes Mathematicae* 6: 290–297.

C. J. G. Evertsz and B. B. Mandelbrot 1992. Multifractal Measures. *In*: *Chaos and Fractals — New Frontier of Science* . Heinz-Otto Peitgen et al. (Eds), Springer Verlag: 921–953.

Fara, H.D. and Scheidegger, A. E. 1961. Statistical geometry of porous media. *Journal Geoph. Res*. 66(10): 3,279-3,284.

J. Feder, 1988. *Fractals*. Plenum Press, NY.

P. Fischer, 1972: On the inequality $\sum p_i f(p_i) \geq \sum p_i f(q_i)$ . *Metrika* 18: 199-208.

Fortin, J., Schnubnel, A. and Guéguen. Y. 2005. Elastic wave velocities and permeability evolution during compaction of Bleuswiller sandstone. *Int J Rock Mech Min Sci* 42:873–889.

Fraser, A. R., Moss, F. J. and Turpie, A., 1976. Reconnaissance gravity survey of Australia, *Geophysic* 41: 1337-1345.

Behzad Ghanbarian-Alavijeh, Humberto Millán and Guanhua Huang 2011. A review of fractal, prefractal and pore-solid-fractal models for parameterizing the soil water retention curve. *Canadian Journal of Soil Science* 91(1): 1-14.

Gilvarry, J. J. 1964. Fracture of Brittle Solids. Distribution Function for Fragment Size in Single Fracture. (Theoretical). *J. Appl. Phys*. 32: 391-399.

Gombár, L. 1983. Correlation of attenuation of elastic waves with other petrophysical and lithological properties. *Geophysical Transactions* 29(3): 217-228.

I.J. Good 1952. Rational decisions. *J. Roy. Stat. Soc. Ser. B*. 14: 107-114.

I.J. Good, 1954. *Uncertainty and Business Decisions*. Liverpool University Press, Liverpool.

Grant, F.S., and West, G.F. 1965. *Interpretation Theory in Applied Geophysics*, McGraw-Hill Book Co., New York.

Grassberger, P. andProcaccia, I. 1983a. Measuring the strangeness of strange attractors. *Physica* 9D, Nos 1 and 2: 189-208.

Grassberger, P. and Procaccia, I. 1983b. Characterisation of strange attractors. *Phys. Rev. Lett.* 50: 346-349.

Gravestock D. I. and Alexander E. M. 1986. Porosity and permeability of reservoirs and caprocks in the Eromanga Basin, South Australia. *The Australian Petroleum Exploration Association Journal* 26: 202-213.

Grenander, Ulf and Szego, Gabor 1958. *Toeplitz Forms and Their Applications*. Berkeley: Univ. of California Press, 2nd edn.

Griffith, L. 1943. A Theory of the Size Distribution of Particles in a Comminuted System. *Can. J. Research* 21A: 57-64.

Guerin, C.A. and Holschneider, M. 1996. Scattering on fractal measures. *J Phys A: Math Gen* 29:7651–67.

Guerin, C.A. and Holschneider, M. 1998. Time-dependent scattering on fractal measures. *J Math Phys* 39(8):4165–94.

Guerin, C. et al. 1997. Electromagnetic scattering from multi-scale rough surfaces. *Wave Random Media* 7:331–49.

Hamilton, E. L. 1972. Compressional wave attenuation in marine sediments. *Geophysics* 37(4): 620-646.

Hammersley J. M. 1983. Origins of percolation theory. *In*: Deutscher, G., Zallen, R. and Adler, J. (Eds.*) Percolation Structures and Processes*. Ann. Israel Phys. Soc. 5: 48-57.

Hammouda, H. M. 1986. *Study and Interpretation of Basement Structural Configuration in the Southern Part of Gulf of Suez using Aeromagnetic and Gravity data*. Ph.D. Thesis, Faculty of Science, Cairo University.

Hansen, J. P. and Skjeltorp, A.T. 1988. Fractal pore space and rock permeability implications. *Physical Review B (Condensed Matter*) 38(4): 2635-2638.

Hashin, Z. 1964: Theory of mechanical behaviour of heterogeneous media. *Appl. Mech. Rev*. 17, No. 1: 1-9.

Hashin, Z. and Shtrikman, S. 1963. A variational approach to the theory of the elastic behaviour of multiphase materials. *J. Mech. Phys. Solids*. 11: 127-140.

Hashin, Z. and Shtrikman, S. 1963. Conductivity of polycrystals. *Phys. Rev* 130(1): 129–133.

P. Hertz1909. Über den gegenseitigen durchschnittlichen Abstand von Punkten, die mit bekannter mittlerer Dichte im Raume angeordnet sind. *Math.Annalen* 64: 387-398.

Hicks, W. G. and Berry, J. E. 1956. Application of continuous velocity logs to determination of fluid saturation of reservoir rocks. *Geophysics* 21(3): 739-754.

B.R. Hunt 1998. The Hausdorff dimension of graphs of Weierstrass functions. *Proc.Am. Math. Soc*. 126:791.

M.A. Ioannidis, M.J. Kwiecien and I.F. Chatzis 1996: Statistical analysis of porous microstructure as a method for estimating reservoir permeability. *J. Pet, Sci. & Eng*. 16: 251-261.

Jánossy,L., Rényi, A. and Aczél, J. 1950. On composed Poisson distributions. Pt.1. *Acta Math.* 1:209-224.

Jarrige, J. J et al. 1986. Inherited Discontinuities and Neogene Structure: The Gulf of Suez and the Northwestern Edge of the Red Sea. *Phil. Trans. R. Soc. Lond*. A317:129-139.

Jing. X.D., Al-Harthy, S. and King, S. 2002. Petrophysical properties and anisotropy of sandstones under true-triaxial stress conditions. *Petrophysics* 43: 358-362.

Kachanov, M. 1994.. Elastic solids with many cracks and related problems. *Adv. Appl.Mech.* 30: 259–345.

Karal, F. C. Jr . and Keller, J. B. 1964. Elastic, electromagnetic and other waves in a random medium. *J. Math. Phys*. 5(4): 537-549.

Kay, I. and Silverman, R. A., 1958. Multiple scattering by a random number of dielectric slabs. *Nouvo Cimento*, IX. Serie X. Suppl. No 2: 626-645.

Keller, J. B. 1964. Stochastic equations and wave propagation in random media. *Proc. Symp. Appl. Math.* 16, pp 145-170.

Kendall, M. G., and Moran, P. A. P. 1963. *Geometrical Probability*. Griffin and Co., London.

Kennedy, D. and Herrick, D. 2004. Conductivity anisotropy in shale-free sandstone. *Petrophysics* 45: 38-58.

Klein, J.D., Martin, P.R. and Allen, D.F. 1997. The petrophysics of electrically anisotropic reservoirs. The Log Analyst 38, No. 3.

Klimentos, Th. and C. McCann 1990. Relationships among compressional wave attenuation, porosity, clay content, and permeability in sandstones. *Geophysics* 55 (8): 998–1014.

Knopoff, L. 1964. Q. *Rev. Geoph*. 2(4): 625-660.

A. Koponen, M. Kataja and J. Timonen 1996. Tortuous flow in porous media. *Phys. Rev. E* 54: 406.

A. Koponen, M. Kataja and J. Timonen 1997. Permeability and effective porosity in porous media. Phys. Rev. E 56: 3319.

Korčak, J. 1940. Deux types fondamentaux de distribution statistique. *Bull. Inst. Int. Stat*. 30: 295-299.

Kriegshäuser, B. et al. 2000. A new multicomponent induction logging tool to resolve anisotropic formations. *SPWLA 40th Logging Symposium*.

Lachenbruch, A. H. 1962. Mechanics of Thermal Contraction Cracks and Ice-wedge Polygons in Permafrost. *Geol. Soc. Am. Spec. Paper* 70: 69 pp.

Lamb, Horace 1895. *Hydrodynamics.* Cambridge University Press.

Landau, L.D. and Lifshitz, E.M., 1980. Statistical Physics. Pt.1. (Vol. 5 of Course of Theoretical Physics). Pergamon Press: Oxford, pp. 106-114.

Lerche, I. 1990. *Basin Analysis. Quantitative Methods*. Pt. I. Academic Press: San Diego.

F. K. Levin and D. J. Robinson 1969. Scattering by a random field of surface scatterers . Geophysics 34: 170-179.

Litwiniszyn, J. 1974. *Stochastic Methods in the Mechanics of Granular Bodies*. International Centre for Mechanical Sciences. Courses and Lecture Notes no. 93. Springer-Verlag: Wien.

Lovejoy, S. and Schertzer, D. 1986. Scale invariance, symmetries, fractals, and stochastic simulations of atmospheric phenomena. *Bull. Am. Meteor. Soc*. 67: 21-32.

Lovejoy, S., Schertzer, D. and Ladoy, P. 1986a. Fractal characterization of inhomogeneous geophysical measuring networks. *Nature* 319: 43-44.

Lovejoy, S., Schertzer, D. and Ladoy, P. 1986b. Outlook brighter on weather forecasts. *Nature* 320: 401.

F. Jerry Lucia: Carbonate Reservoir Characterization. Springer, Berlin-Heidelberg, 1998.

Lynch, A. M. and King, A. R. 1983. A review of parameters affecting the accuracy and resolution of gravity surveys. *Bull. Aust. Soc. Expl. Geophys*., 14:131-142.

Madden, T. R. 1983. Microcrack Connectivity in Rocks: A Renormalisation Group Approach to the Critical Phenomena of Conduction and Failure in Crystalline Rocks. *J. Geophys. Res.* 88: 585-592

Mandelbrot, B. B. 1975. Stochastic models for the Earth's Relief, the Shape and the Fractal Dimension of the Coastlines, and the Number-area Rule for Islands. 72: 3825-3828.

B. Mandelbrot 1982. *The Fractal Geometry of Nature.* W.H. Freeman & Co., NY.

Mateker E. J. Jr. 1971. Lithologic predictions from seismic reflections. *Oil and Gas J*. (Nov. 8, 1971): 96-100.

Matsushita, M. 985. Fractal viewpoint of fracture and accretion, *J. Phys. Soc. Japan*. 54:857-860.

G. Mavko, T. Mukerji, and J. Dvorkin 1998. *The Rock Physics Handbook: Tools for Seismic Analysis in Porous Media*. Cambridge University Press: Cambridge.

Maxwell, James Clerk, 1891. *A Treatise on Electricity and Magnetism*. Clarendon, London (Repr. edn. by Dover, New York, 1954).

J. Mayer, Kh. Khairy and J. Howard 2010. Drawing an elephant with four complex parameters, *American Journal of Physics* 78(2010): 648-649.

J. McCarthy 1956. Measures of the value of information. *Proc. Nat'l. Acad. Sci*. 42(9): 654-655.

Meese A. D. and Walther H. C. 1967. An investigation of sonic velocities in vugular carbonates. *8th SPWLA Symp*., Denver.

Mei, Chiand. C. and Bogdan Vernescu 2010: *Homogenization Methods for Multiscale Mechanics*. World Scientific, Singapore.

Minh, Ch.C et al. 2007. Graphical analysis of laminated sand-shale formations in the presence of anisotropic shales. *World Oil* 228 No. 9.

Morlet , J. 1967. Three stages in seismic data processing. *Geoph. Prosp*. 15(3): 540-541.

Neal, J. T., Langer, A. M., and Kerr, P. F. 1968. Giant Desiccation Polygons of Great Basin Playas. *Geol. Soc. Amer. Bull*. 79: 69-70.

Neasham J. W. 1977. The morphology of dispersed clay in sandstone reservoirs and its effects on sandstone shaliness, pore space and fluid flow properties. *SPE Paper 6858*.

O'Brien , P. N. S., 1960. Seismic energy from explosions. *Geophysical Journal* 3: 29-44.

O'Doherty, R. F. and Anstey, N. A. 1971. Reflections on amplitudes. *Geoph. Prosp.* 19(3): 430-458.

K. Oleschko 1988. Delesse principle and statistical fractal sets: 1. Dimensional equivalents. *Soil & Tillage Research* 49: 255.

Olshevsky, V.V. 1966. *Statistical Properties of Sea Reverberations*. Nauka, Moscow. (In Russian).

Ossenberg, K., 1968: *Vergleich der Eigenschaften des Relaiskorrelators mit denen des klassischen Korrelators*. Ph. D. Dissertation, Hannover.

Alex P. Pentland 1984. Fractal-Based Description of Natural Scenes. *IEEE Transactions on Pattern Analysis and Machine Intelligence* PAMI-6:661-674.

Pirrie, D. and Rollinson, G.K. 2011. Unlocking the applications of automated mineral analysis. *Geology Today* 27: 235–244.

Plotnick, R.F. 1986. A fractal model for the distribution of stratigraphic hiatuses, *J. Geol*. 94: 995–890.

G. Polya, 1957. *How to Solve It?*, 2nd ed., Princeton University Press.

Radlinski AP et al. 1999. Fractal geometry of rocks. *Phys Rev Lett* 82: 3078–81.

L. Bruce Railsback 2002. *An Atlas of Pressure Dissolution Features*. Lecture Notes, Department of Geology, University of Georgia, Athens, Georgia 30602-2501 U.S.A. http://www.gly.uga.edu/railsback/PDFindex1.html

Rapoport 1969. Seismic applications of the correlation method. *Prikladnaya Geofizika* 56. (In Russian).

Alfréd Rényi 1967. *Dialogues on Mathematics*. San Francisco: Holden-Day, Inc.

Rice, S. O. 1944, 1945. The mathematical analysis of random noise. *Bell Syst. Techn. J*. 23, No. 3 (1944); 24, No 1 (1945).

Ritzenberger A. L. and Cohen R. J. 1984. First passage percolation: Scaling and critical exponents. *Phys. Rev. B*. 30(7): 4038-4040.

Rothrock, D. A. and Thorndike, A. S. 1984. Measuring the Sea Ice Floe Size Distribution, *J. Geophys. Res*. 89C: 6477-6486.

Rytov, S. M. 1966. *Introduction to Statistical Radiophysics*. Nauka, Moscow (In Russian).

Samarskii, A.A. 1989. *The Theory of Difference Schemes*. (In Russian.). Nauka, Moscow.

Sayers, C.M. and Kachanov, M. 1995. Microcrack induced elastic wave anisotropy of brittle rocks. *J Geophys Res* 100:4149–4156.

Sazhina, N. and Grushinsky, N. 1971. *Gravity Prospecting*. Mir Publishers, Moscow.

Schertzer, D. and Lovejoy, S. 1985. Generalised scale invariance in turbulent phenomena, *Physic. Chem. Hydrodyn*., 6: 623-635.

Schertzer, D. and Lovejoy, S. 1986. Generalised scale invariance and anisotropic inhomogeneous fractals in turbulence. *In*: *Fractals in Physics* (Eds Pietronero, L. and Tosatti, E.), North-Holland, Amsterdam: 457-460.

Schoen, Richard M. 1984. Conformal deformation of a Riemannian metric to constant scalar curvature. *Journal of Differential Geometry* 20 (2): 479–495.

Schoenberger, M. and Levin, F. K. 1974: Apparent attenuation due to intrabed multiples. *Geophysics* 39(3): 278-291.

Schubnel, A. and Guéguen, Y. 2003. Dispersion and anisotropy in cracked rocks. *J Geophys Res* 108:2001.

Schulz-Rojahn. J. P. and Phillips S. E. 1989. Diagenetic alteration of Permian reservoir sandstones in the Nappameri Trough and adjacent areas, southern Cooper Basin. *Proc. of the Cooper and Eromanga Basins Conf*., Adelaide: 629-645.

Shumway, G. 1960. Sound speed and absorption studies of marine sediments by a resonance method—Part II. *Geophysics* 25(3): 659-682.

Sierpinski, Waclaw (1915). "Sur une courbe dont tout point est un point de ramification". Compt. Rend. Acad. Sci. Paris. 160: 302–305.

Sinha, S.K. 1989. Scattering from fractal surfaces. *Physica D* 38: 310-314.

B. Sterligov 2010. *Analyse probabiliste des relations spatiales entre les gisements aurifères et les structures crustales: developpement méthodologique et applications à l'Yennisei Ridge (Russie).* Ph.D. Thesis, Lomonosov State University, Moscow & Institut des Sciences de la Terre d'Orleáns.

Stroud, D. 1998. The effective medium approximations: Some recent developments. *Superlattices and Microstructures* 23(3/4):567-573.

Tatarski, V. I. 1961. *Wave Propagation in a Turbulent Medium*. Dover Publ. Inc. New York.

Tegland E. R. 1970. Sand-shale ratio determination from seismic interval velocity. *23rd Ann. Midwestern Mtg., SEG, AAPG*, Dallas.

Thompson, D'Arcy W., 1942. *On Growth and Form*. Cambridge University Press, Cambridge.

Světlana Tomiczková 2005. Area of the Minkowski sum of two convex sets. *Proc. 25th Conf. on Geometry & Computer Graphics*, Sept. 12-16, 2005, Prague: 255-260.

Turcotte, D. L. 1986, Fractals and Fragmentation. *J. Geophys. Res*. 9IB, 1921-1926.

Donald L.Turcotte and Gerald Schubert 2002. *Geodynamics* (2nd edn,) . Cambridge University Press.

Turner, M.J., Blackledge, J.M. and Andrews, P.R. 1998. *Fractal Geometry in Digital Imaging*, Academic Press, Cambridge, UK.

Van Damme et al. 1988. On the determination of surface fractal dimension of powders by granulometric analysis. *Journal of Colloid and Interface Science* 122(1):1–8.

C.L. Vavra, Kaldi, J.G., and Sneider, R.M. 1992. Capillary pressure. *In*: *Development Geology Manual*. AAPG Methods in Exploration Series No. 10, Tulsa, OK.

Walsh, J.B. and Brace, W.F. 1984. The effect of pressure on porosity and the transport property of rock. *J. Geophys. Res.* 89B(11): 9425–9431.

Edward W. Washburn 1921. The Dynamics of Capillary Flow. *Physical Review* 17 (3): 273-283.

Waterman, P. C. S. and Truell, R. 1961. Multiple scattering of waves. *J. Math. Phys*. 2(4): 512-537.

J. Wei 1975. Least Square Fitting of an Elephant. *CHEMTECH* 5(2:128–129.

J. E. White 2000: *Seismic Wave Propagation*. *Collected Works of J. E. White*. Society of Exploration Geophysicists.

Wyllie M. R. J., Gregory A. R. and Gardner L. W. 1956. Elastic wave velocities in heterogeneous and porous media. *Geophysics* 21(1): 41-70.

Wiener, Norbert 1949. *Extrapolation, Interpolation, and Smoothing of Stationary Time Series*. New York: Wiley.

Yonezawa, F. and Cohen, M.H. 1983. Granular effective medium approximation. *J. Appl. Phys*. 54: 2895–2899.

Bo-Ming Yu 2005. Fractal character for tortuous streamtubes in porous media. *Chinese Phys. Lett*. 22(1): 158-160.

Zallen R. 1983. Introduction to percolation: A model for all seasons. *In*: Deutscher G., Zallen R. and Adler J. (Eds.) *Percolation Structures and Processes*. *Ann. Israel Phys. Soc*. 5: 4-16.

Ziman J. M. 1979. *Models of Disorder. The Theoretical Physics of Homogeneously Disordered Systems.* Cambridge University Press, Cambridge-London-New York-Melbourne.

Zimmerman, R.W. 1991. *Compressibility of Sandstones*. Elsevier: Amsterdam.